Title

The Evolution of Quiet Flight in Owls (Strigiformes) and Lesser Nighthawks (Chodeiles acutipennis)

Author

Le Piane, Krista

Publication Date

2020

UNIVERSITY OF CALIFORNIA
RIVERSIDE

The Evolution of Quiet Flight in Owls (*Strigiformes*) and Lesser Nighthawks (*Chodeiles acutipennis*)

A Dissertation submitted in partial satisfaction
of the requirements for the degree of

Doctor of Philosophy

in

Evolution, Ecology, and Organismal Biology

by

Krista Le Piane

December 2020

Dissertation Committee:
    Dr. Christopher J. Clark, Chairperson
    Dr. Erin Wilson Rankin
    Dr. Khaleel A. Razak

The Dissertation of Krista Le Piane is approved:

____

____

____

Committee Chairperson

University of California, Riverside

ACKNOWLEDGEMENTS

I thank my Oral Exam Committee: Dr. Khaleel A. Razak (chairperson), Dr. Erin Wilson Rankin, Dr. Mark Springer, Dr. Jesse Barber, and Dr. Scott Curie. Thank you to my Dissertation Committee: Dr. Christopher J. Clark (chairperson), Dr. Erin Wilson Rankin, and Dr. Khaleel A. Razak for their encouragement and help with this dissertation. Thank you to my lab mates, past and present: Dr. Sean Wilcox, Dr. Katie Johnson, Ayala Berger, David Rankin, Dr. Nadje Najar, Elisa Henderson, Dr. Brian Meyers Dr. Jenny Hazelhurst, Emily Mistick, Lori Liu, and Lilly Hollingsworth for their friendship and support.

I thank the Natural History Museum of Los Angeles County (LACM), the California Academy of Sciences (CAS), Museum of Vertebrate Zoology (MVZ) at UC Berkeley, the American Museum of Natural History (ANMH), and the Natural History Museum (NHM) in Tring for access to specimens used in Chapter 1. I would especially like to thank Kimball Garrett and Allison Shultz for help at LACM. I also thank Ben Williams, Richard Jackson, and Reddit user NorthernJoey for permission to use their photos in Chapter 1. Jessica Tingle contributed R code and advice to Chapter 1 and I would like to thank her for her help.

I thank Dr. Pete Bloom for his guidance and training early in this program and Dr. Scott Weldy and the volunteers at the Orange County Bird of Prey Center for their enthusiasm and dedication to Chapter 2. Thank you to Jennifer Brown, Stephen Fetting, Justin Garcia, Carie Battistone, and Theresa Wisneskie for state and federal permits used

in Chapter 2 and March AFB for the donation of a salvage Barn owl to use for feather imaging

The research for Chapter 3 was performed at the University of California Natural Reserve System *(Boyd Deep Canyon Desert Research Center)* Reserve DOI: *(*doi:10.21973/N3V66D). I thank Chris Tracy for his help at Boyd Deep Canyon Research Center.

I thank my advisor, Dr. Christopher J. Clark for his dedication to me and this research. He guided me through countless e-mails, meetings, and manuscript drafts, filled in for me when I needed it most, and was supportive and helpful throughout this process.

This dissertation is based upon work supported by the National Science Foundation Graduate Research Fellowship Program under Grant No. (DGE-1326120) awarded to Krista Le Piane. Any opinions, findings, and conclusions or recommendations expressed in this material are those of the author(s) and do not necessarily reflect the views of the National Science Foundation.

The text of this dissertation, in part, is a reprint of the material as it appears in Evidence that the dorsal velvet of Barn Owl wing feathers decreases rubbing sounds during flapping flight, 2020. The co-author, Christopher J. Clark, listed in that publication directed and supervised the research which forms the basis for this dissertation.

DEDICATION

This dissertation is dedicated to my family, friends, and mentors. Thank you to my wonderful, supportive parents, Kim Le Piane and Karl Le Piane and my brother, Ryan Le Piane for encouraging me to keep going when I wanted to give up. Thank you to my grandparents, Patricia Weckerly, Allen Weckerly, Michelle Le Piane, and Patrick Le Piane for being my biggest cheerleaders. Thank you to my dear friends: Jessica Tingle, Ayala Berger, Anne Hilborn, Ming-Feng Ho, Yongda Zhu, and Mahdi Qezlou for lifting my spirits. Thank you to Sharon Newmann, my high school counselor for planting the seed of a PhD in my mind when I was in high school. Thank you to Gary Waayers for lighting the spark of a love for Biology and to Dr. Gita Kolluru for my undergraduate training. Thank you to Dr. Erin Wilson Rankin for encouraging and supporting me at pivotal moments in this process. Finally, thank you to my advisor, Dr. Christopher J. Clark for believing in me, even when I did not believe in myself. Without all of you, none of this would be possible. Thank you for lifting me onto your shoulders and supporting me through this journey.

ABSTRACT OF THE DISSERTATION

The Evolution of Quiet Flight in Owls (*Strigiformes*) and Lesser Nighthawks (*Chodeiles acutipennis*)

by

Krista Le Piane

Doctor of Philosophy, Graduate Program in Evolution, Ecology, and Organismal Biology
University of California, Riverside, December 2020
Dr. Christopher J. Clark, Chairperson

All locomotion produces sound and flight is no exception. In owls, flight sounds are quieted by three wing and feather features: the leading-edge comb, a modified barb structure that projects dorsally from the front edge of the outermost primary feather (P10), the velvety dorsal surface of flight feathers, and the fringed vane of flight and tail feathers. There are two hypotheses for the evolution of quieting features: stealth and self-masking. Under the stealth hypothesis, we predict quiet flight evolved to aid owls in sneaking up on prey. Under the self-masking hypothesis, we predict quiet flight evolved to aid acoustic hunters in locating prey. To test these hypotheses, we investigated the relationship between leading-edge comb morphology and ecology (Chapter 1), tested the function of the dorsal velvet in Barn Owls (Chapter 2), and investigated the function of quieting features in Lesser Nighthawks, another nocturnal bird (Chapter 3). In Chapter 1, We used phylogenetic generalized least squares (pgls) to test the correlation between comb morphology and the stealth or self-masking scores. We found comb morphology to be correlated with both stealth and self-masking (pgls; DF = 66 test-statistic = -3.92; *P*-

value = 0.0002). In Chapter 2, impairing the dorsal velvet of 10 feathers on 13 barn owls increased broadband sound production and the upstroke increased more than the downstroke, such that the upstroke of manipulated birds was louder than the downstroke, supporting the frictional noise hypothesis. Finally, In Chapter 3, we found Lesser Nighthawks initiated pursuit of prey at a greater distance than the audible detection distance of insects (0.5 m) both when hunting on the ground (1.1 ± 0.2 m; *P*-value = 0.02) and on the wing (2.5 ± 0.4 m; *P*-value <0.0001), suggesting they use visual cues to initiate pursuit of prey under these conditions. This dissertation contributes to a research area which has received little consideration: the role of sound and hearing in predation.

Table of Contents:

List of Figures:

Chapter 1 Figures:

Chapter 2 Figures:

Chapter 3 Figures:

Supplemental Figures:

List of Tables:

Chapter 1 Tables:

Chapter 2 Tables:

Chapter 3 Tables:

Supplemental Tables:

Introduction:

All locomotion produces sound and flight is no exception. In owls and other nocturnal birds, flight sounds are quieted by a suite of wing and feather features. These include: the leading-edge comb, a series of modified barbs that project up from the leading edge of the outermost primary (P10) feather, the velvety dorsal surface of flight feathers, and a fringed vane of wing and tail feathers (Graham 1934).

There are two main hypotheses for the evolution and function of quieting features in owls and other birds: stealth and self-masking (Clark et al. 2020a). Here, we consider stealth a hunting strategy where a predator remains undetected until they are too close for the prey to escape (Heithaus et al. 2002). Under the stealth hypothesis for the evolution of quiet flight, we predict quieting features evolved to aid predators in sneaking up on prey (Clark et al. 2020a). Masking is an auditory phenomenon where the presence of one sound renders another sound inaudible. Here, we consider self-masking an animal's own locomotion-induced sounds (i.e., flight sounds) rendering sounds they may be listening for (i.e., auditory cues from prey) inaudible (Larsson 2012). Under the self-masking hypothesis for the evolution of quiet flight, we predict quieting features evolved to aid auditory hunters in listening for auditory cues from prey.

There are several ways that wings may produce sound, including aerodynamic and frictional sound. Aerodynamic noise is one source of sound production during flight, caused by the formation and shedding of turbulence over the wing (Blake 2017; Rao et al. 2017; Jaworski and Peake 2020). Another source of aerodynamic sound production is caused by the time variation of the forces keeping the bird aloft (i.e., lift and drag) which we term Gutin sound (Gutin 1948; Blake 2017). Gutin sounds have a fundamental frequency equal to the rate birds flap their wings, so they are concentrated below 0.1 kHz. Aerodynamic noise has the highest amplitude at low frequency and declines sharply as frequency increases (Crighton 1991; Rao et al. 2017). Frictional sound, on the other hand, is the hypothesized broadband sound caused when two feathers slide past one another, as occurs during flapping flight (Clark et al. 2020a). Quieting features may work to reduce flight sounds from aerodynamic sources, frictional sources, or both.

Owls are not the only group of species with quieting features. The leading-edge comb is not unique to owls: nocturnal frogmouths (*Podargidae*) have independently evolved a leading-edge comb and Rough-winged Swallows have short comb-like projections on their outer primaries(Mascha 1905; Clark et al. 2020a). The dorsal velvet is also not unique to owls: some hawks, such as the American Kestrel (*Falco sparverius*) and other nocturnal birds, such as Nightbirds (nocturnal members of Caprimulgiformes such as Nightjars, Nighthawks, Pootoos) also have the dorsal velvet (Clark et al. 2020b). The distribution of vane fringes in birds other than owls is unknown, but birds such as Lesser Nighthawks (*Chordeiles acutipennis*) also have vane fringes.

In this dissertation, we investigate the phylogenetic distribution of leading-edge comb morphology across owls related to ecological correlates (Chapter 1), the function of the dorsal velvet in reducing Barn Owl flight sounds (Chapter 2), and the function of quieting features in Lesser Nighthawks (*Chordeiles acutipennis*).

Chapter 1: Phylogenetic analysis suggests owl leading-edge comb evolved to reduce self-masking and aid in stealthy hunting

Abstract:

Owls have evolved excellent hearing and quiet flight which make them efficient nocturnal hunters. Owls' ability to localize sounds is facilitated by the facial disc, a circular arrangement of feathers on the face. Another adaptation for nocturnal hunting is quiet flight. In owls, quiet flight is facilitated by wing and feather features that reduce their flight sounds, including the focus of the present study, the leading-edge comb, which is a series of modified barbs that project up from the leading edge of the outermost primary (P10) feather. Two non-exclusive hypotheses have been proposed to explain the function of quiet flight: stealth and self-masking. According to the stealth hypothesis, silencing features evolved to better approach prey undetected. Under the stealth hypothesis, we predicted owls hunting prey that hear well (i.e., small mammals and flying insects) will have longer combs. According to the self-masking hypothesis, silencing features evolved to aid owls in prey detection, mid-flight. Under the self-masking hypothesis, we predict owls hunting prey acoustically, such as when hunting prey that are not visible (e.g., hidden by grass or snow), will have longer combs. Here, we test these two hypotheses by quantifying the diversity in the leading-edge comb of 147 owl species and facial disc of 66 owl species, and using species accounts to score ecological variables (prey type, hunting strategy, active period, and habitat), which we then used to produce scores for stealth and self-masking reliance (N=66 species). We then used phylogenetic generalized least squares (pgls) to test the correlation between comb morphology and the stealth or self-masking scores for each species. We found support for both the stealth and self-masking hypothesis in that the interaction between stealth and self-masking was highly significant (pgls; DF = 66; t-value = -3.16; *P*-value = 0.003). We consider this evidence that a suite of features which aids in predation evolves to benefit the predator in multiple ways.

Introduction:

Predator-prey interactions can lead to 'arms race' evolution, a cyclical pattern of predatory adaptation and prey counter-adaptation played out on an evolutionary timescale (Brodie and Brodie 1999a). Coevolutionary arms races occur between two tightly locked species, such as between garter snakes and rough-skinned newts (Brodie and Brodie 1999a, 1999b) or between bats and tiger moths (Corcoran et al. 2009; Corcoran and Conner 2012). In both of these examples, the predator is specialized for eating that prey species and the prey species has evolved a defense mechanism in response to a particular predator. When a predator instead eats multiple prey types, selection may instead act on that predator weakly in multiple directions (Slobodkin 1974). Instead of an arms race, predatory characteristics may evolve under "top-down evolution", where predators evolve and prey respond, resulting in escalation, rather than the cyclical pattern predicted by an arms race (Vermeij 1983, 1994).

Here we consider which of these scenarios better applies to an adaptation that hunting owls have for catching prey: quiet flight. As most owl species hunt at night, when light is limited, auditory cues are especially important to both owls and their prey. For a nocturnal hunter, listening for and responding to auditory cues given off by prey aids in the detection and successful capture of prey. For nocturnal prey, such as a mouse, detecting and responding to auditory cues from an approaching predator could mean the difference between life and death. On account of these ecological pressures, nocturnal predators and prey have adaptations to facilitate nocturnal vision (Walls 1942; Ali 2012) and increased ability to localize sounds (Ralls 1967; Payne 1971; Knudsen 1981; Martin 1986). In addition to these adaptations, owls have evolved quiet flight, which aids in nocturnal hunting. Here we ask: did quiet flight evolve to help owls ambush prey (i.e., stealth) in an example of arm's race evolution? Or is quiet flight instead the product of escalation, where silent flight and sound localization ability evolved to help owls detect and capture prey?

The stealth hypothesis is an example of arms race evolution, in which quiet flight is a counter-adaptation against prey that have excellent hearing ability (Clark et al 2020). Owls that hunt prey that use hearing to detect predators are predicted to have enhanced silencing features. Examples of prey with excellent hearing ability are rodents—many of which hear 1-4 kHz sounds well (Ralls 1967; Heffner and Heffner 1985; Heffner et al. 2001; Fay 2012) and flying insects, which are sensitive to a range of frequencies and may use hearing to avoid bird predators (Fournier et al. 2013). Under the stealth hypothesis, we also predict that owls hunting in relatively quiet environments, such as the deserts (Mennitt et al. 2013, 2014), will have increased silencing features because low background sound increases the chance of an owl being detected by prey.

The self-masking hypothesis is an example of escalation, in which quiet flight evolves in concert with owl hearing, to aid in prey detection. Locomotion-induced sound may cause masking, which is the presence of one sound interfering with an animal's ability to perceive sounds from the environment (Larsson 2012). Owls may have evolved quiet flight to reduce self-masking, facilitating prey detection. Barn owls are able to detect prey sounds mid-flight and change their flight path in response to a change in the location of a prey item (Payne 1971; Konishi 1973a; Hausmann et al. 2008). Under the self-masking hypothesis, we predict owls hunting when prey is not easily seen (e.g., when prey hidden under snow or grass) or make a lot of noise that an owl could be listening for (such as small mammals and some arthropods) will have increased quieting features (Payne 1971; Goerlitz et al. 2008). In contrast, owls hunting animals which make little noise during locomotion (i.e., flying insects; Chapter 3) will have decreased silencing features because owls hunting quiet prey will have to use senses other than hearing to detect these prey. Under the self-masking hypothesis, we also predict that increased silencing features are correlated with owl sound localization ability, measured here as the size of the facial disc.

Owls

Owls are a clade of over 200 species in two families (*Strigidae* and *Tytonidae*) (del Hoyo et al. 1999). There is variation in owl ecology: owls hunt a variety of prey, live in different habitats, and some are active during the day, while most are nocturnal (del Hoyo et al. 1999). This diversity means that owls potentially evolved variation in features associated with hunting (i.e., sound localization ability and quiet flight). For example, an owl hunting in the desert where ambient sound levels are sometimes extremely low (Mennitt et al. 2013, 2014) may have greater need to be silent to successfully ambush prey (i.e., a stealthy hunting strategy). Or, an owl hunting prey that is not visible (e.g., hidden under snow) may need to quiet its own flight sounds so it can better detect hidden prey.

Quiet Flight

Owls have several wing features that seem to reduce flight sounds, including the leading-edge comb, a fringed vane of many of their wing and tail feathers, and velvety dorsal surface of their flight feathers (Graham 1934; Konishi 1973a; Bachmann et al. 2007) (Fig. 1.1). The quieting feature that is the focus of this study is the leading-edge comb, comprised of stiff, comb-like barbs that taper as they extend from the leading-edge of a feather (Bachmann et al. 2007; Weger and Wagner 2016). The leading-edge comb is present on the anterior edge of the outermost primary (P10) as well as on P9, P8, and P7 in some species (Fig. 1.1). The leading edge comb varies morphologically among species, as well as down the length of P10 (Weger and Wagner 2016).

Owl Hearing

The sound localization ability of many owls is facilitated by the facial disc, a circular array of feathers that functions similarly to the fleshy pinnae of the mammalian ear in that it captures, amplifies, and funnels high frequency sounds to the inner ear (Konishi 1973a; Norberg 1977; Heffner and Heffner 1992; Heffner et al. 1996). High frequency sounds are important in auditory localization, so these structures increase an animal’s ability to locate sound. The size of the mammalian pinnae is correlated to the range of frequencies with which it interacts (Knudsen and Konishi 1979; Calford and Pettigrew 1984; Rice et al. 1992; Chen et al. 1995). Similarly, the facial disc of a Barn

Owl modifies sounds with a physical wavelength shorter than the size of the disc (approximately >3 kHz for a Barn owl) (Knudsen and Konishi 1979). Owls with prominent facial discs often have also evolved ear asymmetry to further aid in sound localization. Ear asymmetry has evolved independently multiple times (Norberg 1977) in members of *Tyto, Asio, Strix, Ciccaba,* and others. Conversely, owls that lack asymmetrical ears (e.g., Great Horned Owl, Burrowing Owl, Scops Owl) often have reduced facial discs and cannot hear well above 6 kHz (Volman and Konishi 1990; Gutiérrez-Ibáñez et al. 2011). These patterns suggest that facial disc size may scale with the range of frequencies it can alter, i.e., species with larger facial discs may have enhanced sound localization ability. Here, we quantified the variation in the facial disc morphology a phylogenetically-diverse sample of owls and used facial disc size as a proxy for an owls' ability to localize sound.

To test the stealth and self-masking hypotheses for the evolution of quiet flight, we measured variation in the morphology of the leading-edge comb on 168 owl species and facial disc on 66 owl species. On an owl phylogeny, we tested whether indices of self-masking, or indices of stealth, were better correlated with the presence of the leading-edge comb.

Methods:

Feather Measurements

We measured owl skin specimens at the Natural History Museum of Los Angeles County (LACM), the California Academy of Sciences (CAS), Museum of Vertebrate Zoology (MVZ), the American Museum of Natural History (ANMH), and the Natural

History Museum (NHM). When possible, we collected data on three males and three females from each species. We measured 11 traits, including three size measurements (ornithological wing chord, tarsus length, tail length), and eight comb traits shown in Fig. 1.1. These were the total length of the comb on P10; the length of a serration at four places along that length (see Fig. 1.1), At 25% of the length of the comb, we measured the distance between two barbs (Fig. 1.1F) and the width of a single barb at the tip (Fig 1.1G). Finally, we measured barb density (number of barbs per centimeter; Fig. 1.1H). We photographed wings and used ImageJ (Rueden et al. 2017) to measure fine-scale details such as serration length and distance between barbs.

Facial Disc Measurements

Owls have little ocular mobility (Knudsen 1989) and often orient their gaze directly towards sound, such as the shutter of a camera (Knudsen and Konishi 1979). Therefore, we used photographs of live birds obtained from internet sources (listed in Table 1.S1) to measure interspecific variation in the facial disc. In owls, facial feathers are under muscular control, so the facial ruff may vary from image to image. To control for this, we measured three images per species and averaged the measurements (with the exception of *Jubula lettii*; N=1). We only used photos of birds with adult plumage and images where the birds were looking directly at the camera, as indicated by widths of the eyes being approximately equal.

From each photo, we took the measurements as shown in Figure 1.2A. For both the left and right side of the facial disc, we measured from the top of the eye to the top of the disc (Fig. 1.2-1), from the bottom of the eye to the bottom of the facial disc (Fig. 1.2-

2) and from the left or right of the eye to the respective side of the facial disc (Fig. 1.2-3). The edges of the facial disc were determined by the location of the facial ruff, the stiff feathers surrounding the disc, or a change in the orientation or color of the feathers on the face (Fig. 1.2). For example, in species with a poorly developed disc, such as collared owlet (*Glaucidium brodiei;* Fig 1.2C), the facial ruff is not prominent, but it is still possible to determine the edge of the disc based off of feather orientation and color of the feathers. The images we used did not have a size scale, so we scaled our measurements relative to the distance between the eyes (Fig 1.2-4). We chose the distance between the eyes (from the inside of one eye to the inside of the other; Fig. 1.2-4) as a scale because it is fixed and appeared to scale isometrically with body size.

Owls are sexually size dimorphic (Abouheif and Fairbairn 1997), but we combined our data from males and females for three reasons: 1) in a preliminary analysis of the effect of comb morphology on quieting features, only 11 (of 146) species had any sex difference in comb morphology (combs were up to 0.77 mm longer in males of some species and 2.15 mm longer in females of other species, but most of these differences were <0.4mm); 2) we found no differences between male and female owls in the photographs used for our facial disc measurements and; 3) there were not any species for which the sexes scored differently under the stealth and self-masking hypothesis.

Ecology: stealth vs masking scores

We used information about diet, habitat, active period, and hunting strategy from species accounts (del Hoyo et al. 1999; Billerman et al. 2020) to give each species a score for stealth-reliance and masking-reliance (described below).

Diet was defined as specializing on mammals, arthropods, flying insects, fish, or generalist. An owl was considered a specialist if a given prey type was reported to make up >80% of that owl's diet (% by count or mass, when available). When a species account did not include detailed information about the diet (counts or mass), we considered that owl a specialist if only one prey type was listed in the species account. Within arthropod specialists, a small number (N=3) were considered flying insect specialists because they consumed >80% flying insects such as moths and beetles, which we presume were caught in flight. If a species account recorded an owl "mostly" or "primarily" eating insects or other arthropods (such as spiders and scorpions), it was coded as an arthropod specialist, but not a flying-insect specialist. The diet of these owls includes a mix of flying insects and non-flying arthropods. An owl was considered a generalist if it was described as such in a species account or if it was reported to eat three or more types of prey (all owl species that sometimes eat amphibians, reptiles, or birds fell into this category).

The habitats considered were: woodland, forest, desert, grassland, tundra, and generalists and coded by the US National Vegetation Classification System standards (*USNVC*, 2019). Forests were defined as wooded areas with 60-100% canopy cover, woodlands were wooded areas with 25-60% canopy cover, grasslands were areas with low vegetation (<1m high) and <10% canopy cover, tundras were areas in the arctic circle with <10% tree cover, and deserts are open habitats with sparse (<1%) canopy cover (*USNVC,* 2019). We considered an owl a habitat generalist if the species account mentioned multiple types of habitats or if the account described an owl as a habitat generalist.

The active periods considered were nocturnal, diurnal, and crepuscular. In most cases, if a species account mentioned diurnal activity, that owl was coded as diurnal. However, owls such as *Bubo scandiacus,* are diurnal for part of the year because they live above the arctic circle where daylight is present 24-hours for part of the year, but return to nocturnal habits for the rest of the year (Martin 2010). *Bubo scandiacus* and other owls which are nocturnal for part of the year were treated as nocturnal.

The hunting strategies considered were: sit-and-wait, quartering, and hunting through snow. Most owls employ either sit-and-wait (hunting from a perch) or quartering (flying low over the ground) as a hunting strategy (del Hoyo et al. 1999). Hunting through snow is a type of sit-and-wait strategy, but we included it as special hunting strategy because prey is not visible to the owl. Species that ever hunted through snow were coded as hunting through snow. Hunting strategy was unknown for some of the owls in this study (N=11). These owls were treated as sit-and-wait predators because that is the most common hunting strategy.

Stealth

These ecological data were then used to construct a score from 0-3 for stealth. Stealth points were awarded for prey type and habitat (points awarded in each category are presented in Table 1.1). First, owls were awarded 0, 1, or 2 points for stealth reliance relative to prey hearing ability (prey type; Table 1.1). We considered small mammals and flying insects as prey that hear well and owls specializing in hunting small mammals

(N=19) and flying insects (N=3 species) received two points for stealth (Table 1.1). Prey that do not hear well for the purposes of this study are fish (sound does not pass well between air and water) and non-flying arthropods (no reports of using ears to avoid predators). Owls specializing in hunting fish received zero points for stealth (Table 1.1). Owls that eat small mammals or flying insects as part of their diet (including generalists and non-flying insect specialists) were awarded one point for stealth (Table 1.1). Arthropod specialists were awarded one point for stealth because while there are no reports of non-flying arthropods (such as spiders and scorpions) using ears to avoid predators, the diet of arthropod specialists included some flying insects, which do hear well and potentially use ears to avoid predators (Table 1.1).

Second, owls were also scored relative to their propensity to hunt in quiet environments. Owls residing in quiet habitats with little vegetation (deserts and tundras) were given one point for stealth because low background noise increases the chance of auditory detection by their prey (Mennitt et al. 2013, 2014). Owls hunting in woodlands and forest received zero points to stealth because the stealth and self-masking hypotheses do not make contrasting predictions for these habitats (see below). Owls hunting in grasslands also received zero points for stealth because it was conflated with a prey type (small mammals) and it is unclear if grasslands warranted additional points for stealth. We instead awarded points for this prey type rather than the habitat (see below).

There were no points awarded for stealth reliance in hunting strategy, active period, or sound localization ability (Table 1.1). Sit-and-wait hunting strategies do not make contrasting predictions for stealth or self-masking because this hunting strategy requires an owl to both sneak up on prey (stealth) and listen for prey movements (self-masking). We awarded no points for hunting period because nocturnal settings could also require both stealth and self-masking. Finally, sound localization ability is not predicted to be a factor in stealth.

Self-masking

For self-masking, owls were given a score from 0-4 based on prey type, habitat, active period, hunting strategy, and sound localization ability in situations where hearing is important for prey location (Table 1.1). Owls such as *Aegolius funereus* which has a well-developed facial disc and specializes in hunting small mammals through snow (i.e., when prey are not visible) received the highest scores for self-masking. First, we scored owls for their propensity to hunt prey that make a considerable amount of noise during locomotion (i.e., the rustling of leaves, walking on a substrate, etc.). We considered small mammals and non-flying arthropods to be noisy locomotors (Payne 1971; Goerlitz et al. 2008). Owls specializing in hunting small mammals were awarded two points for self-masking. Flying insects are hypothesized to make little noise in flight (Chapter 3) so owls specializing in hunting flying insects received zero points for self-masking (Table 1.1). Owls which hunt insects and other arthropods (arthropod specialists; Table 1.1) received one point for self-masking because the diet of these owls is a mix of flying (quiet locomotors) and non-flying arthropods (noisy locomotors; Table 1.1). Owls hunting three or more types of prey were considered generalists and were awarded one point for masking (Table 1.1). Owls hunting fish were awarded zero points for self-masking.

Owls were not awarded any self-masking points for habitat. Under the self-masking hypothesis, we predict owls hunting in quiet, open environments (deserts and tundras) will have increased silencing features, but the low levels of vegetation in these habitats means there is probably always enough light for owls to hunt by sight rather than sound (Dice 1945; Martin 2017). These conditions do not favor hunting by ear, so zero self-masking points were awarded. We did not award any points (for either selfmasking or stealth) for owls hunting in forests, woodlands, and habitat generalists because the self-masking and stealth hypotheses do not make contrasting predictions for these habitats. We also did not award any points for owls hunting in grasslands because this habitat is conflated with hunting strategy and prey type.

Diurnal and crepuscular owls were awarded zero total points for self-masking, even if they met other criteria, because we assume there is always light available to hunt, resulting in reduced selective pressure for hunting by ear.

Owls received a maximum of one point for hunting strategy for self-masking (Table 1.1). Owls that hunt by coursing were awarded one point for self-masking because these owls are hunting prey that aren’t visible so they must be located using acoustic cues (Table 1.1). Owls that hunt prey through snow (when prey are not visible) were also awarded one point for self-masking (Table 1.1). Barn Owls, which hunt both by quartering and through snow were only given one point for self-masking in hunting strategy. Owls hunting by sit-and-wait were awarded zero points for self-masking.

To score for sound localization ability, owls in the top 25% of relative facial disc size (as measured by the first principle component of disc size; see results) were awarded an additional point for self-masking, since we took facial disc size as a proxy for reliance on hearing (Table 1.1).

Hunting strategy, prey type, and habitat were often correlated to one another. For instance, owls specializing in hunting in grasslands (a habitat) also tend to use coursing (a strategy) and hunt small mammals (a prey type). To provide proportionate weighting for this ecology, we scored these species two points for stealth and three points for self-masking (Table 1.S2).

Since the stealth and self-masking hypotheses are not mutually-exclusive, we made an effort to weigh attributes evenly. We did this by awarding habitat, hunting strategy, and active period points only in situations where either stealth or self-masking was important. For example, no points were awarded to owls living in forests and woodlands because the self-masking and stealth hypotheses do not make mutually exclusive predictions for these habitats: owls hunting in low light could be listening for prey (masking) or sneaking up on prey (stealth; Table 1.1). Conversely, low background sound in open habitats (e.g., deserts and tundras) may mean both prey are able to better hear an approaching owl (stealth) and owls are better able to hear their prey (self-masking), but the low vegetation in these areas means owls may have plenty of light to hunt (reducing the effect of self-masking; Dice 1945; Martin 2017). So, owls hunting in deserts and tundras were awarded 1 point for stealth and zero points for self-masking.

Phylogeny

We made an owl phylogeny, based on a backbone of Slater et al. (2019) who used ultra-conserved elements (UCE) to construct a phylogenetic tree. First, we ultrametricized the Slater et al. (2020) phylogeny in Mesquite version 3.63 (Maddison and Maddison 2019) using the 'arbitrarily ultrametricize' command. Then, we added 29 additional species for which we had data on comb morphology, disc images, or ecological information, to the phylogeny. Additional species were added using the topology of the trees presented in Wink et al. (2009), Dantas et al. (2016), and Wood et al. (2017), or in some cases, according to hypothesized sister relationships, using taxonomy from del Hoyo et al. (1999).

Specifically, *Strix uralensis* was added as sister to *Strix aluco* with *Strix nebulosa* as the outgroup (Wood et al. 2017). *Strix butleri* was placed as sister to *Strix woodfordii* (Wink et al. 2009). *Pulsatrix perspicillata* and *Pulsatrix keoniswaldiana* were added as sister taxa (Wink et al. 2009) with *Pulsatrix melanota* as the outgroup based on taxonomy data (del Hoyo et al. 1999). *Megascops choliba* was placed as sister to *Megascops albogularis* (Dantas et al. 2016). *Megascops kennicottii* was placed a sister to *Megascops asio* (Dantas et al. 2016). *Ketupa zeylonensis* was placed as sister to *Ketupa ketupu* (Wink et al. 2009). *Bubo lacteus* was added outside the clade containing fishing owls (Wink et al. 2009). *Bubo africanus* was placed as sister to *Bubo cinerascens* (del Hoyo et al. 1999). Then, sister species *Bubo bubo* and *Bubo ascalaphus* were added as sister to *B. africanus* and *B. cinerascens* (Wink et al. 2009). Finally, *Bubo virginianus* was placed as sister to *Bubo scandiacus* and these two species were placed outside this part of the *Bubo* clade (Wink et al. 2009). *Asio capensis* was added as sister to *Asio flammeus* (Wink et al. 2009). *Ptilposis leucotis* was added as sister to *Ptilopsis granti* (Wink et al. 2009). *Otus scops* as placed as sister to *Otus elegans* (del Hoyo et al. 1999). *Otus brucei* was placed as the outgroup to these two species (Wink et al. 2009). Sister species *Glaucidum jardinii* and *Glaucidium brasilianum* were added with *Glaucidium gnoma* as the outgroup (Wink et al. 2009). Then, *Glaucidium passerinum* and sister species *Glaucidium perlatum* were added outside these three species (Wink et al. 2009). *Ninox sctructulata* was placed sister to *Athene superciliaris* (formerly *Ninox*) based on species accounts (del hoyo et al, 1999). *Ninox strenua* and *Ninox rufa* were added as sister species and placed as sister to *Ninox sctulata* and *Athene supersciliaris* (Wink et al. 2009). Sister species *Aegolius acadicus* and *Aegolius harrassii* were placed with *Aegolius funereus* as the outgroup (Wink et al. 2009). *Ninox connivens* was placed as sister to *Ninox boobook* (Wink et al. 2009). *Tyto novaehollandiae* was added as sister to *Tyto alba* (Wink et al. 2009). Then, sister species *Tyto tenebricosa* and *Tyto longimembris* were placed sister to *T. alba* and *T. novaehollindae.* We removed *Ptilopsis granti, Glaucidium tephronotum, Xenoglaux lowerii, Otus elegans, Otus gurneyi, Otus rufescens, Otus bakkamoena,* and *Otus spilocephalus* from the Slater (2020) phylogeny because we lacked comb morphology data and/or ecological information for these species.

We added all of the above species assuming they had a branch length of half that of the subtending branch to which it was added (i.e. for a branch length of 1, the new species was added at distance of 0.5 on the preexisting branch, and with a branch length of 0.5 to keep the tree ultrametric). We then transformed the branch lengths using Pagel's method because this was the branch length transformation that produced standard deviations of branch lengths that were not correlated with the independent contrasts of the variables used in our statistical analyses (Comb PC1, Disc PC1, stealth score, masking score; Garland et al. 1999).

Sample size

We measured comb morphology on 146 species of owls (Table 1.S2). We then measured facial disc morphology of owls included in our phylogeny (N=66 species). Species were not included in the phylogenetic analysis if there was not enough ecological information in species accounts to score masking and stealth reliance, there were not enough photos of the facial disc to analyze, or if we could not resolve where they belonged in the phylogeny.

Statistical Analyses

Principal Components Analyses:

We performed three separate principal components analyses (PCA) to distill the variation in our measured body size, comb morphology, and facial disc morphology. We used species averages of the respective variables in each PCA.

Body size

Most of the museum specimens we measured lacked body mass data, so we could not use body mass in our measure of body size. Instead, we computed species averages for folded wing chord length, tarsus length, and length of R1 (N=147 species), then conducted a PCA of the log-10 transformed species-average values for these characters. Component 1 was our proxy for body size, (hereafter “body size”).

Leading-edge comb

To describe the variation in the leading-edge comb, we computed a PCA on log-10 transformed species averages for our comb variables (Comb length 25%, Comb length 75%, width between barbs, and barb density), after removing comb length 50% because it was collinear with comb length 25% (R^2=0.93). Component 1 from this analysis loaded on overall size of the comb (see results *Leading-edge Comb*; Table 1.2) and so we used ("Comb PC1") in our phylogenetic analysis of comb morphology (described below).

Facial Disc

To describe the variation in facial disc, we ran a PCA of the facial ruff features (N=66 species). Measurements from the left side of the face were highly correlated with the respective measurement from the right side of the face (R^2>0.8), so only the right side of the face was included in the analysis. Also, right eye height (collinear with right eye width; R^2=0.9) was removed from the analysis. We did not Log10 transform these facial ruff variables prior to the PCA because there were several values of zero.

Body Size and Diet

To test our hypothesis that body size is correlated to diet, we ran a separate preliminary regression analysis in JMP Pro v 14.0 (*JMP*® 2019) on a subset of owls with detailed information about percentage mammals in the diet (N=44). Body size PC1 was our independent variable and percentage mammals in the diet was our dependent variable. We excluded fishing owls from this analysis because they are large and eat fish instead of mammals.

Collinearity

We checked for collinearity between predictors in models using the function 'vif' in package *car* (Fox and Weisberg 2019) to ensure all variance inflation factors (VIFs) were <3.0. As masking and stealth were collinear, we regressed masking against stealth and extracted the residuals (Dormann et al. 2013), which represented the independent contribution of stealth after accounting for the effect of the masking.

Phylogenetic Analyses

To test our stealth and masking hypotheses, we used the ape (Paradis and Schliep 2018), Geiger (Pennell et al. 2014), and nlme (Pinheiro J et al. 2020) packages in R version 3.6.3 (R Core Team 2020) to calculate a phylogenetic generalized least squares (pgls) regression with Comb PC1 as our dependent variable and stealth score (0-3) and masking score (0-4) as continuous independent variables with body size as a co-variate. We included a stealth x self-masking interaction term to test the hypothesis that silencing features evolved to both aid in prey detection and to help owls sneak up on prey.

Our models were computed using a pgls fit assuming a variance-covariance structure of Brownian motion (Pagel's $\lambda = 1$), as well as using ape's corPagel function which estimates a value of λ based on the data.

Results:

Ecology

The number of owl species with each of the prey types, habitats, active periods, and hunting strategies considered are summarized in Table 1.1. Of measured species (N=66), there were 19 mammal specialists, 13 arthropod specialists (3 of which specialized in flying insects), 3 fish specialists, and 31 generalists

Over 85% of owls in this study were nocturnal (N=58), 7 were diurnal, and *Athene cunicularia* was the only crepuscular owl in this study. Over 50% of owls in this study live in the forest (N=34) and 23% live in woodlands (N=15), with only a small number living in grasslands (N=6), deserts (N=4), the tundra (N=1), and six were habitat generalists. Sit-and-wait predation was the most common hunting strategy (N=43). A small number of owls six hunt through snow (N=7), and six hunt by quartering. The hunting strategy of the remaining 11 owls in this study is unknown.

Stealth and self-masking scores were sometimes based on a small number of categories. For example, while self-masking scores were sometimes based on prey type, habitat, active period, hunting strategy, and sound localization ability, stealth scores relied on prey type and habitat alone. Owl species hunting small mammals and flying insects received the highest scores for stealth. Owls such as *Micrathene whitneyi*, which hunt primarily flying insects received relatively high stealth scores (2) and low self-masking scores (0; Table 1.S2). Species which scored high in self-masking hunted through snow or by coursing, specialized in hunting small mammals, and had highly developed facial discs. Owls such as *Asio clamator* which are generalists in habitat and prey type, but hunt by quartering and have a well-developed facial disc received a relatively low stealth score (1) and high self-masking score (3; Table 1.S2).

Body Size

The PCA of Body Size was based off of three body size variables (folded wing length, tarsus length, and tail length) measured on museum skins from 146 species of owls. PC loadings for Components 1 and 2 of the body size PCA are presented in Table 1.2. PC Scores for individual species are presented in Table 1.S2 and species averages for the measurements used in this PCA are presented in Table 1.S3. Component 1 of this analysis accounted 91.4% of the variation in our body size variables. The first principal component is related to all three body size variables, with strong positive loading on folded wing length (loading: 0.99), tarsus length (loading: 0.93), and tail length (loading: 0.95; Table 1.2). Owls with low Body Size PC1 values, such as *Glaucidium gnoma* (Body size PC1 = -3.5) had small tarsi, wings, and tails while owls with high Body Size PC1 values, such as members of the *Bubo* clade (Body Size PC1: >2.6) had large tarsi, wings, and tails. Body Size PC2 loaded positively on tarsus length and negatively on tail length, such that owls with high Body Size PC2 values such as *Tyto longimembris* (Body Size PC2: 1.5) had larger tarsi and relatively shorter tails (Table 1. 2) Maximum and minimum values along with their associated species names are presented in Table 1.3.

In a separate preliminary analysis of body size PC1 and percentage mammals in the diet of a subset of owls (N=44), body size was found to be related to prey type in that owls that larger owls (with higher body size PC scores) tend to have more mammals in their diet (Fig. 1.3)

Leading-edge comb

We collected leading-edge comb measurements from 860 specimens from 146 species, representing 28 of the 30 owl genera (>90% of all owl genera). The full dataset is presented in Table 1.S3, while species with the most extreme morphologies are listed in Table 1.3. Although we were unable to measure all currently described owl species (~66 of 213 total owl species are missing from Table 1.S3, two of which are from monotypic genera), the species we did measure covered much of the morphological diversity of this trait found within extant owl species.

Loadings for PC1 and PC2 of the comb are presented in Figure 1.4 and values for each variable considered in the PCA is presented in Table 1.2. Comb PC1 was an overall measure of comb size. It loaded strongly and positively on distance between barbs and comb length at 25% and 75%. Comb PC1 had the lowest score in a species with a negligible comb, such as Andean pygmy owl (*G. jardinii*; Fig. 1.4A) to well-developed in Pharaoh eagle-owl (*Bubo ascaphalaus;* Fig. 1.4C;). Comb PC2 described how 'fine-toothed' the comb was, loading heavily on barb density (Fig. 1.1H) and negative loading on distance between barbs (Fig. 1.1F; Table 1.2). Comb PC2 ranged from the relatively stubby, widely spaced out barbs of the comb in Brown hawk owl (*Ninox sctulata;* Fig. 1.4D) to densely packed, thin barbs in Greater Sooty Owl (*Tyto tenebricosa;* Fig 1.4B).

Facial Disc

The first two principle components of facial disc are presented in Figure 1.2, plotted as a function of diurnal/nocturnality and loadings are presented in Table 1.2. Facial Disc PC1 was an overall metric of facial disc size (relative to the interocular distance), and varied from species with a negligible disc such as Collared owlet (*Glaucidium brodiei;* Fig. 1.2C, and other members of the genus *Glaucidium*) to the species with the largest disc, Great Grey owl (*Strix nebulosa;* Fig. 1.2E). Species with low facial Disc PC1 values, such as *G. brodiei* (Fig. 1.2C) tended to have negligible measurements from the top of the eye to the top of the disc (Fig. 1.2-1) and the greater measurements from the side of the eye to the side of the facial disc (Fig 1.2-3). Species with high Facial Disc PC1 values, such as *S. nebulosa* (Fig. 1.2C) had highly developed discs in all directions. Disc PC2 was a metric of eye diameter relative to disc size, and varied from the large-eyed Rufous owl (*Ninox rufa;* Fig. 1.2D) to the small-eyed *Tyto longimembris* (Fig. 1.2F). Most owls are nocturnal (N=58); the diurnal species (N=7) tended to have small eyes and small facial discs, and cluster together in PCAs (blue points in Fig. 1.2). Owls with large eyes (Facial Disc PC2 >0) tended to have small facial discs (Facial Disc PC1<1; Fig. 1.2). No species in this study had large eyes and large facial discs, which indicates there may be a tradeoff between sound localization ability and eyesight (Fig. 1.2).

Phylogenetic Statistics

Leading-edge comb size was significantly positively correlated with facial disc size for both Model 1 (pgls regression, *P* =0.01) and Model 2 (λ=0.87*, P*-value=0.0004; Fig. 1.5; Table 1.4). Comb PC1 is plotted on a phylogeny in Figure 1.4A along with regressions of body size, masking, and stealth scores with comb size. There was not a significant effect of body size on comb morphology in either Model 1 (*P*-value=0.26) or Model 2 (λ=0.87*, P*-value=0.12; Fig. 1.6; Table 1.4). There was a significant effect of stealth score on comb morphology in both Model 1 (*P*-value=0.01) and Model 2 (λ=0.87; *P*-value=0.008; Fig. 1.6). Self-masking score was also correlated with comb size in Model 1 (*P*-value=0.02) and in Model 2 (λ=0.87*, P*-value=0.006; Fig. 1.6; Table 1.4) The stealth x self-masking interaction term was also significant in Model 1 (*P*-value=0.003) and in Model 2 (λ=0.87*, P*-value=0.004; Fig. 1.6; Table 1.4). .

Discussion:

Owls as a clade are exclusively carnivorous aerial raptors. Within this niche they have diversity in ecology, body size, ability to localize sound, and wing and facial disc morphology (Table 1.3). For example, Great grey owls (*Strix nebulosa*) are large, primarily nocturnal owls with large combs, have the largest facial disc of any owl, regularly hunt prey (such as voles, *Microtus* spp) by ear alone through a layer of obscuring snow, indicating excellent sound localization ability (del Hoyo et al. 1999). Fishing owls such as *Ketupa zeylonensis* are large owls which primarily eat fish and, have a short comb. They also have small facial discs and poor hearing above 6 kHz (Table 1.3; Nieboer and Van der Paardt 1977; del Hoyo et al. 1999; Gutiérrez-Ibáñez et al. 2011). Pygmy owls (*Glaucidium spp.*) are small, primarily diurnal owls which eat arthropods, birds, and small mammals (Table 1.3; del Hoyo et al. 1999). They have small eyes, small facial discs, and functionally lack a comb, and are reported to hunt visually (Table 1.3; del Hoyo et al. 1999). These are just a few of the examples of how comb and disc diversity are related to the ecological diversity within owls.

Stealth vs. Self-Masking

Here, we have distilled that ecological diversity into indices of "stealth-reliance" and "masking-reliance" to ask the question: did these predatory features evolve to aid in stealthy hunting as part of a co-evolutionary arms race, or did they evolve to reduce self-masking, as a complement to their ability to localize sound? We found support for both our stealth and self-masking hypotheses, and specifically, the stealth x self-masking interaction term was highly significant (*P*-value = 0.003; Table 1.4). These two hypotheses are not mutually exclusive, statistical support for both suggests that both processes have driven the evolution of quiet flight.

It is likely that stealth is more important for some owls and self-masking is more important for others. Owls such as the Marsh Owl (*Asio capensis*), which had a relatively large leading-edge comb score (Comb PC1 = 1.15) and received a high self-masking score (masking score = 3) for its excellent sound localization ability (measured by Disc PC1 = 3.50) and specialization in hunting mammals by quartering over dense vegetation, self-masking and not stealth (stealth score =1) is likely driving quieting features (Table 1.S2). Conversely, for owls such as the Boobook Owl (*Ninox boobook*), which had a medium leading edge comb (Comb PC1 = 0.41), relatively poor hearing (measured by Facial Disc PC1 = -0.36) and specialized in hunting flying insects, which hear well and may have evolved ears to avoid predators (Fournier et al. 2013) but make little sound for the owl to be listening for (Chapter 3), stealth is instead likely the driver (stealth score =2, masking score = 0; Table 1.S2). There are several examples of owls where both stealth and self-masking are important. For example, owls hunting small mammals often listen for acoustic cues to determine prey location (self-masking) and are selected to reduce flight sounds to sneak up on prey (stealth).

In general, predator-prey interactions are often described as an arms race, an asymmetrical, ever-escalating interaction between species that is played out on an evolutionary timescale in which each adaptation by a predator is matched over evolutionary time by a counter-adaptation in the prey species (Brodie and Brodie 1999a). However, what is noteworthy about this type of coevolutionary arms race is that it is between two tightly connected players: the main predator of the newts are the snakes, and the main diet of the snakes are newts (Brodie and Brodie 1999b). In owls, the stealth hypothesis for the evolution of quiet flight suggests an arms race where owls evolve quiet flight to sneak up on prey and in turn, prey evolve increased hearing ability to better detect and avoid predation from owls. However, there do not appear to be any owls with this same level ecological diet specificity. Even the owls that are specialists (e.g. on rodents) tend to forage on many species of rodents.

Morphology

Among 147 owl species, the leading-edge comb ranges from the well-developed (long, curved dorsally and bent so the barb tips point proximally) comb observed in species like *B. ascaphalaus* (Fig. 1.4C) to the short, negligible comb observed in species like *G. jardinii and N. sctulata* (Fig. 1.4D,C). Sick (1937) described these two extremes in comb morphology as “Bubo” type and “Surnia type”. We found that comb morphology varied more or less continuously from “Surnia” type to “Bubo” type along the first two principle components of shape among the species and morphological parameters we considered (Fig. 1.4). Owls are not the only bird that has a leading-edge comb: nocturnal frogmouths in the genus *Podargus* (Podargidae) have a similar, ambush hunting style and have convergently evolved a comb (Mascha 1905). The prevalence, evolutionary pressures, and physical mechanism of these features in non-owls is unknown.

At this point, not enough is known about how the comb suppresses sound to know whether and how comb size may affect its ability to suppress sound. There are at least three ways the comb might modify sounds made by the owl in flight. First, if the owl flies through turbulent air, as that turbulence impinges on the leading edge of the wing, eddies within that turbulence get stretched by the presence of the leading edge of the wing, resulting in sound (Jaworski and Peake 2020). The morphology of the comb might affect this stretching of ingested turbulence in some way. Second, the comb potentially trips turbulence in the boundary layer of the wing, causing turbulence to develop earlier than it would otherwise; and third, the comb might modify or disrupt stall at high angles of attack (angle of the wing relative to the flow of oncoming air; Neuhaus et al. 1973; Rao et al. 2017). High wing angles of attack are often achieved during the last phase of strike on prey (~1 m away from the prey), where an owl pitches its body up and brings its feet forward, sweeping the wings up and achieving a high angle of attack during the maneuver (Payne 1971a; Konishi 1973a, p. 415). In support of this third mechanism, experiments on owl wings have not found much acoustic effect of the comb at low angles of attack, but have suggested that it reduces sound at high angles of attack, potentially implicating the third mechanism, disrupted stall (Neuhaus et al. 1973; Geyer et al. 2017;

Jaworski and Peake 2020). For none of these potential mechanisms is it clear how variation in comb morphology might affect acoustic performance.

PC 2 of comb morphology loaded on how coarse/fine the comb was among the owls sampled (Fig. 1.4). In owls, the velocity of the wing as it is flapped and the size and shape of the comb will determine how air flows through it. Air flows through the serrations and may prevent aerodynamic separation on the dorsal surface of the wing, which, in turn, may reduce sound production above 2 kHz (Rao et al. 2017). The Reynolds number of the comb (Re=ul/v where u=velocity of wing (assumed to be 5.8 m/s; Wolf and Konrath, 2015); l=diameter of the tip of an individual barb from the comb; v=kinematic viscosity of air) (Koehl 2006) in the species at the two extremes of Comb PC2 varied between Re=2,320 (*Tyto tenebricosa*)and Re=502 (*Ninox sctulata;* Fig. 1.4B,D). This fourfold difference in Re among different owls may have functional significance in terms of how the comb introduces or modifies vortical structures into the flow over the wing. It is unclear how the length of the comb impacts flight sounds because the functional morphology is not understood well enough to know what difference a short or long comb makes for silent flight, i.e. whether and how the longest combs (about 5 mm from feather vane to barb tip; Fig 1.3C), suppresses more sound than a 2.5 mm long comb.

Here we have documented considerable variation in morphology of the facial disc (a circular array of feathers that amplifies sound and funnels it to the ear openings) on 67 species representing the diversity in disc size and shape (Fig. 1.2). The facial disc varies from highly developed, circular array of feathers found in species like *S. nebulosa* (Fig.

2E) to negligible (mainly present from the eye to the ear opening) in species like *N. rufa* and *G. brodiei* (Fig. 1.2 C,D). We have included facial disc measurements as a proxy for sound localization ability, such that owls with large Facial Disc PC1 values (such as *S. nebulosa*) are presumed to have excellent sound localization ability and owls with small Facial Disc PC1 values (such as *G. brodiei*) are presumed to have poor sound localization ability. There is some evidence to support this claim in that owls with well-studied and highly developed sound localization ability such as Barn Owls (*Tyto alba*) and Northern Saw-whet Owls (*Aegolius acadicus*) had relatively high Facial Disc PC1 values (Facial Disc PC1 =1.83 and 0.99, respectively, Table 1.S2; Konishi 1973b; Frost et al. 1989; de Koning et al. 2020). Conversely, owls with poor sound localization ability, such as Brown Fish-Owl (*Ketupa zeylonensis*) had low facial Disc PC1 scores (Facial Disc PC1 = -1.12, Table 1. S2; van Dijk 1973)

Facial disc size was found to be correlated with comb morphology, which suggests that owls with better sound localization ability also have larger combs, and possibly, quieter flight (Fig. 1.5; Table1. 4). This assumes two things: it assumes that a larger facial disc correlates with sound localization ability because large, circular facial discs often evolve with asymmetrical ears (Norberg 1977; Volman and Konishi 1990) and owls with both of these features have excellent sound localization ability. It also assumes that the size of the comb is proportional to the effect it has on airflow.

Body size was not a significant predictor of comb morphology in our multiple regression (*P*-value = 0.26 when λ=1; Table 1.3; Fig. 1.6). It is unclear how body size should scale with comb morphology; unlike most body proportions, which will clearly tend to be larger in larger animals, whether and how the comb should have scaling allometry with body size was not clear *a priori*. Since turbulence impinging on the leading edge might produce sound in a way that does not scale with body size at all (the turbulence is a property of the air the owl flies through, not the owl), at one extreme, it is conceivable that the comb morphology could have no scaling relationship with body size.

We were surprised to find a leading-edge comb in fishing owls (*Ketupa spp, Scotopelia spp*; yellow dots in Fig. 1.4). Graham (1934) claimed that fishing owls do not have a comb or other quieting features. In contrast, we found Fishing owls to cluster in the middle of PC1 for comb size (Fig. 1.4; Table 1.S2). Fishing owls are not predicted to have silencing features under either the stealth and self-masking hypothesis because sound does not travel well between air and water. One explanation for this could be that Fishing owls listen for fish as they splash at the surface of water and fishing owls use those acoustic cues to locate prey. Instead, we found Pygmy owls (*Glaudidium spp*) to have functionally no comb (blue dots in Fig. 1.4). Pygmy owls are mostly diurnal owls which live in forests across the world so they are also predicted to not have quieting features under either the stealth or self-masking hypotheses (Billerman et al. 2020). It is unclear why quieting features are present in fishing owls but absent in pygmy owls, but nocturnality may play a key role in the persistence of quieting features in fishing owls.

There were aspects of comb morphology that we noticed but did not quantify. For example, there was variation in the distribution of comb across the wing. The comb was only present on P10 in Little owls (*Athene spp.*), while it was present on P10, 9, and sometimes even the tips of P8, and P7 in some Horned and Eagle Owls (*Bubo spp.)* and some Wood owls (*Strix spp.*). The leading-edge comb was also present on the alula (thumb feather) of 56 species. The leading-edge comb curved upward (i.e. potentially affecting airflow predominantly on the dorsal surface of the wing) in most species, but the comb stuck straight out from the front of the wing in owls with short, stubby combs like Boobook owls (*Ninox spp.*). In some species, there was variation in curvature such as Barred owl (*Strix varia*), in which the leading-edge comb curves upward on P10 but curves downward on the alula. In order to fully understand the quieting mechanism of the leading-edge comb, the fluid dynamics of the diversity of comb morphologies described here could be investigated.

Concluding Remarks

Here, we have quantified the variation in body size, facial disc morphology, comb morphology, and ecology across a phylogenetically-diverse selection of owls. We have found support for both the stealth and self-masking hypotheses. Quiet flight likely evolved as part of a suite of characteristics which make some owls excellent nocturnal hunters. This evidence is contrary to the assumptions many authors make about quiet flight evolving for stealth in owls. This assumption stems from a commonly held belief that predators and prey coevolve simply because they exist together. Since predators and prey coexist, it is easy to assume that they must evolve together, but this equilibrium can be reached without coevolution (Slobodkin, 1974). For predatory species that are not locked in a tight relationship with one prey species, it is necessary to consider all of the factors that influence a predatory relationship.

Figures:

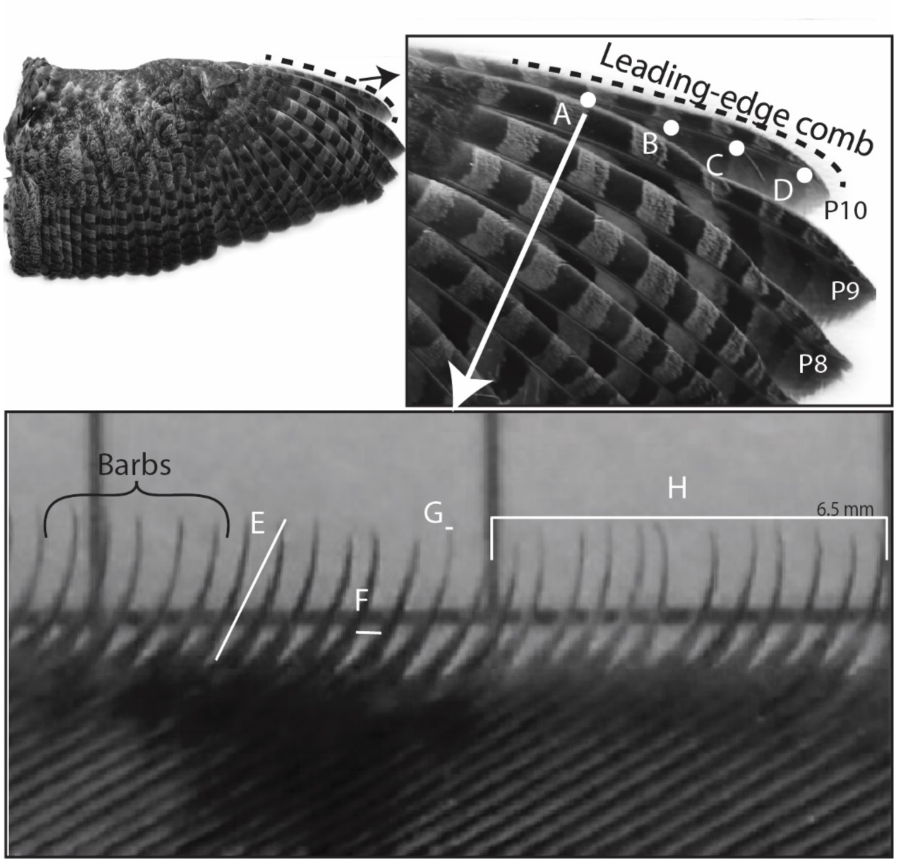

Figure 1.1. Spread wing of a Great Horned Owl (Bubo virginianus) with measurements taken of the leading-edge comb. The dashed line shows the location the leading-edge comb on the outermost flight feather (P10). Length of individual barbs that make up the comb was measured at A) 25%, (B) 50%, C) 75%, and D) 100% the total comb length. E) Measurement of comb length at 25%. Also measured at 25% total comb length was the F) the distance between barbs and G) the width a barb at the tip H) barb density (number of barbs per cm).

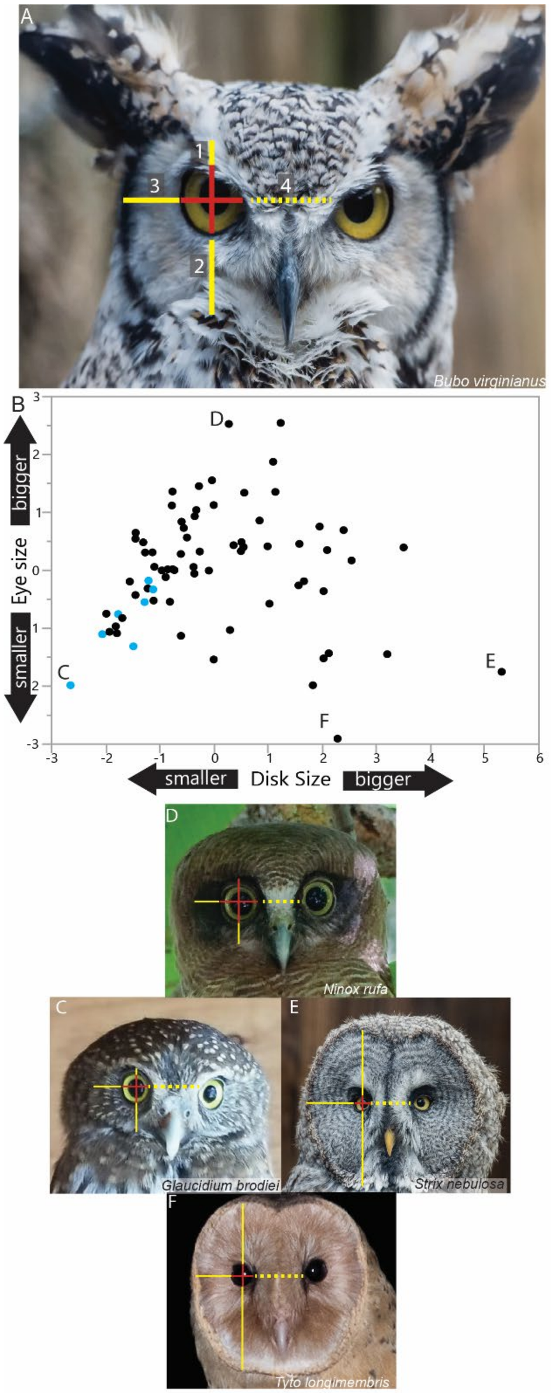
A
1
2
3
4
Bubo virginianus
B
3
2
1
0
1
2
-3
bigger
Eye size
smaller
-3
-2
-1
0
1
2
3
4
5
6
smaller
Disk Size
bigger
D
C
E
F
Ninox rufa
Glaucidium brodiei
Strix nebulosa
Tyto longimembris

Figure 1.2. Principal components analysis of the facial disc of 66 owl species. A) Facial disc measurements taken: 1) from the top of the eye to the top of the disc, 2) from the bottom of the eye to the bottom of the disc, 3) from the left of the eye to the left of the disc. All measurements were computed relative to the interocular distance (4). B) Principal Components Analysis of facial disc measurements. Disc PC 1 represents 59.4% of the variation in the dataset and Disc PC 2 represents 26.9% of the variation. Loadings for the variables used in this PCA are presented in Table 1.2. Light blue circles indicate diurnal owls and black circles indicate nocturnal owls. C-F) owl facial discs representing the diversity of morphology. Photos used with permission: Strix nebulosa and Bubo virginianus photos by Ben Williams. Ninox rufa and Tyto longimembris photos by Richard Jackson. Glaucidium brodiei photo by reddit user NorthernJoey.

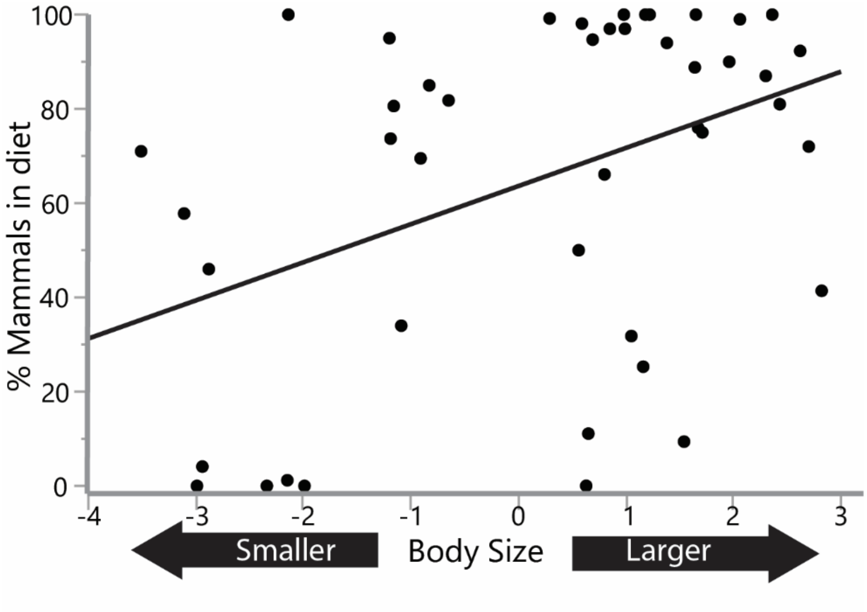

Figure 1.3. Results of a preliminary generalized linear regression (glm) analysis of owl body size by percent mammals in the diet (by count or mass, when available) of 44 owl species. Body size is a significant predictor of the percent mammals in the diet (gls; DF=43; f-ratio=8.76; P-value=0.005). Note that fish eating owls (N=3) are excluded in this analysis because they are large and eat no mammals. Additional species were removed from this analysis because they were lacking specific data on diet**.**

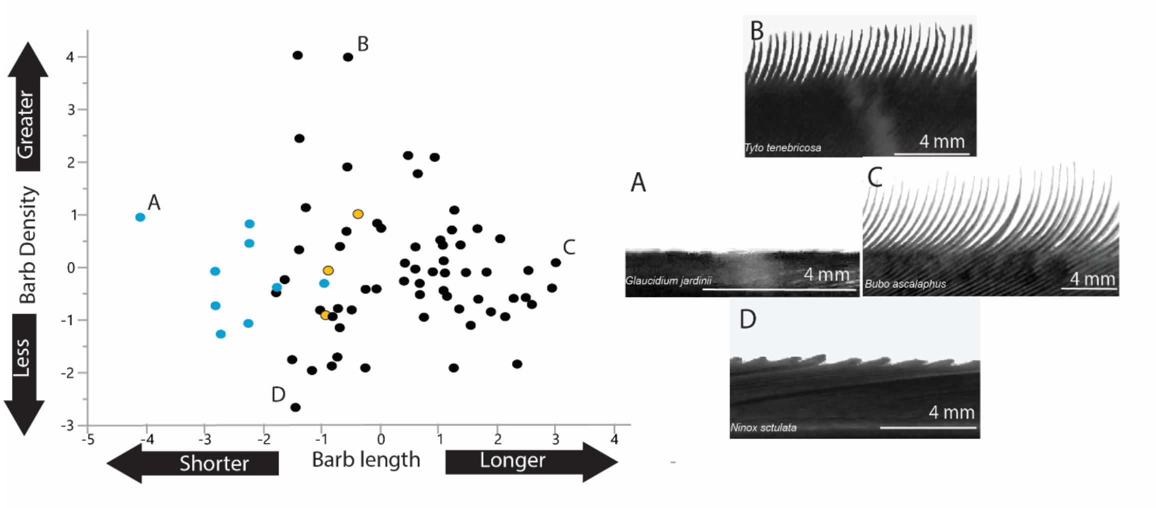

Figure 1.4. Principal Components Analysis of leading-edge comb variables for 147 species of owls. Comb PC1 represented 50.6% of the variation in the dataset. Comb PC2 represented 35.2% of the variation in the dataset. As Comb PC1 increases, barbs become longer. As Comb PC2 increases, Barb density increases and the distance between barbs decreases. Loadings for the variables used in this PCA are presented in Table 1.2. Blue dots represent species with functionally no comb (Glaucidium spp) and yellow dots represent Fishing Owls.

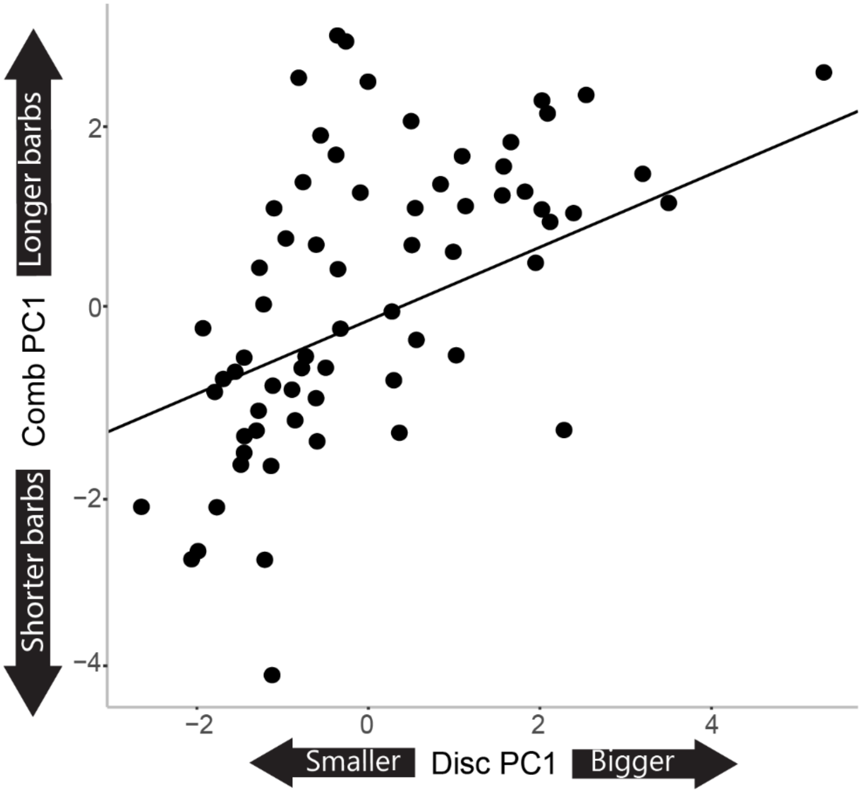

Figure 1.5. Disc PC 1 against Comb PC1 of 66 species of owl. Points are raw data, regression line calculated from pgls (Model 2 in Table 1.4, λ = 0.87). There was a significant effect of Disc PC1 on Comb PC1 (Table 1.4; DF=66; t-value=3.78; P-value = 0.0004).

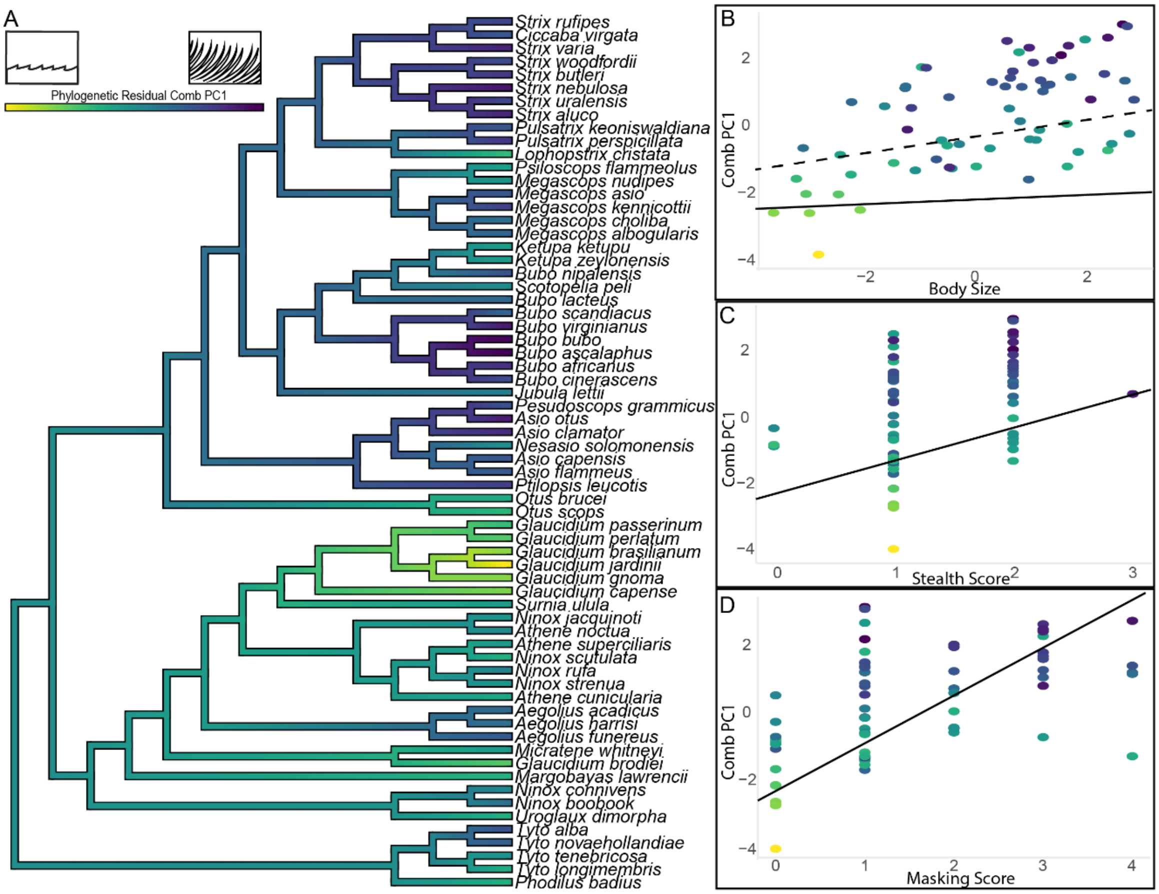

Figure 1.6. Comb morphology on a phylogeny of 66 owl species. A) Phylogeny backbone from Slater et al. (2020). Branch colors indicates reconstructed values of Comb PC 1. Values at internal nodes were reconstructed using fastAnc in Phytools (Revell 2012), which yields the maximum likelihood estimate of ancestral states under a model of Brownian Motion character evolution . Values along branches interpolated with contMap (Revell, 2013). Phylogenetic regressions of Comb PC1 against B) Body size, C) Stealth score, and D) Masking score. Solid regression lines represent the pgls value computed in Model 1, Brownian Motion (Pagel's λ=1; Table 1.4). Plotted values for B, C, and D are raw species numbers, colored according to the phylogenetic residual values of Comb PC1. Dashed line in B represents the results of a separate pgls with Body size as the independent variable and Comb PC1 as the dependent variable (pgls; λ=1; DF=66; test-statistic = 1.84; P-value = 0.07).

Tables:

Table 1.1. Ecology of owls in our phylogenetic analysis (N=66 species) and stealth and self-masking points awarded for each category.

Category	N Species	Stealth Points	Masking Points
Diet		0-2	0-2
Mammals	19	2	2
Arthropods	10	1	1
Flying insects	3	2	0
Fish	3	0	0
Generalist	31	1	1
Habitat		0-1	0
Woodland	15	0	0
Forest	34	0	0
Grassland	6	0	0
Desert	4	1	0
Tundra	1	1	0
generalist	6	0	0
Hunting Strategy		0	0-1
Sit-and-wait	43	0	0
through snow	7	0	1
coursing	6	0	1
unknown	11	0	0
Active Period		0	0
Nocturnal	58	0	0
Diurnal	7	0	0 points total[1]
Crepuscular	1	0	0 points total[1]
Sound localization ability			
Top 25% of facial disc PC1	17	0	1

[1] Diurnal and crepuscular owls received zero points for self-masking, even if they would have received points in another category because we assume these owls always have enough light to hunt visually

Table 1.2. Principal Component loadings for the variables used in each of the three Principal Components Analyses

PCA	Response variable	PC1 Loading	PC2 Loading
Body Size:		91.40%	7.52%
	Tarsus length	0.93	0.36
	Folded wing length	0.99	-0.05
	Tail length	0.95	-0.30
Facial Disc:		59.40%	26.90%
	Eye width	0.18	0.96
	Side of disc	0.84	0.22
	Top of disc	0.88	-0.03
	Bottom of disc	0.94	-0.08
Leading-edge comb:		50.60%	35.20%
	Comb length 25%	0.94	0.15
	Comb length 75%	0.91	0.27
	Distance between barbs	0.57	-0.69
	Barb density	0.01	0.91

Table 1.3. Average, maximum, and minimum values for traits used in Body Size PCA and Comb PCA

Trait	Average	Maximum	Species	Minimum	Species
Tarsus length (cm)	35.2 ±14.8	76.3	*Tyto longimembris*	10.9	*Glaucidium gnoma*
Ornithological chord length (cm)	239.8 ± 96.7	520.6	*Bubo blakistoni*	90.3	*Glaucidium minutissimum*
Tail Length (cm)	126.1 ±54.3	286.5	*Strix nebulosa*	49.1	*Micrathene whitneyi*
Comb Length 25% (mm)	1.45 ± 1.3	5.9	*Strix nebulosa*	0.09	*Glaucidium parkeri*
Comb Length 75% (mm)	0.70 ± 0.62	2.47	*Asio otus*	0.06	*Glaucidium costricanum*
Distance between barbs (mm)	0.28 ± 0.13	0.46	*Bubo nipalensis*	0.13	*Glaucidium jardinii*
Barb Density (barbs/cm)	14 ± 3	25	*Phodilus badius*	10	*Ninox ochracea*

Table 1.4. Phylogenetic correlations of comb morphology.

Dependent Variables			DF	value	t-value	*P*-value	Correlation Structure	Log likelihood
Facial disc	model 1	intercept	66	-0.43	-0.52	0.6	Brownian (λ = 1.0)	-96.18
				0.28	2.66	**0.01**		
	model 2	intercept	66	-0.39	-0.63	0.53	Pagel's λ = 0.87	-94.59
				0.39	3.78	**0.0004**		
Body size, stealth, and, masking	model 1	intercept	66	-0.89	-1.10	0.28	Brownian (λ = 1.0)	-93.59
		body size		0.17	1.13	0.26		
		masking		0.30	2.37	**0.02**		
		stealth		0.88	2.66	**0.01**		
		masking*stealth		-0.54	-3.16	**0.003**		
	model 2	intercept	66	-0.96	-1.54	0.13	Pagel's λ = 0.87	-92.13
		body size		0.21	1.59	0.12		
		masking		0.37	2.85	**0.006**		
		stealth		0.95	2.72	**0.008**		
		masking*stealth		-0.55	-3.02	**0.004**		

[1] Significant *P*-values are bold. Scatterplots of the multiple pgls regression are presented in Fig. 1.6.

Chapter 2: Evidence that the dorsal velvet of Barn Owl wing feathers decreases rubbing sounds during flapping flight

Abstract:

Owls have specialized feather features hypothesized to reduce sound produced during flight. One of these features is the velvet, a structure composed of elongated filaments termed pennulae that project up dorsally from the upper surface of wing and tail feathers. There are two hypotheses of how the velvet functions to reduce sound. According to the aerodynamic noise hypothesis, the velvet reduces sound produced by aerodynamic processes, such as turbulence development on the surface of the wing. Alternatively, under the structural noise hypothesis, the velvet reduces frictional noise produced when two feathers rub together. The aerodynamic noise hypothesis predicts impairing the velvet will increase aerodynamic flight sounds predominantly at low frequency, since turbulence formation predominantly generates low frequency sound; and that changes in sound levels will occur predominantly during the downstroke, when aerodynamic forces are greatest. Conversely, the frictional noise hypothesis predicts impairing the velvet will cause a broadband (i.e., across all frequencies) increase in flight sounds, since frictional sounds are broadband; and that changes in sound levels will occur during the upstroke, when the wing feathers rub against each other the most. Here, we tested these hypotheses by impairing with hairspray the velvet on inner wing feathers (P1-S4) of 13 live Barn Owls (*Tyto alba*) and measuring the sound produced between 0.1-16 kHz during flapping flight. Relative to control flights, impairing the velvet increased sound produced across the entire frequency range (i.e. the effect was broadband) and the upstroke increased more than the downstroke,

such that the upstroke of manipulated birds was louder than the downstroke, supporting the frictional noise hypothesis. Our results suggest that a substantial amount of bird flight sound is produced by feathers rubbing against feathers during flapping flight.

Introduction:

Owls are quiet fliers, meaning the sounds they produce during flight are concentrated at low frequencies (<1 kHz), below the best hearing range of owls and many of their prey species (Konishi 1973a). Barn owls (*Tyto alba*) can localize prey noises in complete darkness and strike at the sound of prey when no visual cues are available (Payne 1971; Konishi 1973a). A hunting Barn Owl may change course after takeoff in response to a change in the location of an acoustic cue, which indicates that the sound of their own flight could potentially interfere with their ability to detect prey midflight (Payne 1971; Konishi 1973a; Hausmann et al. 2008). Reducing flight noise (incidental sounds produced during locomotion) is hypothesized to be selected for, either for improved prey detection and/or for stealth (Clark et al. 2020a).

Barn Owls are best at locating pure tones in the 3-9 kHz frequency bandwidth (Payne 1971; Knudsen et al. 1979). Therefore, if quiet flight evolved to improve prey detection, we expect quieting features have been selected to reduce sound in the 3-9 kHz frequency bandwidth. If quiet flight evolved for stealth (i.e. to allow the owl to better sneak up on prey undetected), silencing features could have evolved to reduce a wide range of frequencies, since many rodents and insects hear well into ultrasonic frequencies (Ralls 1967; Fullard and Yack 1993), although some desert rodents also hear well at low frequencies (< 1 kHz; Webster 1962). In response to one or both of these selective pressures (self-masking or stealth), owls have evolved quiet flight to aid in nocturnal hunting (Clark et al. 2020a).

Owls have evolved multiple wing and feather features to reduce flight noise (Graham 1934). These features include the leading-edge comb, vane fringes, and the subject of this study, the velvet. The velvet is made up of elongated filaments (pennulae) that project up from the dorsal surface of the feathers (Bachmann et al. 2007). In many owls, the pennulae are elongated (up to 1.2 mm) and collectively make feathers soft to the touch (Bachmann et al. 2007). The velvet is hypothesized to function to reduce either aerodynamic or frictional noise produced during flight (Bachmann et al. 2007; Jaworski and Peake 2020).

The elongated pennulae that make up the velvet are hypothesized to be a modified form of fastening barbules (Lucas and Stettenheim 1972; Matloff et al. 2020). Fastening barbules are distal barbules with lobate cilia that project up dorsally, located on the inner vane of flight feathers, in regions of feather overlap (Proctor and Lynch 1993; Wissa et al. 2015; Matloff et al. 2020). Fastening barbules reduce separation of feathers during flight by preventing the vane of neighboring flight feathers from slipping under applied aerodynamic loads (Wissa et al. 2015; Matloff et al. 2020). The absence of fastening barbules in owl feathers may indicate an evolutionary trade-off between feather fastening and reducing flight sounds (Matloff et al. 2020).

Flapping wings are hypothesized to make sound in multiple ways. One source of flight sound is aerodynamic noise, such as sound caused by the formation and shedding of turbulence over the wing (Blake 2017; Rao et al. 2017; Jaworski and Peake 2020). Aerodynamic noise produced by turbulence development and dissipation is highest amplitude at low frequencies, and declines exponentially with increasing frequency. Specifically, the power spectral density of frequency has a characteristic negative slope on a log/log scale (Crighton 1991; Rao et al. 2017). Models of the velvet suggest it could decrease aerodynamic sound production by 2-8 dB in the range of 1-20 kHz, and could modify the slope, but the slope is still expected to be negative (Jaworski and Peake 2013).

A second type of aerodynamic sound is the product of time variation of aerodynamic forces that keep the bird aloft (i.e., lift and drag), which we term Gutin sound (Gutin 1948; Blake 2017). Gutin sound is concentrated at <0.1 kHz, since it has a fundamental frequency of the frequency owls flap their wings (~4 Hz) plus the first few integer harmonics of the wingbeat frequency. The velvet is not hypothesized to affect the Gutin sound.

A different hypothetical source of flight noise in birds is frictional noise (Clark et al. 2020a). Frictional noise is caused by feathers rubbing against neighboring feathers. Feathers rub together when the geometry of the wing changes, as occurs when the wing is opened and closed during takeoff and landing, and during flapping flight (wing morphing of a Barn Owl can be seen in Fig. 20 Wolf and Konrath 2015). We specifically hypothesize that feathers rubbing against feathers will produce broadband sound, akin to the sound produced when Velcro is unfastened or a piece of sandpaper is rubbed against itself (Akay 2002). The sounds of sandpaper or Velcro are atonal and broadband because they are the product of many small asperities interacting semi-autonomously, similar to the milli- and micro-structure of feathers. Broadband sounds of this type need not decline at higher frequencies (Bachmann et al. 2012; Clark et al. 2020; Matloff et al. 2020). Empirical measurements indicate bird wing noises are broadband and can extend into ultrasonic frequencies (Thorpe and Griffin 1962; Fournier et al. 2013).

Here, we conducted experiments to test the function of the dorsal velvet. Under the aerodynamic noise hypothesis, we predicted impairing the velvet will increase predominately low-frequency sound produced during the downstroke, when most of the aerodynamic force keeping the bird aloft is produced (Lentink et al. 2015; Chin and Lentink 2016). We also predicted a greater increase in sound production at low frequencies than high frequencies. Conversely, the frictional noise hypothesis posits the velvet reduces sounds produced by friction between a feather and a neighboring wing feather (reviewed in Clark et al. 2020). Under the frictional noise hypothesis, we predicted impairing the velvet would increase sound levels across a broad range of frequencies (broadband sounds) produced during flapping flight, and may have greatest effects at high frequencies. We also predicted the resulting power spectrum would have a flat slope above 3 kHz. During flapping flight, the feathers are likely to rub the most when the wing deforms during the upstroke. Thus, we predicted impairing the velvet will cause an increase in sound production during the upstroke, rather than the downstroke.

To test these hypotheses, we impaired the velvet of five inner flight feathers (P1-S4) on live Barn Owl wings, by applying hairspray to their dorsal surface. We recorded the sounds Barn Owls make in flight under three experimental conditions: before manipulation, during manipulation, and manipulation removed.

Methods:

Permits

This project was conducted under permits from the U.S. Fish and Wildlife Service (USFWS #. MB41649d-0) and the California Department of Fish and Wildlife (CADFW # 13665) between July and September 2019. All experimental protocols were approved by University of California, Riverside Institutional Animal Care and Use Committee (IACUC) # 20170009. The birds used in this experiment were 13 untrained Barn Owls undergoing rehabilitation to be re-released into the wild. Only adult owls without signs of flight feather molt that could fly across the room (with normal wing kinematics) were used in this experiment.

Experimentation took place in a hard-walled aviary measuring 9.14 m x 4.57 m x 4.57 m at the Orange County Bird of Prey Center (http://www.ocbpc.org/). The space was open to the sky and had no acoustic treatment. We hung sheets to reduce the dimensions of the room to a corridor of approximately 9.14 m x 2.13 m x 2.44 m (Fig. 2.1). The smaller dimensions ensured the birds flew over the microphone at a consistent height with each flight. We set up two microphones at the middle of the room, one below the bird’s flight path and another to right of the flight path (Fig. 2.1).

Experimental regime

A single flight consisted of releasing an owl from the hand approximately 1.8 m behind the microphones. Each owl flew across the room, passing roughly 0.5 m above the bottom microphone), and landed on the opposite wall. Each bird was flown a minimum of six times per experimental treatment. If the bird's wing collided with either microphone during a flight, the bird snapped its bill while flying, or there was abnormally high background noise in a flight, that flight was discarded. As a result, some owls were flown up to 10 times for a given treatment to acquire 6 usable flights. All owls flapped their wings while passing the microphones (none glided).

Manipulations

We applied non-toxic hairspray to the dorsal surface of five flight feathers in the middle of the left and right wing (P1-S4), because these feathers are likely to experience substantial rubbing during flapping flight. In preliminary work, we attempted to manipulate five outer primary feathers (P10-6), as a direct test of the aerodynamic noise hypothesis, but this treatment altered the kinematics of the bird, meaning we could not disentangle acoustic effects that were the product of kinematic changes, from purely acoustic effects. Therefore, we abandoned efforts to manipulate outer wing-feathers. Manipulation of interior flight feathers (P1-S4) had no obvious impact the owls' flight kinematics (and we statistically tested for subtle effects, see below).

We performed two different applications of hairspray: spray and painted. For the spray application (N=4 birds, 86 flights), five pumps (approximately 0.123 g) of Nature's Brands sugar-based organic hair spray (www.HerbalChoiceMari.com) was sprayed onto each of the feathers. The hairspray bottle was held approximately 13 cm from the surface of the feather while spraying. To protect adjacent feathers from incidental treatment, we placed a sheet of paper between the feather being treated and the adjacent feathers. We calibrated the amount of hairspray applied to a single feather by depressing the spray top of the hairspray five times onto a piece of paper and weighing it. The total amount of hairspray applied to the flight feathers was approximately 1.23g. In the painted application (N=9 birds), Andalou Naturals Polyvinylpyrrolidone (PVP)-based hairspray (www.andalou.com) was applied onto the dorsal surface of P1-S4 with a small paintbrush to ensure hairspray was only applied to the intended feathers. We changed hairspray application protocol to (1) increase the amount of hairspray being applied directly to the target feather and (2) reduce the incidental application of hairspray to other parts of the wing. To estimate the amount of hairspray used in the painted application, we applied hairspray to a feather with a small paintbrush and weighed it before and after manipulation. Approximately 6.31g of hairspray in total was painted onto the ten flight feathers. To remove the hairspray, we applied rubbing alcohol to a towel and wiped the hairspray from feathers.

We flew each bird under three experimental conditions: control (pre-treatment), treated with hairspray, and treatment removed before testing the next bird. In the painted application, we changed our protocol to increase the sample size of birds, such that we first measured 6 or more control flights on all of the experimental owls, then applied the hairspray treatment and flew each bird under the manipulated treatment, and finally removed the hairspray with rubbing alcohol and flew each bird under the treatment removed. We performed our experiments this way to ensure the owl feathers had a chance to dry after hairspray was applied and removed. As there was not an available aviary where the bird could sit and freely preen after the second treatment, birds were housed in cardboard carriers between experimental treatments and were therefore not able to preen their feathers.

To ascertain the effect of the manipulation, as well as its removal, we imaged feathers using Environmental Scanning Electron Microscopy (eSEM). We imaged one untreated control feather (unknown secondary), two feathers (S2) pulled from a bird in the spray application after hair spraying, and two unknown secondary feathers that had hairspray painted onto them in the lab to mimic the treatment in the painted application. We then imaged feathers with hairspray-removed by using rubbing alcohol and a paper towel to remove hairspray from one hairspray sprayed feather and one hairspray painted feather before imaging. eSEM images were taken with a Hitachi TM-1000 tabletop eSEM at an accelerating voltage of 1.5kV, and analyzed at the Institute for Integrative Genome Biology (IIGB) facility at UC Riverside.

Video recording

We filmed the middle of the flight path with a camera (Canon XA10 Professional; 30 frames/second, 1920 x 1080) to the side and in line with the microphone on the flight path (Fig. 2.1). In view of the camera, we held a meterstick vertically and horizontally over the microphone in the middle of the flight path to calibrate the image plane.

The purpose of recording video was twofold. First, syncing audio and video recordings allowed us to determine which parts of the flight path was recorded, allowing us to account for distance between the bird and the microphone. We synced audio and video with a short, impulsive sound (snapping fingers) produced in the frame of the camera and adjacent to the microphone before each flight. Second, capturing video allowed us to collect kinematic data such as flight speed and timing of the upstroke and downstroke (Fig. 2.2A). Since the bird did not always fly in the image plane coincident with the spatial calibration, distance in the 3rd dimension, between the bird and camera, varied from trial to trial. To control for this variable distances between camera and bird, we estimated relative flight speed by first measuring the length from the tip of the bird's beak to the end of its tail in pixels using ImageJ2 (Rueden et al. 2017) and then calculated the number of bird-lengths traveled per second. This value was converted to m s^{-1} assuming an owl length of 0.3 m.

The side microphone was intended to capture sounds in line with the owl's ear and without much Gutin sound. However, due to a faulty audio cable in about half of the flights, only quantitative data from the microphone under the bird's flight path will be presented. Patterns of sound production were consistent between the two microphones, apart from the greater need to filter out the Gutin sound in the recordings from below the bird (described next).

Sound Analysis

Sounds were recorded with two Brüel and Kjær 4190 free-field microphones with fuzzy windscreens to prevent pseudosound. The free-field response of these microphones is flat between 3.15 - 20 kHz ± 2dB, with a sensitivity of 50 mV/Pa. We used a Sound Devices 702 recorder with a minimum frequency of 10 Hz and a sampling frequency of 48 kHz, with the gain set to 24.3 dB.

We measured sounds in Raven Pro Version 1.5 (Cornell Lab of Ornithology 2014). We analyzed all of our recordings with a 1500 sample Fast Fourier Transform (FFT) window size. In the waveform, we identified the peak amplitude of the Gutin sound corresponding to upstroke and downstroke of the wingbeat closest to the microphone, and collected data from a 0.02 second window centered around each peak (Fig. 2.2). Then, since low frequency Gutin (Load) sound produced by lift and drag (Blake 2017) dominated the recordings, we applied the software's high pass filter above 100 Hz. The filter was applied four times to eliminate roll-off effects (spectral leakage) and fully eliminate peaks in the waveform that were caused by the wingbeats (Fig. 2.2) [Applying the same filter multiple times was necessary as RAVEN Pro v. 1.5 neither documents their filter parameters nor allows users to edit them (Raven Software Support, pers. comm. Sept. 27 2019)]. We then calculated RAVEN's Filtered Root Mean Squared Amplitude (fRMS Amplitude) of the full spectrum (0.1–16 kHz) as well as three portions of this spectrum (1-3 kHz, 3-7 kHz, 7-16 kHz; Fig. 2.2C). "Filtered" means that we calculated the relative RMS amplitude of each of these *portions* of the spectrum, rather than the entire spectrum (Fig. 2.2C). Similarly, we measured background sound before each flight (when the owl was not flying), following the same procedures as above. The unfiltered background sound of our research space was 52 ± 3.8 dB SPL (ref 20 μPa; 0.01-16 kHz; N=37 flights). After filtering out sound below 0.1 kHz, the background sound was 34.6 ± 3.1 dB SPL (0.1-16 kHz N=468 flights). To subtract background sound from the spectra for individual wing flaps, we converted amplitude in dB to pascals, then subtracted fRMS amplitude of background sound from the respective fRMS amplitude of flight sound. Negative values, in which the background sound was louder than the recorded flight sound, were set to 0 Pa.

We analyzed Gutin sounds (0.01-0.1 kHz) on unfiltered recordings (N = 464 flights). Sound production was analyzed using the same methods described above except the high pass filter was not applied.

The microphone was calibrated relative to a sound source (B&K sound level calibrator 4231; Clark et al. 2013) that produced a 1 kHz tone at 94 and 114 dB, ref 20 µPa, with the recorder's gain set to zero dB. We converted our values to SPL ref 20 µPa after accounting for the difference in gain between the calibration recording versus our experimental setup (Gain of 0 vs 24.3 dB).

Data Analyses

We analyzed differences in sound production across treatment groups for a given frequency range (1-3 kHz, 3-7 kHz, 7-16 kHz and 0.1-16kHz) with a repeated measures ANCOVA using JMP pro version 14 (*JMP*® 2019). A separate ANCOVA was run for each frequency band analyzed. Treatment application (spray, painted) was nested in treatment group (control, hairspray, hairspray-removed) as our independent variable to test for differences in sound production within treatment applications. The dependent variable of our model was Partial Sound Pressure Level (dB pSPL), bird ID was a random effect, and flight speed, distance from the owl to the microphone at the up/down stroke of interest (Fig. 2.2A), flight number (within a treatment group), and stroke (up or down) were covariates. We did not scale pSPL for the effect of distance; rather, we accounted for distance by including distance it as a covariate in the statistics. To test our hypotheses that the effects of experimental treatment would be stroke-specific, we included a stroke × treatment interaction effect.

Although we did not detect any obvious changes in kinematics between the experimental treatments, subtle changes in flight kinematics that we did not notice, if present, could confound our interpretation of the above statistical model. Therefore, in preliminary analyses we also included interaction terms with flight number within a treatment group (i.e., a number from 1-6) and kinematic variables (flight speed, distance from microphone) to test for changes in distance or speed across subsequent trials within a given treatment (as might occur if the animals flew differently from increasing experience with the protocol) Also included was flight speed × treatment group interaction to test if application of hairspray caused the flight speed to change; a treatment x total distance interaction to test if applying the hairspray (or increased experience with the protocol) changed the distance at which the birds flew by the microphone, and a flight number × flight speed interaction to test if flight speed changed over the course of subsequent flights within a treatment. None of these terms were statistically significant, suggesting that any effect of learning, or any effect treatment on flight kinematics, was too small for us to detect.

We calculated effect sizes of our control and treatment groups using Cohen's d, which estimates effect sizes of repeated measures ANCOVA using means, standard deviations, and correlation estimates between two variables (Lenhard and Lenhard 2016).

We then performed post-hoc Tukey HSD tests on the stroke (up vs. down) × treatment interaction to test for differences in sound production during the upstroke and downstroke of birds in different treatment groups. Means are presented ± S.D.

To assess whether there were any changes in the Gutin sound as a function of treatment, sound production from 0.01-0.1 kHz was analyzed using a separate Repeated Measures ANCOVA with SPL of Gutin sound (0.01-0.1 kHz) as our dependent variable, treatment group (control, hairspray, hairspray-removed) as our independent variable. Also included was Bird ID as a random effect and stroke (up, down), flight speed, and total distance from microphone as covariates.

Results:

The owls flew at an average speed of 2.6 ± 0.3 m s^{-1} and passed approximately 0.5 m above the bottom microphone (N=14 owls, 392 flights). All owls flapped their wings when they passed the two microphones; we had no opportunities to study gliding flight.

Gutin sound production (0.01-0.1 kHz) values and the results of the repeated measures ANCOVA of Gutin sounds are presented in Table 2.1. There was a significant difference in Gutin flight sounds between treatment groups (N= 14 birds; 419 flights, f=4.15; DF=4; *P*=0.002; Table 2.1). Post-hoc Tukey HSD test reveals that in the hairspray painted application, the treatment owls' gutin sounds were 1.7 dB louder than the control and the effect size of this treatment is small (Cohen's d = 0.13) There was no other significant effect between groups.

After filtering out the Gutin sound, control (unmanipulated) owl flight sounds were 28.6 ± 12.9 pSPL for the upstroke and 29.67 ± 11.2 pSPL for the downstroke (0.1-16 kHz; distance=0.52 ±0.2 m; N=150 flights).

The intended outcome of the hairspray treatment was to stiffen the velvet. Scanning electron images of the spray treatment showed that the geometry of the pennulae was not changed by the sprayed application (Fig. 2.3C). In the painted application, the pennulae were physically laid down by the paintbrush when the hairspray was applied (Fig. 2.3C). The hairspray-removed treatment was intended to return the flight feathers to their control (unmanipulated) state. However, the SEM image of the hairspray-removed treatments revealed that removing hairspray with alcohol aligned the pennulae with the barbs instead of distributing them along the feather, as in the control (unmanipulated) images (Fig. 2.3C). This indicates that the hairspray-removed treatment was not a return to control status, as was intended.

Sound production (dB) for frequency bandwidths analyzed, for upstrokes and downstrokes, are presented in Table 2.2. Full results of the final statistical model are presented in Table 2.3. In the control flights, the flight sounds were highest amplitude at low frequencies (Table 2.2; 1 – 3 kHz) and the downstroke was louder than the upstroke for all of our control birds in the painted application (all $P<0.05$; Fig. 2.3D). For example, in the control group of the painted application, the downstroke was 6.6 dB (0.1 – 16 kHz; at a distance of 0.5 ± 0.2 m) louder than the upstroke (Table 2.2).

Un-filtered power spectra of background sound in the experimental space, as well as an upstroke and downstroke for one bird are presented in Fig. 2.3A (control) and Fig. 2.3B (hairspray painted). Figure 2.S1 shows the power spectra in Fig. 2.3A, B plotted on a log/log scale. The regression line of the control owl's downstroke had a slope of -21.2 dB/kHz and the slope of the upstroke is -17.7 dB/kHz. The slope of the treatment owl's downstroke was -20.7 dB/kHz and the slope of the upstroke was -13.8 dB/kHz (Fig. 2.S1). The log/log slope of sound production in the downstroke of the treatment group increased by 0.5 dB/kHz and the upstroke of treatment group increased by 3.9 dB/kHz, compared to the controls. This flattening of slope means applying hairspray to flight feathers caused a broadband increase in sound production (0-16 kHz). For example, at 3-7 kHz, sound production increased by 14.7 dB compared to the control (Table 2.3; Fig. 2.3D; N=9 birds, *P*>0.001, f=79.8, df=4, Cohen's d=0.78). The effect of treatment was statistically significant for all frequency bandwidths (Table 2.3; all *P*<0.05). In the treatment-removed group of the painted application, sound production was intermediate to the treatment and control groups of all frequency bandwidths (Table 2.2; Fig. 2.3D). In the spray application, sound production in the treatment-removed group was louder than both the control and treatment groups at all frequency bandwidths (Table 2.2; Fig. 2.3D). Effect sizes for treatment and control owls in the painted application are presented in Table 2.4.

There was a significant interaction between treatment and stroke on sound (e.g., 3-7 kHz; N=9 birds, treatment x stroke *P*<0.0001, f=12.9, df=4). At 3-7 and 7-16 kHz, the upstroke of the painted application treatment group was significantly louder than the downstroke, unlike the control flights (Table 2.3; Fig. 2.3D).

The relationship between flight speed and sound production is presented in Fig. 2.4. There was no significant effect of flight speed on sound production (Table 2.3). In general, birds that flew faster were louder (a 1 ms^{-1} increase in flight speed caused a 3.9 ± 1.9 dB increase for the entire 0.1-16 kHz range). However, in the spray application, there was a negative relationship between flight speed and sound production for the hairspray-removed birds (Fig. 2.S2).

Discussion:

These results support the frictional noise hypothesis. Under this hypothesis, we predicted that impairing the velvet would cause an increase in broadband sound production. We found that applying hairspray to the dorsal surface of flight feathers caused a broadband increase in flight sounds (dB pSPL; Fig. 2.3) but with greatest effects at highest frequencies. At 3-7 kHz, the flight sounds of the painted hairspray group were 14.7 dB louder than the flight sounds of control group. Similarly, in the 7-16 kHz range, painted hairspray birds were 17.1 dB louder than control birds. Additionally, application of hairspray increased the slope of the regression line in the log/log power spectrum by 3.9 for the upstroke (Fig. 2.S1). This increase in sound at all bandwidths and increase in the slope of sound production across all frequencies suggests that the velvet we experimentally impaired suppresses broadband sound consistent with the structural noise hypothesis, and not the aerodynamic noise hypothesis.

Another prediction of the structural noise hypothesis supported by our data is that sound produced during upstroke increased more than the downstroke. This is not consistent with the aerodynamic noise hypothesis, which predicted that impairing the flight feathers would cause sound production to increase during the downstroke because most of the aerodynamic force keeping the bird aloft (and the turbulence associated with it) is produced during the downstroke (Lentink et al. 2015). Before treatment, the downstroke was louder than the upstroke (Table 2.2). However, when hairspray was applied to the flight feathers, sound levels during the upstroke increased such that now the upstroke was louder than the downstroke (Table 2.2; Fig. 2.3D). Further, the sound produced during the upstroke increased by as much as 22.7 dB (7-16 kHz) while the sound produced during the downstroke increased by 11.5 dB (7-16 kHz). This increase in sound production during the upstroke is consistent with an increase in frictional sounds when two feathers rub together. Further, the power spectrum of hairspray-painted birds resembles the power spectrum produced when two pigeon feathers are rubbed together (Matloff et al. 2020 their Fig. 4C).

The sound increase we found during flapping flight is consistent with the sound produced when two pigeon feathers are rubbed together. These results suggest a substantial amount of flight sound is frictional noise and that this sound is produced primarily during the upstroke, when wing deformation causes feathers to rub against one another.

Gutin sounds (<100 Hz) were affected by the treatment application (Table 2.1). However, due to a low effect size (Cohen's d = 0.13) and a greater effect of stroke, total distance, and flight speed on gutin sound production, we conclude that there was a minimal effect of treatment on gutin sound production. Since these sounds are the product of lift and drag production by the wing, this suggests that application and removal of the hairspray had minimal impact on the flight kinematics of the owls in this experiment.

Our prediction that sound production would return back to control levels after hairspray was removed was not supported. Instead, the sound production in the painted hairspray-removed groups was intermediate to the control and hairspray groups and in the spray application, the treatment-removed group was louder than the control and treatment groups at several frequency bandwidths (Table 2.2). Scanning Electron Microscope images of feathers that we subjected to hairspray application and removal revealed that the geometry of the feather microstructure did not return to the control condition after removal of the hairspray (Fig. 2.3C). This likely contributed to elevated sound production levels compared to the control group. In between treatments birds were not able to preen their feathers (i.e., further removing residual hairspray and returning the feather vane to normal) between experimental treatments. Had they preened, we expect the sound production would have returned back to control levels.

In the spray application, the upstroke of the treatment group was not significantly louder than the downstroke (Fig. 2.3D). Scanning electron images of the spray application group revealed that the geometry of the feather microstructure was not altered by the spray application, indicating the pennulae were likely stiffened in place from the hairspray (Fig. 2.3C). When the geometry of the feathers in the spray application was altered by the removal of the hairspray, it caused an increase in broadband sound production. For example, at 7-16 kHz, the upstroke of the hairspray-removed treatment was louder than both the control and hairspray group (Fig. 2.3D). It may be the geometry of the velvet moreso than the stiffness that functions to reduce frictional sounds. Further experimentation is needed to test this hypothesis.

Painting the hairspray onto the feathers allowed us to have more control over where hairspray was applied to the feathers, eliminating incidental application of hairspray to other feathers. In the painted application, the pennulae were physically adhered to the dorsal surface of the feather (Fig. 2.3C), which may have contributed to the increase in sound production during flapping flight.

While painting the dorsal surface of the feather, hairspray was applied inadvertently to the vane fringe of the same feather. The vane fringe is also hypothesized to reduce the sound of aerodynamic and/or frictional flight sound in owls (Clark et al. 2020a; Jaworski and Peake 2020). Stiffening the vane fringe may have contributed to the overall increase in sound production. Therefore, this experiment may not have been a manipulation of the velvet in isolation to other adjacent parts of the feather. For example, applying hairspray onto the dorsal surface of flight feathers may have stiffened the vane of the feather. The trailing vane of Barn Owl feathers is more flexible than the trailing vane of other bird feathers (Bachmann et al. 2007). It is possible that the flexibility of the vane allows for deformation, decreasing the sound produced when two owl feathers are rubbed together. Therefore, stiffening the vane could lead to an increase in frictional sound production.

Biological Implications

Barn Owls are auditory hunters, meaning they can locate prey using auditory cues alone (Payne 1971). They are best at locating sounds in the range of 3-9 kHz (Payne 1971; Knudsen et al. 1979), meaning that of the frequency bandwidths analyzed in this study (0.1-16 kHz, 1-3 kHz, 3-7 kHz, 7-16 kHz), the 3-7 kHz range is especially important to a hunting owl. Barn owls often flap their wings during hunting (Payne 1971; Bruce 1999; Usherwood et al. 2014). Therefore, flapping flight and the sounds produced during it are important to the success of an acoustically hunting owl.

Features associated with silencing frictional flight sounds may have evolved to aid in prey detection and/or stealth. In the above experiments, we have shown that manipulating the dorsal surface of a free-flying barn owl's wings increases the broadband sound produced during flapping flight, including the range of frequencies most important for sound localization in the Barn Owl(3-9 kHz; Payne 1971a; Konishi 1973b, 1973a).The velvet may have evolved to reduce self-noise, enabling owls to better detect prey. Additionally, broadband sound produced during flapping flight may alert potential prey to the presence of an owl. Therefore, suppressing flight sounds above the best hearing range of the owl may be important for stealth. Impairing the velvet with hairspray increased broadband sound production (7-16 kHz) within the hearing range of many potential prey species including birds (Dooling 1992), insects (Fullard and Yack 1993; Fournier et al. 2013), and small mammals (Ralls 1967).The observed patterns of increased sound production are consistent with both the prey detection and stealth hypotheses for the evolution of quiet flight.

The data presented here support the hypothesis that feathers make frictional sounds when they rub together and that the velvet functions to reduce frictional sounds during flapping flight in Barn Owls. The frictional noise hypothesis is further supported by the location and relative development of the velvet on flight feathers because the velvet is longer and more well-developed in regions of feather overlap (Bachmann et al. 2007). Further, the presence of the velvet has been found to reduce the sound produced when two overlapping feathers are separated (Matloff et al. 2020).

Our data do not directly address whether the velvet may also ameliorate aerodynamic sounds. Two more direct tests of the aerodynamic noise hypothesis would have been manipulating primary flight feathers; and to measure sound production during gliding flight. Primary flight feathers are more exposed to the airflow than interior wing feathers, and their outer regions don't rub during regular flapping. However, in preliminary tests, manipulating primary flight feathers (P10-6) altered the flight kinematics of a bird, which risked confounding our result (i.e. it would not be clear whether a measured difference was the result of a change in kinematics, or a change in the underlying acoustic mechanism). So, we decided to manipulate interior flight feathers where the effect of adding hairspray did not appear to impact the owls' flight kinematics in any discernable way.

Measuring sound produced during gliding flight would have been a more direct test of the aerodynamic noise hypothesis because feathers rub much less in gliding than during flapping flight, thus, according to the frictional noise hypothesis, the manipulation we conducted should have no effect on sound produced during gliding. However, every bird in our experiment flapped their wings as they passed the microphones. Future experimentation on live owls trained to glide past the microphone could better address the aerodynamic noise hypothesis.

Figures:

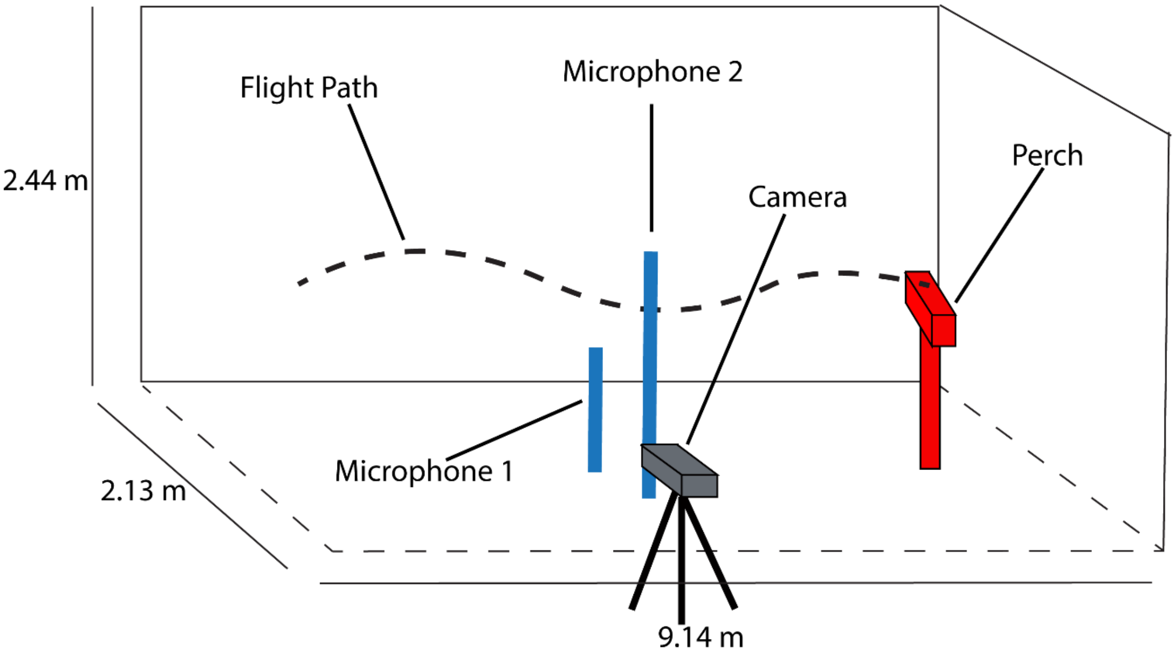

Figure 2.1. Experimental setup. Microphone 1 is positioned below the flight path of the bird and Microphone 2 is place above and to the side of the flight path of the bird.

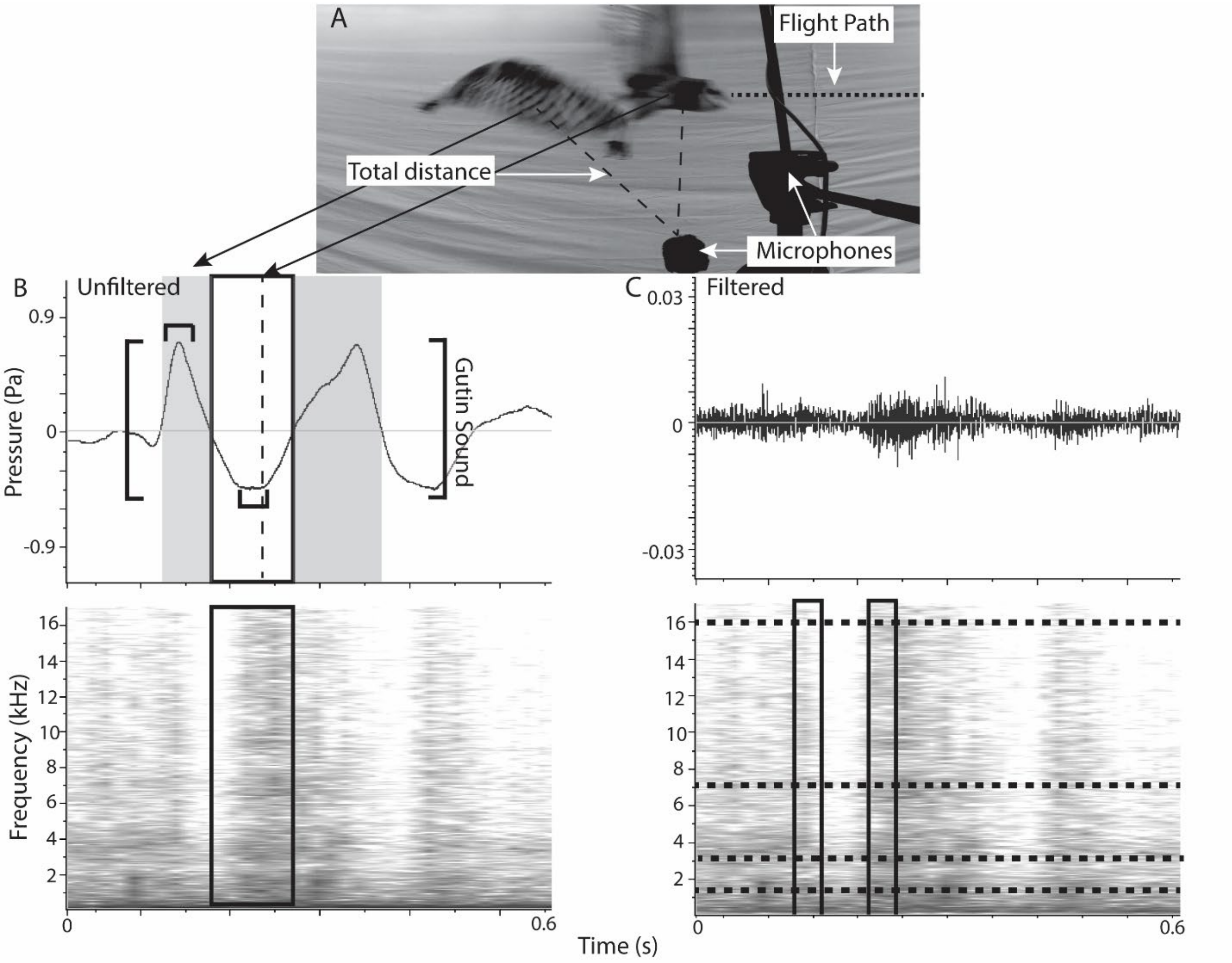

Figure 2.2. **Sound production during flapping flight.** A) Composite image of two frames from video camera showing one upstroke and downstroke. Dashed lines from microphone to owl images indicate two-dimensional distance from the bird to the microphone (total distance). Flight path and microphones are also labeled. B) Unfiltered Waveform in Pascals (Pa) and spectrogram of flight sound before filtering. Gutin (load) sound is labeled. Grey regions indicate downstroke and black box indicates upstroke visible on waveform. Dashed line indicates point during the upstroke where owl is closest to the microphone (0.69 m away from bottom microphone). Brackets indicate 0.02 s window centered around peak amplitude of upstroke and downstroke. Black box indicates upstroke. C) Waveform and spectrogram after applying high pass filter to eliminate Gutin sound. Boxes represent time windows analyzed and dashed lines represent frequency bandwidths analyzed. Note Y-axis scale in comparison to B).

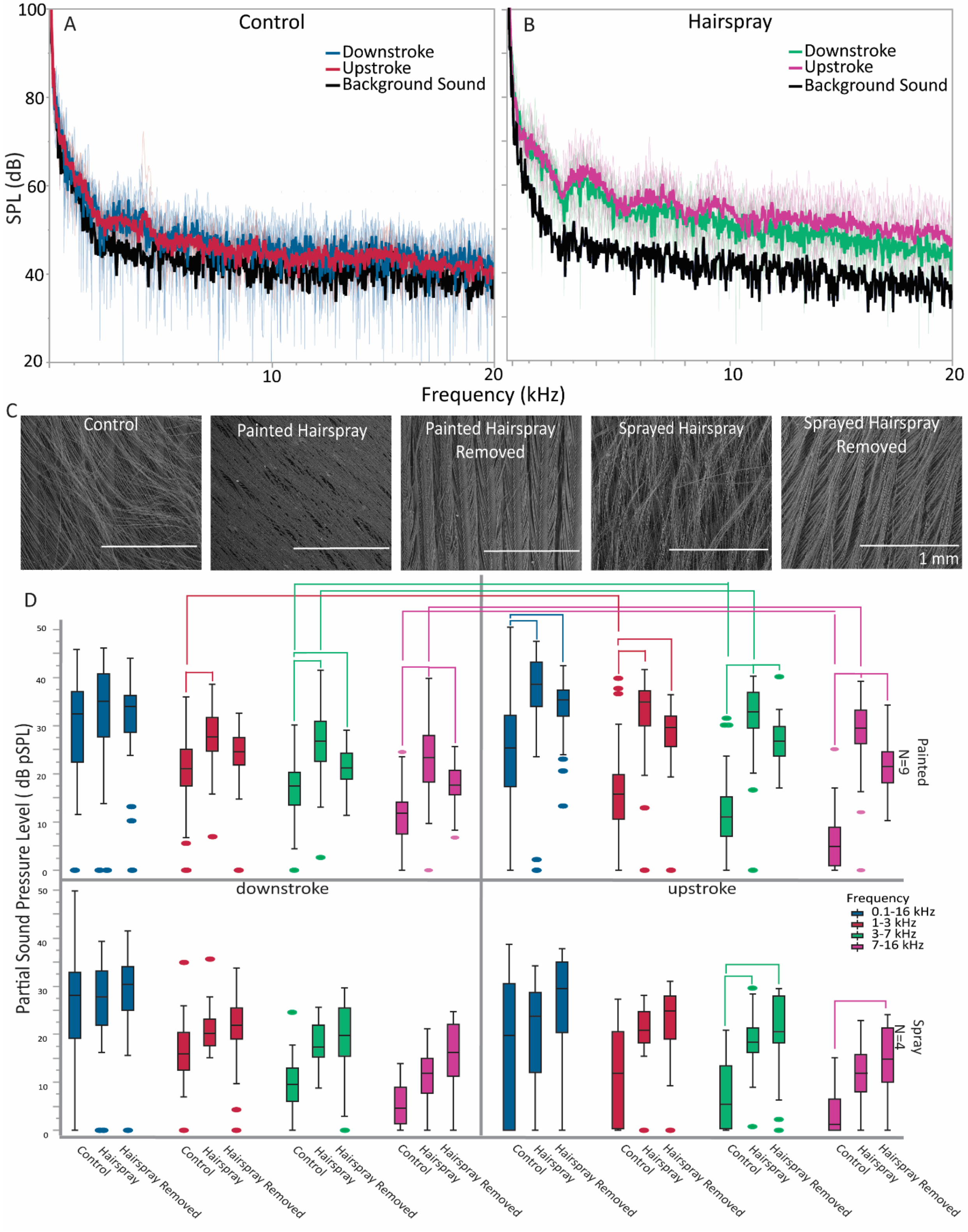
A
Control
Downstroke
Upstroke
Background Sound
SPL (dB)
100
80
60
40
20
10
20
B
Hairspray
Downstroke
Upstroke
Background Sound
10
20
Frequency (kHz)
C
Control
Painted Hairspray
Painted Hairspray Removed
Sprayed Hairspray
Sprayed Hairspray Removed
1 mm
D
Partial Sound Pressure Level (dB pSPL)
50
40
30
20
10
0
downstroke
upstroke
Painted N=9
Spray N=4
Frequency
0.1-16 kHz
1-3 kHz
3-7 kHz
7-16 kHz
Control
Hairspray
Hairspray Removed

Figure 2.3. Wing sound of a Barn Owl (*Tyto alba*). A) Power spectrum (unfiltered) of sound produced during the upstroke and downstroke of a control trial (N=6 flights from 1 bird). Faint lines are individual flights, bold lines are average. B) Power spectrum of upstroke and downstroke at all frequencies of a hairspray painted flight (N=1 Bird; 6 flights). For both A and B, time window was 0.5 seconds (centered around upstroke/downstroke as in Fig. 2.2) and the FFT window size was 1,500 samples. C) Environmental SEM images of the dorsal surface of all treatments (control, hairspray, hairspray-removed) for painted and sprayed applications, respectively. D) Partial Sound Pressure Level (dB pSPL) in the painted (N=9 birds) and sprayed (N=4 birds) treatment groups for the upstroke and downstroke, respectively (mean ± s.d.). Colors represent different frequency bandwidths analyzed. Lines above box and whisker plots indicate statistical significance.

Tables:

Table 2.1. Gutin sound (0.01-0.1 kHz) amplitude (mean ± s.d.) during flapping flight, flight seed (m s $^{-1}$), and total distance (m)

Painted (N = 9 owls)	Upstroke SPL estimate (dB)	Downstroke SPL estimate (dB)	Flight speed (m s $^{-1}$)	Total distance (m)
Control:	91.1 ± 3.53	96.0 ± 4.92	2.5 ± 0.29	0.5 ± 0.2
Hairspray:	92.8 ± 3.34	96.7 ± 4.72	2.5 ± 0.34	0.5 ± 0.2
Hairspray-removed:	91.5 ± 2.99	95.8 ± 4.03	2.6 ± 0.28	0.6 ± 0.3
Spray (N= 4 owls)				
Control:	90.9 ± 5.05	94.6 ± 4.98	2.6 ± 0.35	0.5 ± 0.2
Hairspray:	90.2 ± 3.84	95.1 ± 5.60	2.7 ± 0.35	0.4 ± 0.2
Hairspray-removed:	91.5 ± 2.36	96.0 ± 4.08	2.8 ± 0.24	0.5 ±0.2

[1] The average total distance across analyzed flights was 0.6 ±0.25 m and the average flight speed was 2.6 ± 0.32 m/s (Mean ± s.d.; N = 424 flights). There was a significant effect of treatment on Gutin sound production (Repeated measures ANCOVA; DF=4, F-ratio=4.15, *P*-value=0.002). There was also a significant effect of stroke (DF=1, F-ratio=218.2, *P*<0.0001), total distance (DF=1, F-ratio=41.9, *P*<0.0001), and flight speed (DF= 1, F-ratio=10.82, *P*=0.0011) on Gutin sound production.

Table 2.2. Sound production ± S.E. (dB pSPL) estimated from Post-hoc Tukey HSD tests, after controlling for flight speed ± S.D. (m s^{-1}), and total distance from the owl to the microphone ± S.D. (m) for spray and painted applications.

Spray N=4 owls		0.1-16 kHz	1-3 kHz	3-7 kHz	7-16 kHz	Flight speed (m s^{-1})	Total Distance (m)
Control:	upstroke	25.5 ± 2.70	18.0 ± 1.90	14.4 ± 1.69	11.5 ± 1.67	2.6 ± 0.35	0.6 ± 0.2
	downstroke	30.0 ± 2.73	20.7 ± 1.90	17.0 ± 1.69	12.5 ± 1.67		0.5 ± 0.2
	average	27.7 ± 2.19	19.3 ± 1.56	15.7 ± 1.41	12.0 ± 1.43		
Hairspray:	upstroke	28.9 ± 2.60	26.1 ± 1.82	24.2 ± 1.62	17.6 ± 1.61	2.7 ± 0.35	0.5 ± 0.2
	downstroke	28.5 ± 2.60	24.6 ± 1.82	21.5 ± 1.62	15.6 ± 1.60		0.4 ± 0.2
	average	28.7 ± 2.03	25.3 ± 1.46	22.9 ± 1.32	16.6 ± 1.35		
Hairspray-removed:							
	upstroke	32.0 ± 2.71	27.6 ± 1.88	25.7 ± 1.67	20.4 ± 1.65	2.8 ± 0.24	0.5 ± 0.2
	downstroke	31.1 ± 2.70	24.1 ± 1.88	22.3 ± 1.67	19.0 ± 1.65		0.4 ± 0.2
	average	31.6 ± 2.10	25.8 ± 1.50	24.0 ± 1.36	19.7 ± 1.39		
Painted N=9 owls							
Control:	upstroke	20.6 ± 1.88	14.1 ± 1.37	9.6 ± 1.25	3.81 ± 1.30	2.5 ± 0.29	0.5 ± 0.2
	downstroke	27.2 ± 1.88	19.9 ± 1.37	15.5 ± 1.25	9.58 ± 1.30		0.5 ± 0.2
	average	23.9 ± 1.57	17.0 ± 1.19	12.5 ± 1.10	6.69 ± 1.18		
Hairspray:	upstroke	34.3 ± 1.91	30.6 ± 1.39	29.7 ± 1.26	26.5 ± 1.31	2.5 ± 0.34	0.5 ± 0.2
	downstroke	32.0 ± 1.90	26.1 ±1.38	24.7 ± 1.26	21.1 ± 1.30		0.6 ± 0.3
	average	33.1 ± 1.58	28.4 ± 1.19	27.2 ± 1.11	23.8 ± 1.18		
Hairspray-removed:							
	upstroke	31.5 ± 1.92	26.8 ± 1.40	25.0 ± 1.27	19.1 ± 1.31	2.6 ± 0.28	0.6 ± 0.2
	downstroke	30.5 ± 1.94	23.4 ± 1.41	21.0 ± 1.28	16.4 ± 1.32		0.7 ± 0.3
	average	31.0 ± 1.60	25.1 ± 1.20	22.8 ± 1.11	17.8 ± 1.19		

[1] To account for variation in background sound during experimentation, background sound has been removed from the SPL estimate.

[2] Reported pSPL values. Distance from the owl to the microphone (Total distance) and flight speed were included as covariates in the whole model (Table 2.3). The average total distance across all flights was 0.5 ± 0.23 m (mean ± s.d.; N=468 flights).

Table 2.3. **Repeated measures ANCOVA of sound production at different treatment groups. Frequency bandwidths were analyzed separately (N=13 owls, 392 flights)**

		.01-16 kHz		1-3 kHz		3-7 kHz		7-16 kHz	
	DF	F-ratio	*P*-value	F-ratio	*P*-value	F-ratio	*P*-value	F-ratio	*P*-value
Treatment [application]	4	10.1	**<0.0001**	35.6	**<0.0001**	79.2	**<0.0001**	119	**<0.0001**
Stroke	1	0.97	0.33	1.02	0.31	3.27	0.07	1.85	0.18
Total distance	1	6.24	**0.01**	3.89	**0.05**	3.33	0.07	4.98	**0.03**
Flight Speed	1	2.96	0.09	3.66	0.06	0.78	0.38	2.41	0.12
Flight number	1	1.86	0.17	2.58	0.11	1.71	0.19	1.01	0.32
Stroke*treatment [application]	4	2.68	**0.03**	8.32	**<0.0001**	12.9	**<0.0001**	13.0	**<0.0001**

[1] Significant *P*-values are boldface.

Table 2.4. **Effect sizes (Cohen's d) for control and treatment flights of owls in the painted application group.**

	Treatment	Sound Production (dB pSPL) (Mean ± S.D.)	Correlation	Cohen's D
0.1-16 kHz:	Control	23.9 ± 15.8		
	Hairspray	33.1 ± 15.7	-0.44	0.34
1-3 kHz:	Control	17.0 ± 12.0		
	Hairspray	28.4 ± 11.8	-0.44	0.56
3-7 kHz:	Control	12.5 ± 11.1		
	Hairspray	27.2 ± 10.9	-0.44	0.78
7-16 kHz:	Control	6.7 ± 11.9		
	Hairspray	23.8 ± 11.7	-0.44	0.85

Chapter 3: Evidence that Lesser Nighthawks (*Chordeiles acutipennis*) use visual cues to hunt

Abstract:

Lesser Nighthawks (*Chordeiles acutipennis*) are nocturnal insectivorous birds with adaptations for nocturnal hunting. These include large eyes and two features thought to reduce their flight sounds: a velvety dorsal surface of their flight feathers and a fringed edge of their wing and tail feathers. Two hypotheses as to why flying animals evolve quiet flight are for stealth and to reduce self-masking. The stealth hypothesis posits quieting features help predators approach prey undetected. The self-masking hypothesis instead theorizes silencing features help auditory hunters, during flight, listen for the sound of prey. A necessary component of the self-masking hypothesis is that the predator must use acoustic cues to hunt. To address this question, here we ask: is there evidence that Lesser Nighthawks use auditory or visual cues to find prey when hunting? To assess the audibility of their prey, we recorded flight sounds of a beetle and moth species that are likely prey of nighthawks. At a distance of 0.01 m from a microphone, nearfield insect flight sounds for the beetle (*Chlorochroa sayi*) were 63 dB SPL with a fundamental frequency of 82 ± 1.6 Hz and 72 dB SPL with a fundamental frequency of 58 ± 12 Hz for the moth (*Hyles lineata*). Assuming that nearfield sound levels decline with the square of distance, their flight sounds diminish to 0 dB within 0.5 m. Then, to test if Lesser Nighthawks use acoustic or visual cues from flying insects to locate their prey, we recorded videos of wild Lesser Nighthawks hunting from a perch on the ground (N=5 flights) and on the wing (N=29 flights) in the presence of a bright light. The

apparent detection distances at which they began pursuing prey was 1.1 ± 0.2 m (perched on ground) and 2.5 ± 0.4 m (on the wing). Lesser Nighthawks initiated pursuit of prey at a greater distance than the audible detection distance of insects both when hunting on the ground (P-value = 0.02) and on the wing (P-value <0.0001), suggesting they use visual cues to initiate pursuit of prey under these conditions. There is not yet any evidence that nighthawks hunt their prey by ear. This implies that the function of quiet flight in Lesser Nighthawks is not to reduce self-masking during hunting.

Introduction:

Lesser nighthawks (*Chordeiles acutipennis*) are nocturnal insectivores residing in deserts across North and South America (Latta and Baltz 1997). They primarily hunt flying insects (such as beetles and moths) by aerially hawking (flying low over vegetation to chase prey in flight), or sallying out from a perch (often on the ground), and sometimes chasing insects on foot on the ground (Latta and Baltz 1997). Lesser Nighthawks have several adaptations for nocturnal hunting including, two wing features thought to be associated with quiet flight (Woods 1924; Clark et al. 2020b) and increased nighttime vision (Nicol and Arnott 1974).

These two features are: a fringed vane of their flight and tail feathers, and a velvety dorsal surface of flight feathers (Clark et al. 2020b, p. 4). In owls, dorsal velvet apparently functions by reducing the broadband (sound production across all audible frequencies) frictional sound of two feathers rubbing together, which occurs naturally during flapping flight (LePiane and Clark 2020). Owl flight sounds have the greatest acoustical amplitude (dB SPL) at low frequencies (0-1 kHz) and the amplitude is lower at higher frequencies (LePiane and Clark 2020). When the dorsal velvet on Barn Owl flight feathers was experimentally impaired, sound production increased across all frequencies, particularly during the upstroke, suggesting that the velvet reduces rubbing sounds produced when feathers slide past one another during the upstroke (LePiane and Clark 2020). When two pigeon feathers that lack the velvet are slid past each other, they produce a broadband sound (Matloff et al 2020), similar to the sound produced when two pieces of sandpaper are rubbed together (Akay 2002).

Here, we hypothesize that the dorsal velvet on flight feathers of Nightbirds (nocturnal members of *Caprimulgiformes* such as Nightjars, Nighthawks, Pootoos) functions in reducing the high frequency components of flight sounds. There is some evidence to support this claim: a recording of the Mexican Whip-poor-will (*Antrostomus arizonae*) flight sounds at close range showed little sound above 3 kHz, suggesting that high frequency sounds present in the flight of most birds (Thorpe and Griffin 1962) are suppressed in this species, presumably by the presence of the velvet (Clark et al. 2020a, p. 25).

Nocturnal birds may benefit from quiet flight in multiple ways; quiet flight may enable them to sneak up on prey, avoid their own predators, listen for conspecifics, and/or listen for auditory cues from prey. Here, we are interested in how the flight sounds produced by Lesser Nighthawks impact the interaction between Lesser Nighthawks and their flying insect prey.

In the context of a predator-prey interaction, the two hypotheses for the function of quieting features in predators are stealth and self-masking (auditory phenomenon of sound produced by an animal making sounds they may be listening for inaudible). Under the stealth hypothesis, we predict that quieting features evolved to help predators sneak up on prey, which aids in a stealthy hunting strategy. Under the self-masking hypothesis, we predict silencing features evolved to help the predator locate the prey (Clark et al. 2020a).

The first hypothesis for the function of quiet flight in birds is stealth, under which we predict that quieting features enable predators to sneak up on prey. Lesser Nighthawks specialize in flying insects, such as moths and beetles, which may have evolved ears for predator avoidance (Fournier et al. 2013). Some species of moth, for example, have evolved high frequency hearing that helps them detect the echolocation clicks of bat predators (Conner and Corcoran 2012). It is possible that the velvet and the vane fringe evolved in nighthawks to quiet the frequencies of flight sound that fall into the most sensitive hearing frequencies of their prey.

The second hypothesis for the function of quiet flight in birds is self-masking. Under the self-masking hypothesis, we predict Lesser Nighthawks use sound to locate prey. A key assumption of the self-masking hypothesis is that predators use auditory cues to detect prey. Little is known about the hearing of Lesser Nighthawks, but Caprimulgiformes do not seem to have the same auditory specializations as owls, such as an enlarged inner ears (Peacock et al. 2020). Nonetheless, they are cited as having "excellent hearing" in species accounts (Latta and Baltz 1997; Cleere 2010). The closest relative of the Lesser Nighthawk with a known auditory curve (a measure of sound pressure level sensitivity relative to sound frequency) is the Oilbird (*Steatornis* *caripensis*). Oilbirds are most sensitive at 2 kHz (0 dB) and their sensitivity declines sharply at both higher and lower frequencies (Konishi and Knudsen, 1979, p.425). For example, they can detect a 0.5 kHz sound at about 25 dB and a 0.25 kHz sound at about 35 dB (Konishi and Knudsen 1979). There are several ecological differences between Oilbirds and Lesser Nighthawks, the most relevant of which is that Oilbirds use low frequency sounds to echolocate, something no other caprimulgid is known to do. However, as the hearing abilities of no other caprimulgid have been measured, here we assumed that Lesser Nighthawks have similar hearing abilities to Oilbirds.

If Lesser Nighthawks hunt flying insects by sound, what might they be listening for? Flying insects generally produce sound in only one way: they produce wing tone. This sound is audible (to humans) at the wingbeat frequency, in which the dominant frequency is either the fundamental or one of the harmonics just above the fundamental, such as 2f (the 2nd harmonic; Dudley 2000). This low-frequency wing tone is an inevitable byproduct of flapping wings. The sound close to the animal is nearfield sound, which declines as distance squared (Clark and Mistick 2020). Here, we use Clark and Mistick's (2020) model which predicts insect flight sound levels based off of wingbeat frequency and insect body mass, and assume nearfield propagation, to estimate the sound levels of flying insects that are likely prey of Lesser Nighthawks.

The other primary sense birds use to hunt is vision. Species accounts of Lesser Nighthawks mention they are probably primarily visual hunters (Latta and Baltz 1997; Cleere 2010). The evidence of visual hunting cited in these species accounts is: 1) Lesser Nighthawks have adaptations for nocturnal vision (Nicol and Arnott 1974) and 2) they prefer to hunt during dusk and dawn, and are more active during the full moon (Latta and Baltz 1997), but this may be in response to the availability of insect prey, which also follow this activity pattern (Quiring 1994). Further evidence of visual hunting would be head movements before takeoff to catch an insect. Birds use head movements to visually locate prey and aid in depth perception (Kral 2003). Black Phoebes (*Sayornis nigricans*), hunt in a similar way to a perched Lesser Nighthawk (they sit on a perch and make short, sallying flights to catch insects) have been recorded turning their heads an average of 17 times to look at an insect before takeoff (Gall and Fernández-Juricic 2009).

Here, we assessed whether Lesser Nighthawks use primarily sound or vision to locate prey. Under the auditory hunting hypothesis, we predict that Lesser Nighthawks are orienting to prey either by turning their heads or changing the direction of their flight path in response to audible insects. Under the visual hunting hypothesis, we predict Lesser Nighthawks use head turns before takeoff, and that those head turns occur at distances greater than the audible detection distance of their prey.

To test our hypotheses that Lesser Nighthawks use sound or vision to locate prey, we recorded the flight sounds of insects at our field site and used a model to predict the audible detection distance of insects in the environment. Then, we recorded videos of Lesser Nighthawks hunting on the ground and on the wing to determine how far they are from an insect when they begin pursuing prey.

Methods:

Study site

We conducted all experiments at Boyd Deep Canyon Research Center (reserve DOI: doi:10.21973/N3V66D) in June and July 2019 in the week surrounding the full moon of each month. Experiments took place between 9 pm and 3 am. The temperatures during experimentation in June were 20.4-29.9°C and temperatures during July experimentation were 24.1-34.5°C. Average wind speed was 1.28-23.8 kph with gusts of 4.2-47.3 kph.

Insect Recordings

To attract insects, at Boyd Deep Canyon we set up a UV light (20 W UVLED lamp by YKDTronics) on a tripod during one night of Nighthawk data collection in July 2019. Sounds were recorded with a Brüel and Kjær 4190 free-field microphone with a windscreen. The free-field response of this microphone is flat between 3.15 - 20 kHz ± 2dB, with a sensitivity of 50 mV/Pa attached to a Sound Devices 702 recorder with a minimum frequency of 10 Hz and a sampling frequency of 48 kHz, with the gain set to 24.3 dB. Insects were held 1-2 cm away from the microphone and encouraged to fly directly away (horizontally) from the microphone.

Sound recordings were analyzed using Raven Pro version 1.5 (Cornell Lab of Ornithology 2014). In Raven Pro, we collected the wingbeat frequency of the insects by finding the first six wingbeats visible on the recording and dividing the number of wingbeats (six) by the time elapsed. Then, as an estimate of sound pressure levels, we used Raven Pro's Root Mean Square Amplitude which we converted to dB reference 20 μPa. The microphone was calibrated relative to a sound source (B&K sound level calibrator 4231; Clark et al. 2013) that produced a 1 kHz tone at 94 and 114 dB, ref 20 μPa, with the recorder's gain set to zero dB. We converted our values to SPL ref 20 μPa after accounting for the difference in gain between the calibration recording versus our experimental setup (Gain of 0 vs 24.3 dB).

We calculated the predicted sound levels as a function of distance using the following equation (Clark and Mistick 2020):

$\mathrm{SPL}= mg\,\mathrm{Sin(wt)}/(4\pi r^2) + f\,mg\,\mathrm{Cos\,(wt)}/(2cr)$

where SPL = the amplitude of the insect's wing in Pascals, c = the speed of sound (340 m/s); r = distance from the insect in meters, mg = mass of insect (in kg) times gravity, 9.8 $\mathrm{m\ s^{-2}}$. The term containing Sine is the nearfield while the term containing Cosine is the farfield. As the data indicated that the farfield sound was far below (>20 dB) the nearfield sound at all distances at which it would be audible, we dropped the Cosine term. In that case, to calculate the maximum amplitude of the sound we set the Sine(wt) term equal to 1.

Insects were photographed and identified to species based on morphology. Insect mass was estimated using body lengths reported in the literature (Cartron et al. 2008; Windsor et al. 2014), based off of the model presented in Rogers et al. (1976): W=0.0305xL where W= weight (mg) and L=body length (mm).

Insect flight sounds were then compared to the audiogram of an Oilbird (Konishi and Knudsen 1979) to determine hypothesized audible detection distances.

Assessment of Hypothesized Audible Detection Distance

We found the fundamental frequency of our recorded insect flights to be 82.2 ± 1.6 Hz for the beetle (*Chlorochroa sayi*; mass=0.37 mg; N=2 animals) and 57.8 ± 12.2 Hz for the moth (*Hyles lineata;* mass=1.03 mg; N=5 animals). The nearfield sound was louder than the farfield sound for all of our modeled distances, so we will focus on the nearfield sound (N=5 insects, 2 species; Table 3.S1). At 0.01 m, insect flight sounds of the beetle and the moth were 63 dB and 72 dB, respectively (Fig. 3.1). We predict insect flight sounds decline to ~35 dB at a distance of 0.05-0.075 m (Table 3.S1). Oilbirds can hear low frequency sounds (~250 Hz) at about 35 dB and their sensitivity decreases with decreasing frequency (Konishi and Knudsen 1979; p. 425). At a distance of 0.5 m from the beetle and the moth, modeled flight sounds were -4.7 dB and 4.3 dB, respectively. Sound intensities of -4.7 and 4.3 dB at low frequencies (57-82 Hz) are therefore likely inaudible to Lesser Nighthawks, so we conservatively used 0.5 m as our hypothesized audible detection distance.

Video Recordings

We captured videos of Lesser nighthawks (*Chordeiles acutipennis*) foraging from a perch on the ground and in flight. To record birds foraging in flight (N=29 flights), we found a flock of foraging birds (often 5+ birds foraging together) and positioned a directional light (Nite Rider Pro 2200 race, 2200 Lumens, or LEPOWER LED flood light, 1600 lumens) such that it illuminated a nearby bush to allow observation of the birds hunting. Video was recorded using a Canon XA10 Professional (30 frames/second, 1920 x 1080) on a tripod. We were specifically interested in recordings where birds changed direction during flight to chase a visible insect (Fig. 3.2). Videos of Nighthawks hunting from a perch on the ground (N=3) were recorded from inside a vehicle. The bird was illuminated by the vehicle's headlights. For videos of birds foraging from the ground, number of head turns and rate of head turning [number of head turns/head turning bout length (s)] were recorded.

Using Adobe Premiere Pro version 14.3.1, we extracted stills from the videos at the frame in which the bird noticed an insect. If the bird was foraging in flight, we extracted the frame before the bird changed direction (Fig. 3.2). If the bird was foraging from the ground, we extracted the frame where the bird first moves its head in the direction of an insect (Fig. 3.3). We also recorded if the attack was successful and whether the insect made an evasive maneuver. If the insect made an evasive maneuver, we recorded the distance between the insect and the Lesser Nighthawk at the frame before the insect moved away from the bird.

Images were then analyzed in Image J (Rueden et al. 2017). From each video still, we collected the body size of the Nighthawk (measured from the head to the tail) and distance between the bird and the insect (converted to meters using body length of 0.2 m as the scale Latta and Baltz 1997). Since we recorded video using one camera, actual distances from the insect to the nighthawk are unknown. Measured distances are likely an underestimate of the actual distance between the insect and the nighthawk.

Statistical analysis

To test our hypotheses that Lesser nighthawks use sound or vision to locate prey, we performed two one-sample t-tests where we tested the mean detection distance (m) against a hypothesized audible detection distance (0.5 m). We performed two separate one sample t-tests, one for videos of birds foraging in flight (N= 29 flights) and one for birds foraging from a perch on the ground (N=5 videos). We used Levene's test to ensure homogeneity of variance (Levene's *P*-value = 0.099) and thus proceeded with the t-test. Full model output for predicting audible distance of insect flight sounds are presented in Table 3.S1.

Results:

A summary of our observed mean detection distances for birds foraging on the wing and form the ground are presented in Table 3.1. Lesser Nighthawks changed direction in flight or turned their heads in response to insects at distances greater than 0.5 m (Fig. 3.4).

Lesser Nighthawks detect insects at a greater distance than the hypothesized audible detection distance both when foraging from the ground (one-tailed t-test; DF=4, test statistic = 2.9; *P*-value = 0.02) and in flight (DF= 28; test statistic = 2.35; *P*-value <0.0001; Table 3.2). In all of our recorded predation interactions, Lesser Nighthawks detected insects at a distance greater than 0.5 m.

All of the recorded foraging events from the ground resulted in successful prey capture. The birds took an average of 2.8 seconds from first detection to prey capture (Table 3.3). The majority of birds (3/5) turned their head once before taking off in the direction of an insect. The remaining two birds turned their heads two and three times before takeoff, respectively.

Lesser Nighthawks were found hunting flying insects which were a similar size to the insects we recorded. All of the foraging attempts from the ground were successful

(Table 3.S2). For birds foraging in flight, 12 predation attempts were successful, 15 predation attempts were unsuccessful, and the success of the remaining two attempts is unknown (Table 3.S2). Of the 15 unsuccessful predation attempts, four of them resulted in an evasive maneuver from an insect. Insect evasions occurred when the bird was a very short distance (within centimeters) away from the insect.

Discussion:

Here, we considered the function of quieting wing features in Lesser Nighthawks. The two hypotheses for the function of quieting features in predators are stealth and self-masking. Unser the stealth hypothesis, we predicted Lesser Nighthawks have evolved quieting features to reduce the high frequency components of their flight sounds, which enables them to sneak up on flying insects. Under the self-masking hypothesis, we predict Lesser Nighthawks evolved quieting features to accurately detect the location of flying insects using auditory cues.

We tested these hypotheses by testing whether Lesser Nighthawks use sound or vision to locate prey. First, we considered the sounds the insects in their environment make while flying relative to the hypothesized hearing ability of Lesser Nighthawks. Insect flight sounds are relatively low frequency (fundamental frequency: 82.2 ± 1.6 Hz for the beetle and 57.8 ± 12.2 Hz for the moth). While auditory thresholds of Lesser Nighthawks is unknown, Oilbirds have a low-frequency (~250 Hz) detection threshold >35 dB (Konishi and Knudsen 1979). If Lesser Nighthawks have the same detection threshold, and if the 4th harmonic of the wing sounds (which is roughly 250 Hz) is proportional to the fundamental frequency, our insect flight sound model suggests Lesser

Nighthawks would detect insect flight sounds at roughly 0.05-0.075 m, the distance at which the insect flight sounds reach 35 dB (Fig. 3.1; Table 3.S1).

The self-masking hypothesis for quiet-flying predators requires these predators use sound to hunt. Lesser Nighthawks are orienting to prey either by turning their heads (if hunting from the ground; Fig. 3.3) or changing the direction of their flight path (Fig. 3.2) at distances greater than our hypothesized audible detection distance (one-tailed t-test *P*-values <0.05*;* Table 3.2; Fig. 3.4). It is possible that Lesser Nighthawks use insect flight sounds in the last phase of a hunt (when the insects are within 0.075 m), but here we have shown that Lesser Nighthawks are using their vision to locate and chase prey.

The predatory interactions we observed were under higher levels of light than nighthawks may typically experience. It is possible that Lesser Nighthawks used light to hunt because it was provided to them. But there is already some information in species accounts that indicates Lesser Nighthawks and other Nightbirds are visual hunters. They have adaptations for nighttime vision (Nicol and Arnott 1974), are found to hunt primarily during dusk and dawn, and are more active during the full moon (Cleere 1999). All of these conditions (dusk, dawn, full moon) have lower illuminance than the light conditions we provided in this experiment (a full moon provides 0.05-0.1 lumens m^{-2}; Hänel et al. 2018).

The stealth hypothesis predicts Lesser Nighthawks have evolved quieting features to sneak up on insects. Many flying insects have ears tuned to high frequency sounds (Conner and Corcoran 2012) and many insects have been found to listen for and avoid the flight sounds of birds with more noisy flight (Fournier et al. 2013). Here, we found few predatory flights that resulted in an insect maneuver (N=3). Instead, insects often flew towards the oncoming Lesser Nighthawk (Fig. 3.2). When insects did maneuver away from Lesser Nighthawks, it occurred within centimeters of the bird. This suggests the flying insects Lesser Nighthawks hunted either were not actively listening for bird flight sounds or they did not detect the approaching bird until they were a short distance away. While the dorsal velvet was previously found to reduce high frequency rubbing flight sounds in Barn Owls the function of the velvet in Lesser Nighthawks has not been experimentally tested. But it is likely that the velvet on Lesser Nighthawk flight feathers reduces flight sounds in the range of frequencies their insect prey is most sensitive to. Future work should examine the flight sounds of Lesser Nighthawks to assess the role of velvet in avoiding detection by their insect prey.

Figures:

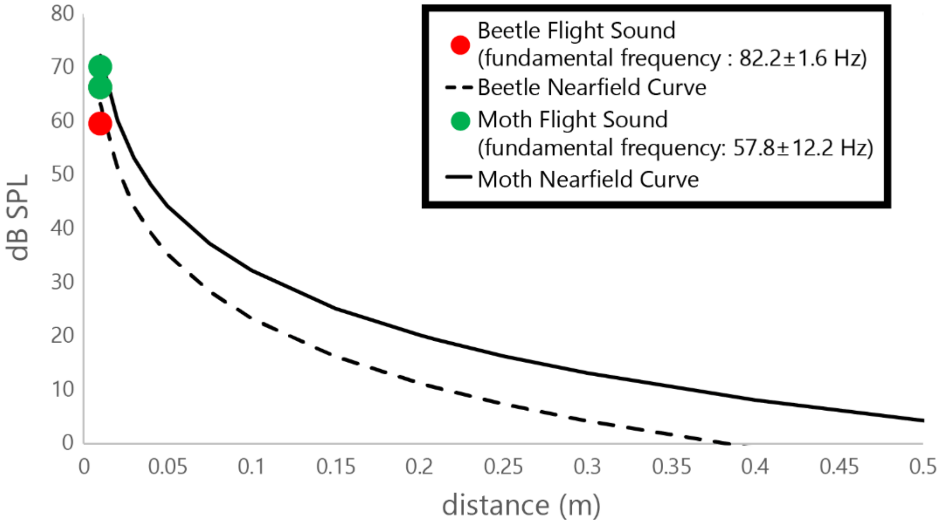

Figure 3.1. An estimate of insect wing tone as a function of distance. Red dots represent Beetle flight sounds (*Chlorochroa sayi;* N=2 recordings) and the estimated Sound Pressure Levels (dB) as a function of distance for beetle flight sounds is represented by the dashed lines. Green dots indicate Moth recordings (*Hyles lineata;* N=5 recordings) and the solid line represents the nearfield sound production at different distances. The fundamental frequency (Wing Beat Frequency) indicated.

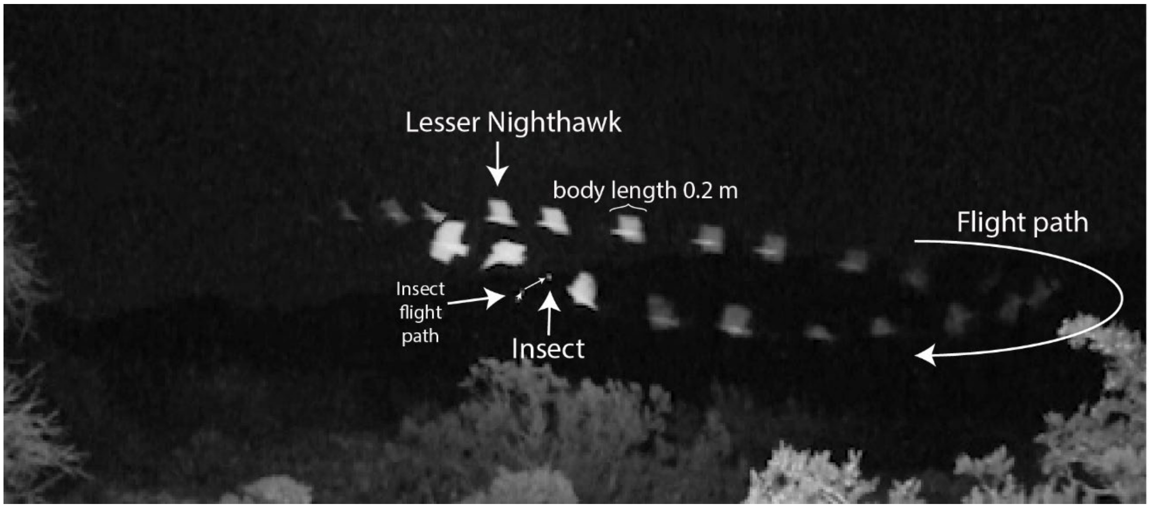

Figure 3.2. **An example of Lesser Nighthawk hunting an insect on the wing.** The Lesser Nighthawk makes a 180-degree maneuver (indicated by the flight path arrow) after detecting the location of an insect (depicted). The flight path of the insect is indicated by the small arrows. Note that the insect moves in the direction of the Lesser Nighthawk, apparently unaware of its fate. Detection distances were relative to the body length of a Lesser Nighthawk (indicated; 0.2 m)

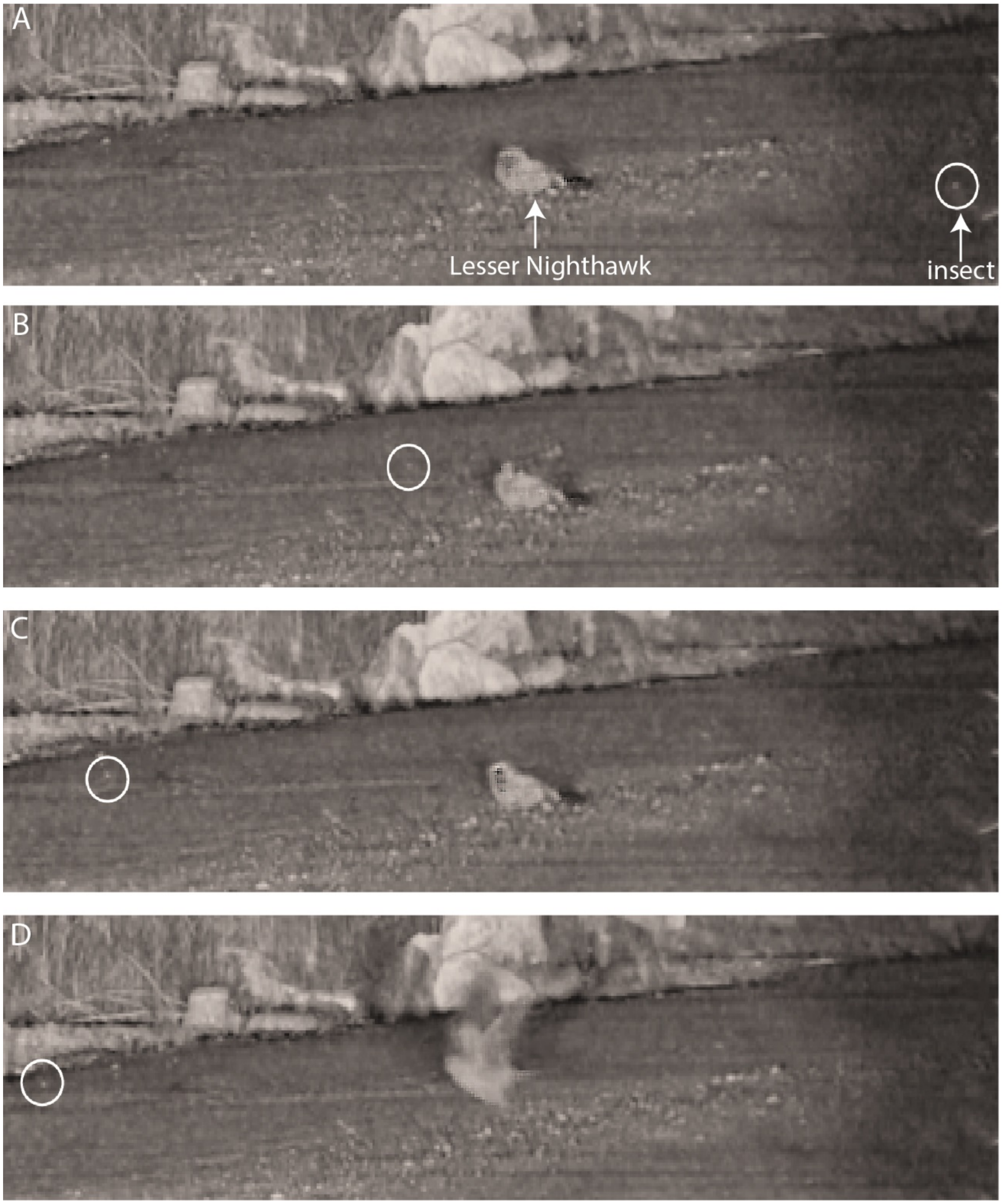

Figure 3.3. An example of a Lesser Nighthawk foraging from the ground. In frame A, the Lesser Nighthawk is looking towards the camera when an insect flies into the frame (white circle). B) The Lesser Nighthawk notices the insect and turns its head away from the camera to look at the insect C) As the insect moves to the right, the Lesser Nighthawk turns its head again before D) takeoff.

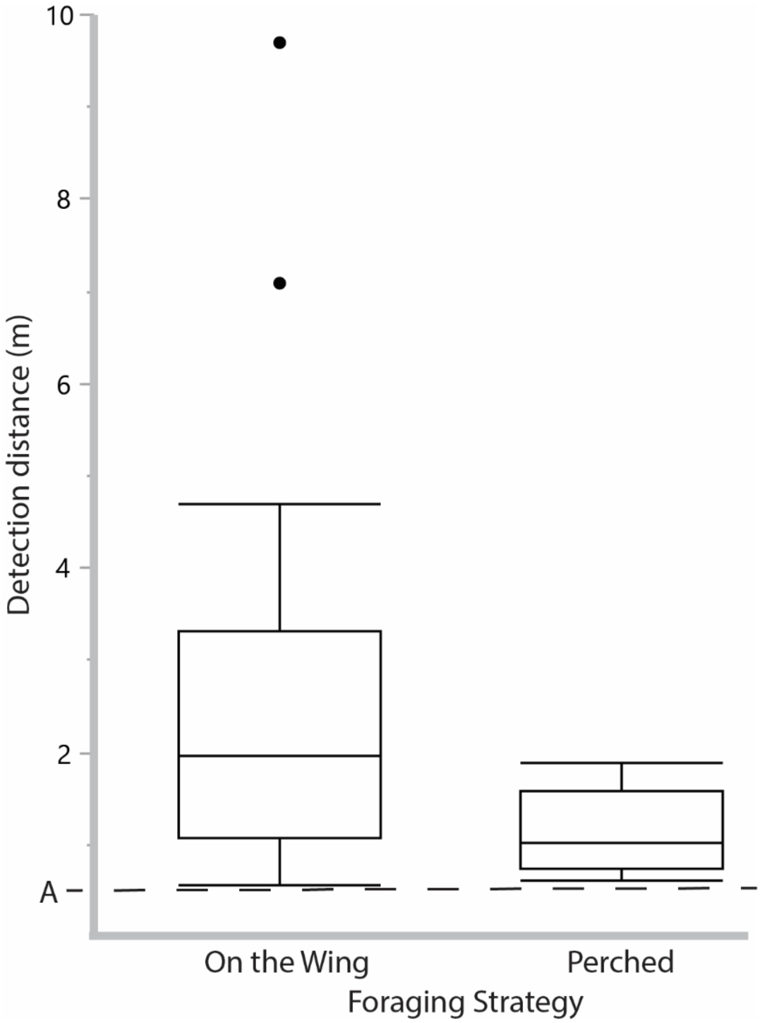

Figure 3.1. Detection distances for Lesser Nighthawks foraging on the wing and perched on the ground. Box plots show mean ± standard error. Dashed Line (A) indicates the hypothesized audible detection distance of insects in the environment (0.5 m).

Tables:

Table 3.1. A summary of detection distances for Lesser Nighthawks foraging on the wing and in flight.

Foraging Strategy	N	Mean detection distance (m)	Std. Dev	Std. Error Mean
On the wing	29	2.5	2.01	0.37
Perched	5	1.1	0.48	0.22

Table 3.2. Results of our one-tailed t-tests for mean detection distance against the hypothesized audible detection distance of insects (0.5 m).

	Test value = 0.5 m			
Foraging Strategy	t-value	DF	*P*-value (one-tailed)	Mean Difference
On the Wing	5.34	28	<0.0001	4.84
Perched	2.93	4	0.02	2.43

Table 3.3. Number of head turns, time from first head turn to takeoff, and head turn bout rate (turns/s) for Lesser Nighthawks foraging on the ground.

Head turns	Head turn bout length (s)	Head turn bout rate (turns/s)
2	0.84	2.4
1	0.48	2.1
1	0.16	6.3
1	0.50	2.0
3	2.6	1.2

Conclusions:

Sound production and its role in predatory interactions is a topic which has received little study. For example, how owls (an auditory predator) hear and hunt mice is unknown. Further, it is unclear how the sounds produced by owl wings during flight travel through the air and whether they impact the birds' ability to detect prey.

This dissertation builds on study about owl hearing from a psychoacoustics perspective (Konishi 1973b; Knudsen et al. 1979) and owl wing and feather features form an engineering perspective (Wagner et al. 2017). The aim of this dissertation was to bridge the fields of psychoacoustics and engineering to address quiet flight in owls and other nocturnal birds from an ecological perspective.

In pursuit of this goal, Chapter 1 investigated how quieting features vary with ecology in owls. I found that increased quieting features are correlated with both stealth and self-masking, indicating that sneaking up on and/or listening for prey may drive the evolution of quieting features. Then, in Chapter 2, I tested the function of the dorsal velvet in quieting Barn Owl flight, and found that the velvet reduces the sound produced when two feathers slide past one another during flapping flight. In this chapter, we found that a substantial amount of flight sound occurs from feather rubbing caused by wing morphing during flapping flight. Finally, in Chapter 3, I investigated the feeding ecology of Lesser Nighthawks to address the function of quieting features in these birds. I found that Lesser Nighthawks use vision to locate prey and considered this evidence against the self-masking hypothesis for the function of quiet flight.

This dissertation contributes to the growing field of bioacoustics in predatory interactions. But there are many questions about quiet flight and predation which remain unanswered, for example, it is still unclear how wing and flight sounds impact a birds' ability to localize prey. Are owls which are considered "loud fliers" (e.g., *Glaucidium spp.*) diurnal because their flight sounds prohibit them from sneaking up on or locating prey at night? Further, it is unclear what the function of quiet flight is in other nocturnal birds. How do quieting features function in these birds and why might they have evolved?

Studying sound and hearing in predation is crucial to understanding how human-made (anthropogenic) noise impacts acoustic predators. For example, there is evidence that anthropogenic noise impacts the distribution of animals (McClure et al. 2013; Ware et al. 2015) and decreases Northern Saw-whet owls' ability to hunt (Mason et al. 2016). But further study is needed to investigate how anthropogenic noise impacts acoustic predators so we can learn how to lessen the acoustic impact of human behavior.

Bibliography:

Abouheif E, Fairbairn DJ. 1997. A comparative analysis of allometry for sexual size dimorphism: assessing Rensch's rule. The American Naturalist 149:540–562.

Akay A. 2002. Acoustics of friction. The Journal of the Acoustical Society of America 111:1525–48.

Ali MA. 2012. Vision in Vertebrates Springer Science & Business Media.

Bachmann T, Blazek S, Erlinghagen T, Baumgartner W, Wagner H. 2012. Barn Owl Flight. In: Tropea C, Bleckmann H, editors. Nature-Inspired Fluid Mechanics: Results of the DFG Priority Programme 1207 ”Nature-inspired Fluid Mechanics” 2006-2012. Notes on Numerical Fluid Mechanics and Multidisciplinary Design Berlin, Heidelberg: Springer Berlin Heidelberg. p. 101–17.

Bachmann T, Klän S, Baumgartner W, Klaas M, Schröder W, Wagner H. 2007. Morphometric characterisation of wing feathers of the barn owl *Tyto alba pratincola* and the pigeon *Columba livia*. Frontiers in Zoology 4:23.

Billerman SM, Keeney BK, Rodewald PG, Schulenberg TS (Eds.). 2020. Birds of the World Ithaca, N.Y.: Cornell Lab of Ornithology.

Blake WK. 2017. Mechanics of Flow-Induced Sound and Vibration, Volume 2: Complex Flow-Structure Interactions Academic Press.

Brodie ED, Brodie ED. 1999a. Predator-Prey Arms Races: Asymmetrical selection on predators and prey may be reduced when prey are dangerous. BioScience 49:557–68.

Brodie ED, Brodie ED. 1999b. Costs of Exploiting Poisonous Prey: Evolutionary Trade-Offs in a Predator-Prey Arms Race. Evolution 53:626–31.

Bruce MD. 1999. Family Tytonidae (Barn-owls). In: del Hoyo J, Elliot A, Sargatal J, editors. Handbook of the Birds of the World Barcelona: Lynx Editions. p. 34–75.

Calford MB, Pettigrew JD. 1984. Frequency dependence of directional amplification at the cat's pinna. Hearing research 14:13–19.

Cartron J-LE, Lowrey T, Mygatt J. 2008. A Field Guide to the Plants and Animals of the Middle Rio Grande Bosque UNM Press.

Chen QC, Cain D, Jen PH. 1995. Sound pressure transformation at the pinna of *Mus domesticus*. J Exp Biol 198:2007–23.

Chin DD, Lentink D. 2016. Flapping wing aerodynamics: from insects to vertebrates. Journal of Experimental Biology 219:920–32.

Clark CJ, Elias DO, Prum RO. 2013. Hummingbird feather sounds are produced by aeroelastic flutter, not vortex-induced vibration. Journal of Experimental Biology 216:3395–3403.

Clark CJ, LePiane K, Liu L. 2020a. Evolution and ecology of silent flight in owls and other flying vertebrates. Integr Org Biol.

Clark CJ, LePiane K, Liu L. 2020b. Evolutionary and ecological correlates of quiet flight in nightbirds, hawks, falcons, and owls. Integrative and Comparative Biology.

Clark CJ, Mistick EA. 2020. Humming hummingbirds, insect flight tones, and a model of animal flight sound. Journal of Experimental Biology.

Cleere N. 1999. Lesser Nighthawk. In: del Hoyo J, Elliot, J., Sargatal, J., editors. Handbook of the Birds of the World Barcelona, Spain: Lynx Edicions. p. 302–86.

Cleere N. 2010. Nightjars: A Guide to Nightjars and related birds Helm.

Conner WE, Corcoran AJ. 2012. Sound strategies: the 65-million-year-old battle between bats and insects. Annual review of entomology 57:21–39.

Corcoran AJ, Barber JR, Conner WE. 2009. Tiger moth jams bat sonar. Science 325:325–327.

Corcoran AJ, Conner WE. 2012. Sonar jamming in the field: effectiveness and behavior of a unique prey defense. Journal of Experimental Biology 215:4278–4287.

Cornell Lab of Ornithology. 2014. Raven Pro: Interactive Sound Analysis Software (Version 1.5) Ithaca, N.Y.

Crighton D. 1991. Airframe Noise. In: Hubbard HH, editor. Aeroacoustics of Flight Vehicles: Theory and Practice Hampton, VA: National Aeronautics and Space Admin Langley Research Center.

Dantas SM, Weckstein JD, Bates JM, Krabbe NK, Cadena CD, Robbins MB, Valderrama E, Aleixo A. 2016. Molecular systematics of the new world screech-owls (Megascops: Aves, *Strigidae*): biogeographic and taxonomic implications. Molecular Phylogenetics and Evolution 94, Part B:626–34.

de Koning M, Beatini JR, Proudfoot GA, Gall MD. 2020. Hearing in 3D: Directional Auditory Sensitivity of Northern Saw-Whet Owls (*Aegolius acadicus*). Integr Comp Biol.

del Hoyo J, Elliot A, Sargatal J. 1999. Handbook of the birds of the world Barcelona, Spain: Lynx Editions.

Dice LR. 1945. Minimum Intensities of Illumination Under Which Owls Can Find Dead Prey by Sight. The American Naturalist 79:385–416.

Dooling RJ. 1992. Hearing in Birds. In: Webster DB, Popper AN, Fay RR, editors. The Evolutionary Biology of Hearing Springer New York. p. 545–59.

Dormann CF, Elith J, Bacher S, Buchmann C, Carl G, Carré G, Marquéz JRG, Gruber B, Lafourcade B, Leitao PJ. 2013. Collinearity: a review of methods to deal with it and a simulation study evaluating their performance. Ecography 36:27–46.

Dudley R. 2000. The biomechanics of insect flight: form, function, evolution Princeton University Press.

Fay RR. 2012. Comparative Hearing: Mammals Springer Science & Business Media.

Fournier JP, Dawson JW, Mikhail A, Yack JE. 2013. If a bird flies in the forest, does an insect hear it? Biology Letters 9:20130319.

Fox J, Weisberg S. 2019. An R Companion to Applied Regression. 3rd ed Thousand Oaks, CA: SAGE Publications.

Frost BJ, Baldwin PJ, Csizy M. 1989. Auditory localization in the northern saw-whet owl, *Aegolius acadicus*. Can J Zool 67:1955–59.

Fullard JH, Yack JE. 1993. The evolutionary biology of insect hearing. Trends in Ecology & Evolution 8:248–52.

Gall MD, Fernández-Juricic E. 2009. Effects of Physical and Visual Access to Prey on Patch Selection and Food Search Effort in a Sit-and-Wait Predator, the Black Phoebe. The Condor 111:150–58.

Garland T, Midford PE, Ives AR. 1999. An Introduction to Phylogenetically Based Statistical Methods, with a New Method for Confidence Intervals on Ancestral Values. Integr Comp Biol 39:374–88.

Geyer TF, Claus VT, Hall PM, Sarradj E. 2017. Silent owl flight: The effect of the leading edge comb. International Journal of Aeroacoustics 16:115–34.

Goerlitz HR, Greif S, Siemers BM. 2008. Cues for acoustic detection of prey: insect rustling sounds and the influence of walking substrate. Journal of Experimental Biology 211:2799–2806.

Graham RR. 1934. The silent flight of owls. Journal of the Royal Aeronautical Society 38:837–843.

Gutiérrez-Ibáñez C, Iwaniuk AN, Wylie DR. 2011. Relative Size of Auditory Pathways in Symmetrically and Asymmetrically Eared Owls. BBE 78:286–301.

Gutin L. 1948. On the Sound Field of a Rotating Propeller. National Advisory Committee for Aeronautics.

Hänel A, Posch T, Ribas SJ, Aubé M, Duriscoe D, Jechow A, Kollath Z, Lolkema DE, Moore C, Schmidt N, Spoelstra H, Wuchterl G, Kyba CCM. 2018. Measuring night sky brightness: methods and challenges. Journal of Quantitative Spectroscopy and Radiative Transfer 205:278–90.

Hausmann L, Plachta DTT, Singheiser M, Brill S, Wagner H. 2008. In-flight corrections in free-flying barn owls (*Tyto alba*) during sound localization tasks. Journal of Experimental Biology 211:2976–88.

Heffner HE, Heffner RS. 1985. Hearing in two cricetid rodents: wood rat (*Neotoma floridana*) and grasshopper mouse (*Onychomys leucogaster*). Journal of Comparative Psychology 99:275.

Heffner RS, Heffner HE. 1992. Evolution of Sound Localization in Mammals. In: Webster DB, Popper AN, Fay RR, editors. The Evolutionary Biology of Hearing New York, NY: Springer New York. p. 691–715.

Heffner RS, Koay G, Heffner HE. 1996. Sound localization in chinchillas III: Effect of pinna removal. Hearing Research 99:13–21.

Heffner RS, Koay G, Heffner HE. 2001. Audiograms of five species of rodents: implications for the evolution of hearing and the perception of pitch. Hearing Research 157:138–52.

Heithaus M, Dill L, Marshall G, Buhleier B. 2002. Habitat use and foraging behavior of tiger sharks (*Galeocerdo cuvier*) in a seagrass ecosystem. Marine Biology 140:237–48.

Howe MS, Howe MS. 1998. Acoustics of Fluid-Structure Interactions Cambridge University Press.

Jaworski JW, Peake N. 2013. Aerodynamic noise from a poroelastic edge with implications for the silent flight of owls. Journal of Fluid Mechanics 723:456–479.

Jaworski JW, Peake N. 2020. Aeroacoustics of Silent Owl Flight. Annual Review of Fluid Mechanics 52.

JMP®. 2019. Cary, NC: SAS Institute, Inc.

Knudsen EI. 1981. The Hearing of the Barn Owl. Scientific American 245:113–25.

Knudsen EI. 1989. Fused Binocular Vision is Required for Development of Proper Eye Alignment in Barn Owls. Visual Neuroscience 2:35–40.

Knudsen EI, Blasdel GG, Konishi M. 1979. Sound localization by the barn owl (*Tyto alba*) measured with the search coil technique. J Comp Physiol 133:1–11.

Knudsen EI, Konishi M. 1979. Mechanisms of sound localization in the barn owl (*Tyto alba*). J Comp Physiol 133:13–21.

Koehl M a. R. 2006. The Fluid Mechanics of Arthropod Sniffing in Turbulent Odor Plumes. Chem Senses 31:93–105.

Konishi M. 1973a. How the Owl Tracks Its Prey: Experiments with trained barn owls reveal how their acute sense of hearing enables them to catch prey in the dark. American Scientist 61:414–24.

Konishi M. 1973b. Locatable and Nonlocatable Acoustic Signals for Barn Owls. The American Naturalist 107:775–85.

Konishi M, Knudsen EI. 1979. The oilbird: hearing and echolocation. Science 204:425–27.

Kral K. 2003. Behavioural–analytical studies of the role of head movements in depth perception in insects, birds and mammals. Behavioural Processes 64:1–12.

Larsson M. 2012. Incidental sounds of locomotion in animal cognition. Anim Cogn 15:1–13.

Latta SC, Baltz ME. 1997. Lesser Nighthawk (*Chordeiles acutipennis*). Birds N Am.

Lenhard W, Lenhard A. 2016. Calculation of Effect Sizes. Psychometrica. (https://www.psychometrica.de/effect_size.html).

Lentink D, Haselsteiner AF, Ingersoll R. 2015. In vivo recording of aerodynamic force with an aerodynamic force platform: from drones to birds. Journal of The Royal Society Interface 12:20141283.

LePiane K, Clark CJ. 2020. Evidence that the dorsal velvet of Barn Owl wing feathers decreases rubbing sounds during flapping flight. Integr Comp Biol.

Lucas A, Stettenheim P. 1972. Structure of Feathers. In: Avian Anatomy: Integument p. 247.

Maddison WP, Maddison DR. 2019. Mesquite: a modular system for evolutionary analysis.

Martin G. 2010. Birds by night. London, England. A&C Black Publishers.

Martin GR. 1986. Sensory capacities and the nocturnal habit of owls (*Strigiformes*). Ibis 128:266–77.

Martin GR. 2017. The Owls' Solutions to Nocturnality. In: The Sensory Ecology of Birds. 1st ed New York, New York: Oxford University Press. p. 128–32.

Mascha E. 1905. The structure of wing-feathers. In: Smithsonian Miscellaneous Collections Washington, D.C.: Smithsonian Institution. p. 1–30.

Mason JT, McClure CJW, Barber JR. 2016. Anthropogenic noise impairs owl hunting behavior. Biological Conservation 199:29–32.

Matloff LY, Chang E, Feo TJ, Jeffries L, Stowers AK, Thomson C, Lentink D. 2020. How flight feathers stick together to form a continuous morphing wing. Science 367:293–97.

McClure CJ, Ware HE, Carlisle J, Kaltenecker G, Barber JR. 2013. An experimental investigation into the effects of traffic noise on distributions of birds: avoiding the phantom road. Proceedings of the Royal Society B: Biological Sciences 280:20132290.

Mennitt D, Fristrup KM, Sherrill K, Nelson L. 2013. Mapping sound pressure levels on continental scales using a geospatial sound model. In: Proceedings of Inter-Noise p. 1–11.

Mennitt D, Sherrill K, Fristrup K. 2014. A geospatial model of ambient sound pressure levels in the contiguous United States. The Journal of the Acoustical Society of America 135:2746–64.

Neuhaus W, Bretting H, Swiss B. 1973. Morphological and functional studies of the" silent "flight of owls (*Strix aluco*) compared to the flight of ducks (*Anas platyrhynchos*). Biologische Zentralblatt 92:495–512.

Nicol JAC, Arnott HJ. 1974. Tapeta lucida in the eyes of goatsuckers (*Caprimulgidae*). Proc R Soc Lond B 187:349–52.

Nieboer E, Van der Paardt M. 1977. Hearing of the African Woodowl, *Strix woodfordii*. Netherlands Journal of Zoology 27:227–29.

Norberg RA. 1977. Occurrence and Independent Evolution of Bilateral Ear Asymmetry in Owls and Implications on Owl Taxonomy. Philosophical Transactions of the Royal Society B: Biological Sciences 280:375–408.

Paradis E, Schliep K. 2018. ape 5.0: an environment for modern phylogenetics and evolutionary analyses in R. Bioinformatics 35:526–28.

Payne RS. 1971. Acoustic Location of Prey by Barn Owls (*Tyto alba*). Journal of Experimental Biology 54:535–73.

Peacock J, Spellman GM, Greene NT, Tollin DJ. 2020. Scaling of the avian middle ear. Hearing Research 108017.

Pennell MW, Jonathan M Eastman, Graham J Slater, Joseph W Brown, Josef C Uyeda, Richard G FitzJohn, Michael E Alfaro, Luke J Harmon. 2014. geiger v2.0: an expanded suite of methods for fitting macroevolutionary models to phylogenetic trees. Bioinformatics 30:2216–18.

Pinheiro J, Bates D, Sarkar D. 2020. Nlme: Linear and Nonlinear Mixed Effects Models, R package R Core Team.

Proctor NS, Lynch PJ. 1993. Manual of Ornithology: Avian Structure & Function Yale University Press.

Quiring DT. 1994. Diel activity pattern of a nocturnal moth, *Zeiraphera canadensis,* in nature. Entomologia Experimentalis et Applicata 73:111–20.

R Core Team. 2020. R: A Language and Environment for Statistical Computing Vienna, Austria: R Foundation for Statistical Computing.

Ralls K. 1967. Auditory sensitivity in mice: *Peromyscus* and *Mus musculus*. Animal Behaviour 15:123–28.

Rao C, Ikeda T, Nakata T, Liu H. 2017. Owl-inspired leading-edge serrations play a crucial role in aerodynamic force production and sound suppression. Bioinspir Biomim 12:046008.

Revell LJ. 2012. phytools: an R package for phylogenetic comparative biology (and other things). Methods in Ecology and Evolution 3:217–23.

Rice JJ, May BJ, Spirou GA, Young ED. 1992. Pinna-based spectral cues for sound localization in cat. Hearing Research 58:132–52.

Rogers LE, Hinds WT, Buschbom RL. 1976. A general weight vs. length relationship for insects. Annals of the Entomological Society of America 69:387–389.

Rueden CT, Schindelin J, Hiner MC, DeZonia BE, Walter AE, Arena ET, Eliceiri KW. 2017. ImageJ2: ImageJ for the next generation of scientific image data. BMC Bioinformatics 18:529.

Slobodkin LB. 1974. Prudent Predation Does Not Require Group Selection. The American Naturalist 108:665–78.

Thorpe WH, Griffin DR. 1962. Lack of Ultrasonic Components in the Flight Noise of Owls. Nature 193:594–95.

Usherwood JR, Sparkes EL, Weller R. 2014. Leap and strike kinetics of an acoustically ‘hunting’ barn owl (*Tyto alba*). Journal of Experimental Biology 217:3002–5.

USNVC (United States National Vegetation Classification) (No. V2.03). 2019. United States National Vegetation Classification Database Washington, D.C.: Federal Geographic Data Committee, Vegetation Subcommittee.

van Dijk TV. 1973. A Comparative Study of Hearing in Owls of the Family *Strigidae*. Netherlands Journal of Zoology 23:131–67.

Vermeij GJ. 1983. Intimate associations and coevolution in the sea. In, Coevolution, edited by DJ Futuyma & M. Slatkin Sinauer Associates, Sunderland, Mass.

Vermeij GJ. 1994. The Evolutionary Interaction Among Species: Selection, Escalation, and Coevolution. Annual Review of Ecology and Systematics 25:219–36.

Volman SF, Konishi M. 1990. Comparative Physiology of Sound Localization in Four Species of Owls. Brain Behav Evol 36:196–215.

Wagner H, Weger M, Klaas M, Schröder W. 2017. Features of owl wings that promote silent flight. Interface Focus 7:20160078.

Walls GL. 1942. The vertebrate eye and its adaptive radiation, The vertebrate eye and its adaptive radiation Oxford, England: Cranbrook Institute of Science.

Ware HE, McClure CJ, Carlisle JD, Barber JR. 2015. A phantom road experiment reveals traffic noise is an invisible source of habitat degradation. Proceedings of the National Academy of Sciences 112:12105–12109.

Webster DB. 1962. A Function of the Enlarged Middle-Ear Cavities of the Kangaroo Rat, *Dipodomys*. Physiological Zoology 35:248–55.

Weger M, Wagner H. 2016. Morphological Variations of Leading-Edge Serrations in Owls (*Strigiformes*). Plos One 11:e0149236.

Windsor SP, Bomphrey RJ, Taylor GK. 2014. Vision-based flight control in the hawkmoth Hyles lineata. J R Soc Interface 11.

Wink M, El-Sayed A-A, Sauer-Gürth H, Gonzalez J. 2009. Molecular Phylogeny of Owls (*Strigiformes*) Inferred from DNA Sequences of the Mitochondrial Cytochrome b and the Nuclear RAG-1 gene. Ardea 97:581–91.

Wissa A, Han AK, Cutkosky MR. 2015. Wings of a Feather Stick Together: Morphing Wings with Barbule-Inspired Latching. In: Wilson SP, Verschure PFMJ, Mura A, Prescott TJ, editors. Biomimetic and Biohybrid Systems. Lecture Notes in Computer Science Springer International Publishing. p. 123–34.

Wood JR, Mitchell KJ, Scofield RP, De Pietri VL, Rawlence NJ, Cooper A. 2017. Phylogenetic relationships and terrestrial adaptations of the extinct laughing owl, Sceloglaux albifacies (Aves: *Strigidae*). Zool J Linn Soc 179:907–18.

Woods RS. 1924. Notes on the Life History of the Texas Nighthawk. The Condor 26:3–6.

Supplemental Materials:

Table.1.S1. Photograph sources for facial disc analysis.

Species	Link
Aegolius acadicus	https://idfg.idaho.gov/species/taxa/19992
	https://www.boisestatepublicradio.org/post/mountain-west-voices-owl-hand
	https://www.sdakotabirds.com/species/northern_sawwhet_owl_info.htm
Aegolius funereus	https://www.fotosearch.com/IMB001/ibxhje03984733/
	https://www.naturepl.com/stock-photo-tengmalm-s-boreal-owl-aegolius-funereus-perched-on-branch-kuusamo-image01384845.html
	https://www.shutterstock.com/video/clip-3806273-boreal-owl-aegolius-funereus-small-northern-woods
Aegolius harrisi	http://carolinabirds.org/Images3LG/Owl,_Buff-fronted_Nortondefeis.jpg
	https://i.pinimg.com/originals/ec/9a/17/ec9a17aa83c67a72d838f81e6e7f4a10.jpg
	https://www.hbw.com/ibc/species/buff-fronted-owl-aegolius-harrisii
Asio capensis	https://www.alamy.com/stock-photo-marsh-owl-south-africa-12604901.html
	https://www.flickr.com/photos/arnolouise/4814323325
	https://www.joelsartore.com/bir025-00499/
Asio clamator	http://dev.seviradigital.com/birdier/bird/pseudoscops-clamator/5b0f522f35863
	https://i.pinimg.com/originals/a7/a9/8f/a7a98ff8dd59502f61a4ab076aed5ffd.jpg
	https://www.hbw.com/ibc/photo/striped-owl-asio-clamator/adult-bird-perch
Asio flammeus	http://www.littlethetford.org/?page_id=1765
	http://www.luontoportti.com/suomi/en/linnut/short-eared-owl
	https://www.hbw.com/ibc/photo/short-eared-owl-asio-flammeus/short-eared-owl-perched-post-along-teller-road
Asio grammicus	https://www.alamy.com/jamaican-owl-pseudoscops-grammicus-perched-on-a-branch-in-jamaica-in-the-caribbean-image240028817.html
	https://www.flickr.com/photos/paulbjones/5644709542
	https://www.hbw.com/species/jamaican-owl-pseudoscops-grammicus
Asio otus	https://dissolve.com/stock-photo/Long-eared-owl-Asio-otus-captive-United-Kingdom-rights-managed-image/102-D246-38-127
	https://www.monaconatureencyclopedia.com/asio-otus/?lang=en
	https://www.sdakotabirds.com/species/long_eared_owl_info.htm

Athene cunicularia	https://sv.wikipedia.org/wiki/Pr%C3%A4rieuggla#/media/File:Burrowing_Owl_(Athene_cunicularia)_(2261438123).jpg
	https://www.gettyimages.com/detail/photo/studio-portrait-of-a-burrowing-owl-athene-high-res-stock-photography/670872861
	https://www.shutterstock.com/image-photo/burrowing-owl-athene-cunicularia-marco-island-94174939
Athene noctua	https://dissolve.com/stock-photo/Little-owl-athene-noctua-couple-perched-branch-Negev-royalty-free-image/101-D30-21-029
	https://www.hbw.com/ibc/photo/little-owl-athene-noctua/wire
	https://www.hbw.com/ibc/species/little-owl-athene-noctua
Bubo africanus	https://www.123rf.com/photo_48903949_spotted-eagle-owl-bubo-africanus-4-years-old-in-front-of-a-white-background.html
	https://www.dreamstime.com/stock-photos-spotted-eagle-owl-bubo-africanus-image24622923
	https://www.flickr.com/photos/therealthings/38903541395
Bubo ascalaphus	https://www.deanbricknellphotography.com/Owls/i-Fc4bT3K/
	https://www.eyalbartov.com/ISRAEL/BIRDSOFISRAEL/Owls/%D7%90%D7%95%D7%97-%D7%9E%D7%93%D7%91%D7%A8%D7%99-Pharaoh/i-mLT8mNx
	https://www.zoochat.com/community/media/pharaoh-s-eagle-owl-bubo-ascalaphus.221566/
Bubo bubo	https://www.monaconatureencyclopedia.com/bubo-bubo/?lang=en
	https://www.peregrinefund.org/explore-raptors-species/Eurasian_Eagle-owl
	https://www.robertharding.com/preview/832-379254/eurasian-eagleowl-bubo-bubo-adult-portrait-winter-zdarske/
Bubo cinerascens	https://www.hbw.com/ibc/photo/greyish-eagle-owl-bubo-cinerascens/front-view-adult-ground-night
	https://www.hbw.com/ibc/photo/greyish-eagle-owl-bubo-cinerascens/greyish-eagle-owl-hunting-insects-road-night
	https://www.zoochat.com/community/media/greyish-eagle-owl-bubo-cinerascens.209989/
Bubo ketupu	https://www.flickr.com/photos/avianphotos/11847230674
	https://www.flickr.com/photos/marklouisbenedict_photography/26103360584
	https://www.whywelovebirds.com/p754480775
Bubo lacteus	https://en.wikipedia.org/wiki/Verreaux%27s_eagle-owl#/media/File:2012-giant-eagle-owl.jpg
	https://www.123rf.com/photo_48904005_verreaux-s-eagle-owl-bubo-lacteus-3-years-old-in-front-of-a-white-background.html
	https://www.pinterest.ca/pin/7388786868665423/
Bubo nipalensis	https://commons.wikimedia.org/wiki/File:Bubo_nipalensis_-_M%C3%A9nagerie_Paris_01.JPG
	https://fog.ccsf.edu/~jmorlan/India/Spot-belliedEagle-OwlIMG_3465.htm
	https://www.pinterest.com/pin/424534702348498435/?lp=true
Bubo scandiacus	https://leesbird.com/kids-section/bible-birds/bible-birds-owls/78-snowy-owl-bubo-scandiacus-2-by-raymond-barlow/

	https://photodune.net/item/snowy-owl-bubo-scandiacus/22381511
	https://www.123rf.com/photo_54784992_snowy-owl-bubo-scandiacus-perched-on-a-post-making-eye-contact-with-piercing-yellow-eyes-light-snowf.html
Bubo virginianus	https://adlayasanimals.wordpress.com/2015/02/01/great-horned-owl-bubo-virginianus/
	https://fineartamerica.com/featured/great-horned-owl-bubo-virginianus-zssd.html
	https://www.owlpages.com/owls/species.php?i=300
Glaucidium brasilianum	https://hiveminer.com/Tags/brasilianum%2Cglaucidium/Timeline
	https://www.hbw.com/ibc/photo/ferruginous-pygmy-owl-glaucidium-brasilianum/cabure-chico-glaucidium-brasilianum
	https://www.hbw.com/ibc/species/ferruginous-pygmy-owl-glaucidium-brasilianum
Glaucidium brodiei	https://flickr.com/photos/68466173@N02/48027990903
	https://www.dreamstime.com/stock-photo-collared-owlet-glaucidium-brodiei-standing-stump-morning-close-up-image98231302
	https://www.inaturalist.org/guide_taxa/785957
Glaucidium californicum	https://alchetron.com/Pygmy-owl
	https://www.alamy.com/stock-photo/glaucidium-californicum.html
	https://www.flickr.com/photos/shyalbatross/3165903504
Glaucidium capense	https://commons.wikimedia.org/wiki/File:African_barred_owlet,_Glaucidium_capense,_in_the_tree_we_were_camped_under_at_Savuti,_Chobe_National_Park,_Botswana_(33770053142).jpg
	https://emuwren.tumblr.com/post/89706287094/the-african-barred-owl-glaucidium-capense-is-a
	https://www.pinterest.com/pin/465489311468676826/
Glaucidium gnoma	https://brendanmcgarry.photoshelter.com/image/I0000quGm6Huo0Dk
	https://dissolve.com/stock-photo/Northern-Pygmy-Owl-Glaucidium-gnoma-swarthi-Vancouver-Island-royalty-free-image/101-D1294-11-602
	https://www.mindenpictures.com/search/preview/mountain-pygmy-owl-glaucidium-gnoma-western-montana/0_00558083.html
Glaucidium jardini	https://birdscolombia.com/2018/07/27/buhito-andino-andean-pygmy-owl-glaucidium-jardinii/
	https://www.flickr.com/photos/jjarango/29026123775
	https://www.flickr.com/photos/marytorresescobar/16036621492
Glaucidium passerinum	https://www.123rf.com/photo_101259046_eurasian-pygmy-owl-glaucidium-passerinum-.html
	https://www.agefotostock.com/age/en/Stock-Images/Rights-Managed/BWI-BLWS049435
	https://www.picfair.com/pics/01871344-dwerguil-eurasian-pygmy-owl-glaucidium-passerinum

Glaucidium perlatum	https://sanwild.site/2018/03/21/pearl-spotted-owl-almost-ready-to-be-released/
	https://www.hbw.com/ibc/photo/pearl-spotted-owlet-glaucidium-perlatum/adult-perched-dusk
	https://www.hbw.com/ibc/species/pearl-spotted-owlet-glaucidium-perlatum
Glaucidium tephronotum	https://www.africanbirdclub.org/afbid/search/birddetails/species/831/23143
	https://www.biolib.cz/cz/taxonimage/id230412/
	https://www.hbw.com/ibc/species/red-chested-owlet-glaucidium-tephronotum#photos
Jubula letti	https://www.oiseaux.net/birds/maned.owl.html
Ketupa zeylonensis	https://indianbirds.thedynamicnature.com/2017/04/brown-fish-owl-ketupa-zeylonensis.html
	https://www.discoverlife.org/mp/20p?see=I_LHT26269&res=640
	https://www.juzaphoto.com/life.php?l=en&s=ketupa_zeylonensis
Lophostrix cristata	https://commons.wikimedia.org/wiki/File:Coruja-de-crista_(Lophostrix_cristata).jpg
	https://www.hbw.com/ibc/photo/crested-owl-lophostrix-cristata/adult-bird-perched
	https://www.hbw.com/ibc/photo/crested-owl-lophostrix-cristata/bird-perched-0
Margaobyas lawrencii	https://www.flickr.com/photos/birdshots-birdlister/27054844330
	https://www.hbw.com/ibc/photo/bare-legged-screech-owl-margarobyas-lawrencii/cuban-screech-owl-gymnoglaux-lawrencii
	https://www.naturepl.com/stock-photo-nature-image01599320.html
Megascops asio	https://www.allposters.com/-sp/A-Captive-Eastern-Screech-Owl-Megascops-Asio-at-Ryerson-Woods-Posters_i9432016_.htm
	https://www.dreamstime.com/stock-image-eastern-screech-owl-megascops-asio-image8365791
	https://www.owlpages.com/owls/species.php?i=189
Megascops choliba	https://species.wikimedia.org/wiki/Megascops_choliba
	https://www.owlpages.com/owls/species.php?i=220
	https://www.owlpages.com/owls/species.php?i=939
Megascops kennicotti	https://dissolve.com/stock-photo/Western-Screech-Owl-Interior-Megascops-kennicottii-macfarlanei-royalty-free-image/101-D1294-11-759
	https://www.owlpages.com/owls/species.php?i=167
	https://www.picfair.com/pics/06271014-westelijke-schreeuwuil-western-screech-owl-megascops-kennicottii
Megascops nudipes	https://neotropical.birds.cornell.edu/Species-Account/nb/species/prsowl/overview
	https://www.hbw.com/ibc/photo/puerto-rican-screech-owl-megascops-nudipes/adult-tree

	https://www.owling.com/puerto-rican-screech-owl/
Micrathene whitneyi	https://www.alamy.com/elf-owl-micrathene-whitneyi-adult-image277615908.html https://www.inaturalist.org/taxa/20379-Micrathene-whitneyi https://www.naturemobile.org/en/species/2700/micrathene-whitneyi
Mimizuku gurneyi	https://animals.fandom.com/wiki/Giant_Scops_Owl?file=142188972.mWjJJlkm.IMG_3226web.jpg https://www.flickr.com/photos/28722516@N02/2848122238 https://www.owlpages.com/owls/species.php?i=277
Nesasio solomensis	https://www.hbw.com/ibc/photo/fearful-owl-nesasio-solomonensis/adult-perched-nesting-tree-massive-fig https://www.hbw.com/ibc/photo/fearful-owl-nesasio-solomonensis/bird-tree https://www.hbw.com/ibc/photo/fearful-owl-nesasio-solomonensis/seen-perched-huge-fig-after-tough-and-slippery-walk
Ninox boobook	https://canberra.naturemapr.org/Community/Species/Sightings/15079 https://www.owlpages.com/owls/species.php?i=1026 https://www.owlpages.com/owls/species.php?i=798
Ninox connivens	https://animals.fandom.com/wiki/Barking_Owl https://www.owlpages.com/owls/species.php?i=778 https://www.shutterstock.com/image-photo/barking-owl-ninox-connivens-close-portrait-1186603186
Ninox jacquinoti	https://www.conservapedia.com/images/3/3e/Southern_boobook.jpg https://www.hbw.com/ibc/photo/west-solomons-boobook-ninox-jacquinoti/pair-outside-their-roost-hole https://www.hbw.com/ibc/photo/west-solomons-boobook-ninox-jacquinoti/solomons-boobook-perched-its-nesting-tree-called
Ninox rufa	http://laurieross.com.au/border_galleries/owls/ https://www.gettyimages.co.nz/detail/photo/rufous-owl-ninox-rufa-at-the-taronga-zoo-high-res-stock-photography/670870507 https://www.pinterest.com/pin/260997740877687310/?lp=true
Ninox scutulata	http://www.birdsofbangladesh.com/viewtopic.php?t=22&p=49 https://www.owlpages.com/owls/species.php?i=810 https://www.owlpages.com/owls/species.php?i=814
Ninox strenua	https://leesbird.com/2012/12/09/ians-bird-of-the-week-powerful-owl/78-powerful-owl-ninox-strenua-by-ian-1/ https://www.agefotostock.com/age/en/Stock-Images/Rights-Managed/MPC-00526121 https://www.mindenpictures.com/search/preview/powerful-owl-ninox-strenua-australia/0_00525914.html
Ninox superciliaris	https://www.flickr.com/photos/65768681@N06/16743342078/

	https://www.flickr.com/photos/sylvie-et-rene/13610577915
	https://www.owlpages.com/owls/species.php?i=818
Otus albogularis	https://www.hbw.com/ibc/photo/white-throated-screech-owl-megascops-albogularis/dorsal-view-adult-perched
	https://www.hbw.com/ibc/photo/white-throated-screech-owl-megascops-albogularis/frontal-view
	https://www.hbw.com/species/white-throated-screech-owl-megascops-albogularis
Otus bakkamoena	http://www.uilenhartjes.nl/index.php/en/owls/little-owls/product/12-otus-bakkamoena
	https://i.pinimg.com/originals/c4/33/c9/c433c940aeafea829f48eeb8cb1e9001.jpg
	https://www.alamy.com/stock-photo-young-indian-scops-owl-otus-bakkamoena-in-front-of-white-background-31375770.html
Otus brucei	https://indianbirds.thedynamicnature.com/2016/12/pallid-scops-owl-otus-brucei.html
	https://www.birdguides.com/gallery/birds/otus-brucei/639609/
	https://www.pbase.com/image/151304794
Otus flammeolus	https://www.alamy.com/stock-photo-female-flammulated-owl-otus-flammeolus-southern-okanagan-valley-british-43909966.html
	https://www.flickr.com/photos/shyalbatross/3618716292
	https://www.joelsartore.com/bir025-00139/?context=flammulated+owl&index=5
Otus podarginus	https://paddlingpalau.net/blog/archives/07-2019
	https://www.hbw.com/species/palau-owl-pyrroglaux-podargina
	https://www.owlpages.com/owls/species.php?i=921
Otus scops	https://fineartamerica.com/featured/european-scops-owl-otus-scops-photostock-israel.html
	https://www.hbw.com/ibc/photo/eurasian-scops-owl-otus-scops/perched-branch
	https://www.hbw.com/ibc/species/eurasian-scops-owl-otus-scops
Otus spilocephalus	https://www.flickr.com/photos/9691141@N07/5080126222/
	https://www.owlpages.com/owls/species.php?i=79
	https://www.reddit.com/r/Superbowl/comments/7mha8d/mountain_scops_owl_otus_spilocephalus/?ref=readnext
Phodilus badius	https://en.wikipedia.org/wiki/Oriental_bay_owl#/media/File:Oriental_bay_owl,_Phodilus_badius_-_Khao_Yai_National_Park.jpg
	https://www.art.com/products/p48945757962-sa-i11132991/joel-sartore-a-common-bay-owl-phodilus-badius-badius-at-penang-bird-park.htm
	https://www.owlpages.com/owls/species.php?i=64
Ptilopsis leucotis	https://depositphotos.com/221668638/stock-photo-northern-white-faced-owl-ptilopsis.html
	https://elements.envato.com/northern-white-faced-owl-ptilopsis-leucotis-1-PB25K5D
	https://www.123rf.com/photo_65482065_closeup-of-an-endangered-northern-white-faced-owl-ptilopsis-leucotis-.html

Pulsatrix koeniswaldania	http://carolinabirds.org/People/SanchesDarioLG/Owl,_Tawny-browed_DarioSanches.jpg
	https://birdier.com/bird/pulsatrix-koeniswaldiana/5b5626b7a0ac2
Pulsatrix melanonata	https://www.hbw.com/ibc/photo/band-bellied-owl-pulsatrix-melanota/adult-perched-tree
	https://www.pinterest.com/pin/476607573038206276/
	https://www.whywelovebirds.com/p838359474/h267DAEBB
Pulsatrix perspicillata	https://i.pinimg.com/originals/60/30/3e/60303ecd97344061f19fbb134edc0cc2.jpg
	https://www.fotosearch.com/CSP169/k17391554/
	https://www.youtube.com/watch?v=crZqkxOjp2k
Scotopelia peli	https://www.alamy.com/pels-fishing-owl-with-tiger-fish-scotopelia-peli-okavango-river-delta-botswana-image181667092.html
	https://www.igoterra.com/photo_info.asp?photoid=215979
	https://www.rockjumperbirding.com/dt_gallery/gallery-tours-zambia-south-luangwa-extension/pels-fishing-owl-by-jonathan-rossouw
Strix aluco	https://www.123rf.com/photo_65765563_young-tawny-owl-in-forest-strix-aluco.html
	https://www.alamy.com/stock-photo-tawny-owl-sitting-on-a-branch-strix-aluco-89966177.html
	https://www.owlpages.com/owls/species.php?i=410
Strix butleri	https://amirbendov.zenfolio.com/strix-hadorami-final-article--14-10-2017-pdf.pdf
	https://thedrunkbirder.wordpress.com/2015/08/22/unravelling-the-mystery-of-the-omani-owl/
	https://www.hbw.com/ibc/species/omani-owl-strix-butleri
Strix nebulosa	https://www.123rf.com/photo_70113018_great-grey-owl-perched-atop-a-tree-in-winter-strix-nebulosa-.html
	https://www.owlpages.com/owls/species.php?i=508
	https://www.owlpages.com/owls/species.php?i=518
Strix rufipes	http://www.fotonaturaleza.cl/details.php?image_id=13115
	https://www.deviantart.com/woodwose/art/Strix-rufipes-133322725
	https://www.pinterest.com/pin/150237337555752977/?lp=true
Strix uralensis	https://commons.wikimedia.org/wiki/File:Strix_uralensis_0a1.JPG
	https://www.123rf.com/photo_96591866_the-ural-owl-strix-uralensis-is-a-medium-sized-nocturnal-owl-found-in-europe-and-northern-asia-.html
	https://www.flickr.com/photos/pokerbrit/6166203339

Strix varia	https://dissolve.com/stock-photo/Juvenile-Barred-Owl-Strix-royalty-free-image/101-D869-59-943
	https://pixels.com/featured/barred-owl-strix-varia-closeup-michael-russell.html
	https://www.hbw.com/ibc/species/barred-owl-strix-varia#photos
Strix virgata	http://www.ecoregistros.org/site_en/imagen.php?id=51777
	https://en.wikipedia.org/wiki/Mottled_owl#/media/File:Mottled_Owl.jpg
	https://www.flickr.com/photos/21182099@N05/37491156876
Strix woodfordii	https://www.alamy.com/stock-photo-african-wood-owl-strix-woodfordii-perched-on-a-mossy-bank-50583002.html
	https://www.hbw.com/ibc/photo/african-wood-owl-strix-woodfordii/african-wood-owl-perched-1
	https://www.hbw.com/ibc/photo/african-wood-owl-strix-woodfordii/bird-perched
Surina ulula	http://www.jaakphoto.com/en/2012/03/#592
	https://dissolve.com/stock-photo/Northern-Hawk-Owl-Surnia-ulula-perched-Prince-Albert-royalty-free-image/101-D1294-14-246
	https://www.hbw.com/ibc/photo/northern-hawk-owl-surnia-ulula/northern-hawk-owl-perched-0
Tyto alba	https://pixels.com/featured/barn-owl-tyto-alba-portrait-hudson-tom-vezo.html
	https://www.allposters.com/-sp/Female-Barn-Owl-Tyto-Alba-World-Owl-Trust-Muncaster-Castle-Ravenglass-Cumbria-UK-Captive-Posters_i3159879_.htm
	https://www.robertharding.com/preview/1219-174/barn-owl-tyto-alba-resting-perched-roadside-wooden/
Tyto longimembris	https://www.biolib.cz/en/image/id315687/
	https://www.owlpages.com/owls/species.php?i=48
	https://www.owlpages.com/owls/species.php?i=916
Tyto novaehollandiae	https://commons.wikimedia.org/wiki/File:Tyto_novaehollandiae_castanops_male_2_-_Port_Arthur.jpg
	https://www.owlpages.com/owls/species.php?i=36
	https://www.owlpages.com/owls/species.php?i=37
Tyto tenebricosa	https://www.owlpages.com/owls/species.php?i=57
	https://www.owlpages.com/owls/species.php?i=59
	https://www.pinterest.com/pin/407786941231095808/?lp=true

Uroglaux dimorpha	http://1.bp.blogspot.com/-7NH5lRZ1ykw/Toxgl6sT6YI/AAAAAAAAAIo/8wv262f2DEY/s1600/Hawk-Owl%252C+Papuan-GV.JPG
	https://www.agefotostock.com/age/en/Stock-Images/Rights-Managed/MEV-10850058
	https://www.hbw.com/ibc/species/papuan-hawk-owl-uroglaux-dimorpha

Table 1.S2. Disc PC1, Comb PC1, Stealth, and Masking scores, and ecology for species used in pgls.

Species	Disc PC1	Disc PC2	Comb PC1	Comb PC2	Size PC1	Size PC2	Stealth (0-3)	Masking (0-4)	Prey type	Habitat	Active Period	Hunting Strategy
Aegolius acadicus	0.99	0.41	0.61	-0.03	-2.14	-0.43	2	2	mammals	forest	nocturnal	sit-and-wait
*Aegolius funereus**	2.39	0.69	1.04	0.51	-1.20	-0.62	2	4	mammals	forest	nocturnal	through snow
*Aegolius harrisi**	1.95	0.76	0.48	2.10	-1.56	0.37	1	2	generalist	forest	nocturnal	unknown
*Asio capensis**	3.50	0.40	1.15	-0.55	1.34	0.46	1	3	generalist	grassland	nocturnal	quartering
*Asio clamator**	2.09	0.35	2.15	-0.93	0.80	-0.19	1	3	generalist	generalist	nocturnal	quartering
*Asio flammeus**	2.02	-1.52	1.08	0.41	0.85	-0.37	2	4	mammals	grassland	nocturnal	quartering
Asio otus	-0.01	-1.54	2.50	-0.57	0.59	-0.60	2	3	mammals	grassland	nocturnal	quartering
Athene cunicularia	-1.28	-0.55	-1.16	-1.94	-0.65	0.91	1	0	generalist	grassland	crepuscular	sit-and-wait
Athene noctua	-1.93	-1.06	-0.24	-0.42	-1.16	0.63	1	1	generalist	woodland	nocturnal	sit-and-wait
Athene superciliaris	-1.55	-0.19	-0.73	-1.69	-0.46	-0.19	1	1	generalist	forest	nocturnal	sit-and-wait
Bubo africanus	0.50	0.33	2.06	0.54	1.54	0.04	2	1	generalist	desert	nocturnal	sit-and-wait
Bubo ascalaphus	-0.36	-0.06	3.01	0.09	2.62	0.35	2	1	generalist	desert	nocturnal	sit-and-wait
Bubo bubo	-0.26	0.32	2.95	-0.39	2.70	-0.43	2	1	generalist	desert	nocturnal	sit-and-wait
Bubo cinerascens	-0.76	0.02	1.38	0.42	1.71	0.32	2	1	generalist	desert	nocturnal	sit-and-wait
Bubo lacteus	0.51	0.49	0.68	-0.30	2.82	-0.08	1	1	generalist	woodland	nocturnal	sit-and-wait
Bubo nipalensis	-0.09	0.00	1.27	-1.90	2.66	-0.13	1	1	generalist	forest	nocturnal	sit-and-wait
Bubo scandiacus	-0.61	-1.13	0.69	-0.52	2.06	-0.73	3	3	mammals	tundra	nocturnal	through snow
Bubo virginianus	-0.81	-0.54	2.54	-0.06	1.96	-0.40	1	1	generalist	generalist	nocturnal	sit-and-wait
Ciccaba virgata	0.54	0.40	1.09	0.12	0.56	-0.16	1	1	generalist	forest	nocturnal	sit-and-wait
Glaucidium brasilianum	-1.21	-0.18	-2.82	-0.08	-2.88	-0.19	1	0	generalist	woodland	diurnal	sit-and-wait
Glaucidium brodiei	-2.65	-1.98	-2.23	0.82	-2.94	0.00	1	0	generalist	forest	diurnal	sit-and-wait

Glaucidium capense	-1.99	-0.75	-2.72	-1.26	-1.99	-0.32	1	0	arthropods	woodland	diurnal	sit-and-wait
Glaucidium gnoma	-2.06	-1.10	-2.81	-0.73	-3.51	-0.81	1	0	generalist	forest	diurnal	sit-and-wait
Glaucidium jardinii	-1.12	-0.33	-4.10	0.94	-2.72	0.03	1	0	generalist	forest	diurnal	unknown
Glaucidium passerinum	-1.49	-1.31	-1.76	-0.38	-3.11	-0.46	1	0	generalist	forest	diurnal	sit-and-wait
Glaucidium perlatum	-1.77	-0.76	-2.24	0.45	-2.37	-0.31	1	0	arthropods	woodland	diurnal	sit-and-wait
Jubula lettii	-1.22	-0.31	0.02	0.73	0.82	-0.66	1	1	arthropods	forest	nocturnal	unknown
Ketupa ketupu	-0.89	-0.12	-0.93	-0.90	1.84	0.34	0	0	fish	forest	nocturnal	sit-and-wait
Ketupa zeylonensis	-1.12	-0.52	-0.88	-0.06	2.36	0.27	0	0	fish	woodland	nocturnal	sit-and-wait
Lophopstrix cristata	-1.14	0.31	-1.78	-0.48	0.97	-0.53	1	1	arthropods	forest	nocturnal	unknown
Margarobyas lawrencii	-0.60	0.84	-1.50	-1.74	-1.02	0.62	1	1	arthropods	forest	nocturnal	sit-and-wait
Megascops albogularis	-0.96	0.00	0.76	-0.94	-0.43	-0.27	1	1	arthropods	forest	nocturnal	unknown
Megascops asio	-1.10	0.06	1.09	-0.44	-1.19	0.18	1	1	generalist	forest	nocturnal	sit-and-wait
Megascops choliba	-1.27	0.31	0.43	0.08	-1.09	-0.32	1	1	generalist	woodland	nocturnal	sit-and-wait
Megascops kennicottii	-0.38	0.06	1.69	-0.60	-0.91	0.06	1	1	generalist	woodland	nocturnal	sit-and-wait
Megascops nudipes	-1.45	0.55	-0.57	0.68	-0.56	0.24	1	1	arthropods	forest	nocturnal	unknown
Micrathene whitneyi	-1.69	-0.82	-0.81	-0.93	-2.99	0.29	2	0	flying insects	woodland	nocturnal	sit-and-wait

Nesasio solomonensis	-0.73	0.00	-0.56	1.89	1.10	0.19	2	2	mammals	forest	nocturnal	unknown
Ninox boobook	-0.36	0.93	0.41	-0.26	0.63	-0.15	2	0	flying insects	generalist	nocturnal	sit-and-wait
Ninox connivens	-0.33	1.04	-0.25	-1.90	1.16	-0.42	1	1	generalist	generalist	nocturnal	sit-and-wait
Ninox jacquinoti	-0.78	1.12	-0.69	-1.14	-0.25	0.39	1	1	arthropods	forest	nocturnal	unknown
Ninox rufa	0.27	2.53	-0.06	-0.41	1.64	-0.48	2	2	mammals	woodland	nocturnal	sit-and-wait
Ninox scutulata	-1.45	0.65	-1.44	-2.64	-0.38	-0.47	1	1	arthropods	forest	nocturnal	sit-and-wait
Ninox strenua	-0.50	0.57	-0.68	0.39	2.43	-0.60	2	2	mammals	forest	nocturnal	sit-and-wait
Otus brucei	-0.86	0.02	-1.27	1.12	-1.40	0.36	1	1	arthropods	woodland	nocturnal	sit-and-wait
Otus scops	-1.45	-0.43	-1.63	-0.23	-2.15	0.10	1	1	generalist	woodland	nocturnal	sit-and-wait
*Pseudoscops grammicus**	1.56	-0.26	1.23	0.70	0.33	0.24	1	1	generalist	woodland	nocturnal	unknown
Phodilus badius	0.36	0.43	-1.41	3.99	-0.42	0.53	1	1	generalist	forest	nocturnal	sit-and-wait
Psiloscops flammeolus	-0.61	0.28	-1.02	-0.81	-2.34	-0.01	2	0	flying insects	forest	nocturnal	sit-and-wait
*Ptilopsis leucotis**	1.09	1.87	1.67	0.73	-0.83	-0.11	2	3	mammals	generalist	nocturnal	sit-and-wait
*Pulsatrix koeniswaldiana**	1.13	1.35	1.12	-0.11	1.28	-0.55	1	1	generalist	forest	nocturnal	sit-and-wait
Pulsatrix perspicillata	-0.56	0.73	1.90	-0.84	1.38	-0.35	2	2	mammals	forest	nocturnal	sit-and-wait
Scotopelia peli	0.56	1.34	-0.37	1.00	2.74	0.10	0	0	fish	forest	nocturnal	sit-and-wait
*Strix aluco**	2.02	-0.36	2.29	-0.59	0.98	-0.49	2	3	mammals	woodland	nocturnal	sit-and-wait
*Strix butleri**	1.66	-0.19	1.83	-0.09	1.05	0.35	1	2	generalist	woodland	nocturnal	unknown
*Strix nebulosa**	5.31	-1.75	2.60	-0.70	2.36	-1.33	2	4	mammals	forest	nocturnal	through snow
*Strix rufipes**	1.58	0.46	1.56	-1.09	0.69	-0.34	2	3	mammals	forest	nocturnal	sit-and-wait
*Strix uralensis**	3.20	-1.45	1.48	-0.10	2.30	-0.86	2	3	mammals	forest	nocturnal	through snow

*Strix varia**	2.54	0.17	2.35	-1.82	1.67	-0.67	1	3	generalist	forest	nocturnal	through snow
Strix woodfordii	0.84	0.86	1.36	-0.79	0.65	-0.17	1	1	generalist	woodland	nocturnal	sit-and-wait
Surnia ulula	0.30	-1.03	-0.82	-1.86	0.29	-1.14	2	3	mammals	forest	nocturnal	through snow
*Tyto alba**	1.83	-1.98	1.28	1.07	1.18	0.90	2	4	mammals	generalist	nocturnal	quartering; through snow
*Tyto longimembris**	2.28	-2.91	-1.38	2.42	1.65	1.51	2	4	mammals	grassland	nocturnal	quartering
*Tyto novaehollandiae**	2.12	-1.43	0.94	2.07	1.22	0.84	2	3	mammals	forest	nocturnal	sit-and-wait
Tyto tenebricosa	1.02	-0.58	-0.54	3.95	0.99	1.04	2	2	mammals	forest	nocturnal	sit-and-wait
Uroglaux dimorpha	-1.31	0.48	-1.38	0.33	0.05	-0.50	1	1	generalist	forest	nocturnal	unknown

*Species in the top 25% of Disc PC1 score, awarded a point for masking

Table 1.S3 Species averages of raw comb measurements used in Principal components analysis. Values presented as mean ± s.d.

species	N	Length of R1 (cm)	Tarsus length (cm)	Folded wing length (cm)	Comb length 25% (mm)	Comb length 50% (mm)	Comb length 75% (mm)	Comb length 100% (mm)	Distance between barbs (mm)	Barb density (barbs/cm)	Tip width (mm)
Aegolius acadicus	6	73.17 ± 3.97	16.39 ± 2.68	140.83 ± 9.11	1.38 ±0.38	1.27 ± 0.16	0.68 ± 0.26	0.38 ± 0.17	0.34 ±0.16	14.2 ± 1.0	0.14 ± 0.1
Aegolius funereus	6	99 ± 7.13	19.49 ± 5.72	174.5 ± 8.26	1.48 ± 0.61	1.40 ± 0.52	1.08 ± 0.54	0.32 ± 0.07	0.32 ± 0.07	15.7 ± 2.0	0.11 ± 0.03
Aegolius harrisi	1	63	23.24	176	2.27	1.58	0.71	0.24	0.25	20.00	0.09
Aegolius tengmalma	1	86	19.38	160	1.77	1.53	0.96	0.28	0.28	19.00	0.09
Asio abyssinicus	1	170	39.09	362	2.70	2.73	2.49	0.20	0.41	13.00	0.17
Asio capensis	6	145 ± 6.93	52.35 ± 3.15	290.5 ± 17.11	1.92 ± 0.2	1.70 ± 0.17	0.68 ± 0.31	0.19 ± 0.17	0.36 ± 0.2	14 ± 1.79	0.10 ± 0.02
Asio clamator	6	147.83 ± 9.33	36.67 ± 5.9	272.17 ± 31.52	3.01 ± 0.83	2.9 ± 0.58	1.60 ± 0.43	0.42 ± 0.15	0.37 ± 0.1	11.8 ± 1.0	0.15 ± 0.06
Asio flammeus	6	145.83 ± 6.43	33.51 ± 3.53	310.33 ± 7.84	1.35 ± 0.29	1.40 ± 0.41	1.30 ± 0.30	0.44 ± 0.29	0.29 ± 0.05	16.0 ± 1.0	0.12 ± 0.03

Asio grammicus	4	122 ± 3.37	38.69 ± 2.4	221.75 ± 11.79	2.02 ± 0.47	1.83 ± 0.30	1.05 ± 0.41	0.27 ± 0.17	0.25 ± 0.04	16 ± 2.0	0.12 ± 0.03
Asio otus	6	145 ± 9.47	29.03 ± 2.14	296.5 ± 7.04	2.89 ± 0.32	2.67 ± 0.31	2.47 ± 0.56	0.57 ± 0.24	0.38 ± 0.07	12.5 ± 1.0	0.07 ± 0.01
Asio stygius	8	161.56 ± 8.55	38.95 ± 4.26	321.11 ± 20.91	1.71 ± 0.28	1.64 ± 0.10	1.27 ± 0.37	0.47 ± 0.21	0.32 ± 0.09	15 ± 1.7	0.10 ± 0.04
Heteroglaux blewitti	1	75	25.58	160	0.28	0.31	0.29	0.25	0.17	17.00	0.09
Athene bramba	9	82 ± 6.36	25.07 ± 2.71	157 ± 6.2	0.83 ± 0.30	0.60 ± 0.18	0.47 ± 0.16	0.19 ± 0.04	0.35 ± 0.16	13.78 ± 1.72	0.15 ± 0.06
Athene cunicularia	7	80.38 ± 6.44	38.18 ± 4.95	167.63 ± 10.11	0.26 ± 0.12	0.32 ± 0.16	0.24 ± 0.13	0.20 ± .014	0.35 ± 0.10	11.5 ± 1.31	0.12 ± 0.07
Athene noctura	6	72.67 ± 5.39	30 ± 3.44	160.83 ± 2.86	0.78 ± 0.03	0.58 ± 0.22	0.36 ± 0.10	0.17 ± 0.10	0.28 ± 0.03	13.67 ± 1.21	0.18 ± 0.04
Bubo africanus	4	166.83 ± 17.52	47.34 ± 7.66	322 ± 16.92	3.73 ± 0.83	3.17 ± 0.79	1.78 ± 0.89	0.34 ± 0.05	0.25 ± 0.03	14.8 ± 2.49	0.14 ± 0.02
Bubo ascalaphus	3	209.33 ± 10.02	69.77 ± 6.17	386 ± 13.23	5.07 ± 0.79	3.9 ± 0.52	2.92 ± 0.26	0.27 ± 0.05	0.36 ± 0.06	14.33 ± 0.58	0.16 ± 0.09
Bubo blackistoni	4	261.2 ± 16.28	65.03 ± 8.42	520.6 ± 30.71	0.56 ± 0.37	0.49 ± 0.26	0.39 ± 0.23	0.27 ± 0.11	0.3 ± 0.13	14.25 ± 1.71	0.1 ± 0.03
Bubo bubo	6	252.17 ± 29.76	53.51 ± 8.84	440.5 ± 41.37	5.6 ± 0.43	4.42 ± 0.53	2.55 ± 0.45	0.24 ± 0.15	0.36 ± 0.08	12.83 ± 1.47	0.1 ± 0.03
Bubo cinerascens	6	167.17 ± 2.32	55.16 ± 7.42	313.33 ± 11	3.18 ± 0.3	2.95 ± 0.41	0.86 ± 0.47	0.2 ± 0.04	0.31 ± 0.03	15.17 ± 1.72	0.1 ± 0.05
Bubo coromandus	6	201.17 ± 24.98	51.66 ± 11.06	322.83 ± 137.53	1.52 ± 0.49	0.65 ± 0.44	0.3 ± 0.29	0.13 ± 0.04	0.27 ± 0.04	13.17 ± 1.83	0.11 ± 0.06

Bubo desertorum	5	187 ± 10.02	61.28 ± 4.22	345 ± 11.34	4.54 ± 0.69	3.33 ± 0.64	1.78 ± 0.11	0.34 ± 0.1	0.33 ± 0.04	14.2 ± 1.1	0.11 ± 0.01
Bubo lacteus	6	231.67 ± 14.64	61.02 ± 3.27	458.67 ± 13.76	1.91 ± 0.33	1.2 ± 0.63	0.62 ± 0.4	0.24 ± 0.16	0.29 ± 0.09	13.33 ± 1.75	0.16 ± 0.04
Bubo leucostictus	9	191 ± 11.11	35.96 ± 3.58	318.33 ± 10.49	1.43 ± 0.59	0.61 ± 0.25	0.29 ± 0.11	0.17 ± 0.06	0.29 ± 0.12	14.22 ± 1.09	0.15 ± 0.07
Bubo nipalensis	6	221.33 ± 7.28	57.18 ± 8.1	454 ± 17.45	3.09 ± 1.03	1.64 ± 1.1	0.42 ± 0.2	0.25 ± 0.13	0.46 ± 0.17	11.33 ± 1.21	0.11 ± 0.05
Bubo philippensis	2	166 ± 8.49	56.39 ± 0.16	355 ± 11.31	1.3 ± 0.58	1.46 ± 0.32	0.98 ± 0.96	0.26 ± 0.03	0.22 ± 0.03	14.5 ± 0.71	0.17 ± 0
Bubo poensis	10	154.8 ± 11.53	45.62 ± 4.22	314.2 ± 19.04	3.18 ± 0.44	2.67 ± 0.82	0.85 ± 0.37	0.29 ± 0.08	0.41 ± 0.07	13.4 ± 0.52	0.12 ± 0.03
Bubo scandiacus	6	218.67 ± 6.59	39.9 ± 9.56	420.17 ± 29.05	2.38 ± 1.38	1.9 ± 1.17	0.47 ± 0.34	0.13 ± 0.05	0.33 ± 0.05	12.67 ± 1.97	0.15 ± 0.06
Bubo shelleyi	2	235	52.84	453	5.33	4.9	1.2	0.3	0.68	11	0.09
Bubo solomensis	3	145.67 ± 9.29	44.99 ± 4.08	281.33 ± 26.03	0.61 ± 0.01	0.74 ± 0.26	0.61 ± 0.43	0.2 ± 0.07	0.25 ± 0.08	20 ± 5	0.18 ± 0.07
Bubo sumatraus	6	178.5 ± 7.23	50.69 ± 4.83	363.33 ± 12.37	2.54 ± 0.76	1.33 ± 0.89	0.23 ± 0.09	0.2 ± 0.08	0.32 ± 0.08	12.67 ± 1.51	0.17 ± 0.08
Bubo virginianus	12	211.67 ± 25.89	45.68 ± 3.24	355.92 ± 28.68	4.34 ± 0.99	3.27 ± 1.21	1.92 ± 0.7	0.37 ± 0.2	0.4 ± 0.15	14.25 ± 1.14	0.12 ± 0.06
Ciccaba albitarsis	2	143.5 ± 4.95	41.8 ± 1.82	275 ± 5.66	0.99 ± 0.56	1.37 ± 0.06	1.75 ± 0.63	1.13 ± 1.02	0.21 ± 0.21	17.5 ± 3.54	0.14 ± 0.08
Ciccaba huhula	6	145.33 ± 11.52	36.91 ± 2.13	257.67 ± 17.13	1.94 ± 0.78	1.72 ± 0.57	0.75 ± 0.24	0.27 ± 0.09	0.32 ± 0.15	13.67 ± 2.07	0.1 ± 0.05

Cryptolaugx rostrata	1	73	22.79	143	0.99	1.69	0.53	0.29	0.18	21	0.06
Glaucidium brasilianum	6	66 ± 3.74	16.25 ± 0.63	93 ± 5.69	0.17 ± 0.06	0.12 ± 0.03	0.1 ± 0.02	0.09 ± 0.03	0.24 ± 0.09	14.5 ± 1.97	0.1 ± 0.03
Glaucidium brodiei	6	62 ± 2.45	17.01 ± 0.35	90.17 ± 0.41	0.19 ± 0.01	0.23 ± 0	0.25 ± 0.03	0.19 ± 0.01	0.21 ± 0	17.17 ± 0.41	0.1 ± 0.02
Glaucidium californicum	5	62.82 ± 9.88	15.29 ± 3.07	93 ± 9.19	0.42 ± 0.12	0.28 ± 0.11	0.26 ± 0.04	0.14 ± 0.07	0.28 ± 0.08	14.67 ± 1.75	0.14 ± 0.06
Glaucidium capense	6	76.33 ± 6.71	17.94 ± 1.67	138.33 ± 6.92	0.11 ± 0.03	0.12 ± 0.03	0.16 ± 0.06	0.15 ± 0.03	0.18 ± 0.09	10.5 ± 1.64	0.16 ± 0.12
Glaucidium costaricum	3	56 ± 4.58	15.79 ± 0.99	95.67 ± 0.58	0.19 ± 0.16	0.09 ± 0.05	0.06 ± 0.03	0.04 ± 0.01	0.17 ± 0.08	17 ± 1	0.07 ± 0.03
Glaucidium cuculoides	6	79.83 ± 9.28	19.53 ± 2.2	151 ± 6.07	0.16 ± 0.08	0.16 ± 0.12	0.12 ± 0.04	0.13 ± 0.04	0.19 ± 0.05	14.5 ± 1.64	0.09 ± 0.02
Glaucidium gnoma	2	62 ± 1.41	10.86 ± 0.26	92 ± 7.07	0.14 ± 0.06	0.18 ± 0.06	0.15 ± 0.01	0.11 ± 0.04	0.29 ± 0	15 ± 0	0.16 ± 0.03
Glaucidium jardini	6	60.67 ± 4.63	17.43 ± 0.77	105.5 ± 6.38	0.15 ± 0.08	0.09 ± 0.03	0.13 ± 0.04	0.1 ± 0.04	0.13 ± 0.04	14.17 ± 1.83	0.09 ± 0.03
Glaucidium lawrencii	3	80.33 ± 2.89	32.1 ± 2.48	151.33 ± 6.66	0.32 ± 0.13	0.29 ± 0.05	0.18 ± 0.01	0.26 ± 0.1	0.26 ± 0.12	10.67 ± 0.58	0.12 ± 0.06
Glaucidium minutissimum	4	50.25 ± 3.4	14.79 ± 0.7	90.25 ± 5.12	0.17 ± 0.08	0.16 ± 0.04	0.16 ± 0.06	0.11 ± 0.02	0.26 ± 0.01	14 ± 1.83	0.09 ± 0.02
Glaucidium parkeri	2	53 ± 4.24	15.51 ± 0.64	95 ± 2.83	0.09 ± 0.02	0.12 ± 0	0.14 ± 0.03	0.14 ± 0.01	0.19 ± 0.19	13.5 ± 2.12	0.05 ± 0
Glaucidium passerinum	5	59.33 ± 4.63	13.04 ± 1.88	106.83 ± 6.18	0.21 ± 0.1	0.22 ± 0.06	0.2 ± 0.02	0.12 ± 0.02	0.29 ± 0.04	15.2 ± 0.45	0.11 ± 0.05

Glaucidium perlatum	6	76.33 ± 4.27	17.49 ± 2.07	107.83 ± 2.86	0.18 ± 0.08	0.27 ± 0.08	0.23 ± 0.07	0.17 ± 0.06	0.21 ± 0.06	15.67 ± 0.82	0.09 ± 0.04
Glaucidium radiatum	7	71.43 ± 7.25	18.86 ± 1.24	130.14 ± 6.34	0.22 ± 0.13	0.19 ± 0.08	0.26 ± 0.14	0.19 ± 0.09	0.25 ± 0.09	13 ± 1	0.07 ± 0.01
Glaucidium siju	6	63.5 ± 3.89	17.06 ± 1.89	103.5 ± 5.72	0.12 ± 0.02	0.17 ± 0.04	0.14 ± 0.04	0.13 ± 0.02	0.27 ± 0.14	14.33 ± 1.03	0.08 ± 0.02
Glaucidium tephronotum	10	83.7 ± 10.15	14.89 ± 2.47	113.7 ± 10.83	0.21 ± 0.18	0.23 ± 0.18	0.2 ± 0.15	0.25 ± 0.27	0.19 ± 0.07	10.8 ± 3.01	0.1 ± 0.04
Jubula letti	3	167.5 ± 7.77	31.45 ± 2.73	281.5 ± 10.41	1.84 ± 0.06	1.82 ± 0.61	0.48 ± 0.18	0.09 ± 0.01	0.19 ± 0.07	14.67 ± 1.15	0.1 ± 0.03
Ketupa flavipes	6	204 ± 30.13	66.63 ± 11.44	425.5 ± 48.49	0.47 ± 0.19	0.53 ± 0.19	0.36 ± 0.22	0.3 ± 0.24	0.25 ± 0.18	13.67 ± 3.27	0.1 ± 0.04
Ketupa javanensis	2	170 ± 14.14	56.67 ± 7.52	346.5 ± 0.71	0.76 ± 0.24	0.65 ± 0.01	0.29 ± 0.01	0.3 ± 0.04	0.12 ± 0.01	11.5 ± 0.71	0.11 ± 0.01
Ketupa ketupu	7	167.86 ± 14.31	56.45 ± 6.52	335 ± 9.9	0.58 ± 0.33	0.57 ± 0.29	0.39 ± 0.22	0.25 ± 0.16	0.2 ± 0.11	10.29 ± 4.75	0.08 ± 0.04
Ketupa zeylonensis	6	185.86 ± 12.47	60.97 ± 6.54	409.71 ± 11.27	0.88 ± 0.76	0.65 ± 0.5	0.33 ± 0.13	0.23 ± 0.13	0.23 ± 0.05	12.83 ± 2.64	0.14 ± 0.07
Lophostrix cristata	6	164.83 ± 12.88	33.68 ± 4.09	298.67 ± 7.94	0.43 ± 0.24	0.23 ± 0.06	0.25 ± 0.15	0.24 ± 0.06	0.24 ± 0.07	12.17 ± 0.41	0.12 ± 0.04
Megascops asio	6	80.11 ± 1.66	25.33 ± 3.6	167.67 ± 8.52	2.07 ± 0.92	1.61 ± 1.02	0.6 ± 0.42	0.21 ± 0.1	0.36 ± 0.17	14.5 ± 1.05	0.12 ± 0.03
Megascops choliba	5	96.33 ± 2.16	22.4 ± 3.02	170 ± 7.72	1.35 ± 0.2	1.21 ± 0.56	0.65 ± 0.29	0.34 ± 0.05	0.33 ± 0.08	14.83 ± 1.6	0.1 ± 0.02
Micrathene whitneyi	13	49.14 ± 7.21	16.96 ± 2.22	108.71 ± 3.47	0.49 ± 0.29	0.43 ± 0.23	0.3 ± 0.13	0.16 ± 0.07	0.27 ± 0.09	12.5 ± 1.99	0.1 ± 0.06

Mimizuku gurneyi	1	145	41.55	295	1.89	1.46	1.03	0.69	0.17	18	0.11
Ninox affinis	4	113.75 ± 21.33	24.38 ± 2.48	190.25 ± 20.56	0.46 ± 0.29	0.35 ± 0.12	0.34 ± 0.1	0.22 ± 0.1	0.28 ± 0.14	11.75 ± 2.06	0.15 ± 0.1
Ninox badeckeri	1	92	20.49	187	1.55	1.9	1.02	0.33	0.17	19	0.07
Ninox boobook	6	143.5 ± 7.01	36.31 ± 4.1	250.33 ± 9.81	1.64 ± 0.12	1.36 ± 0.25	0.51 ± 0.38	0.2 ± 0.06	0.32 ± 0.06	13.67 ± 0.52	0.11 ± 0.04
Ninox connivens	6	166.83 ± 11.07	36.37 ± 3.57	314.33 ± 10.5	0.66 ± 0.29	0.57 ± 0.31	0.31 ± 0.14	0.18 ± 0.08	0.42 ± 0.27	11 ± 0.63	0.14 ± 0.02
Ninox dimorpha	7	137.86 ± 16.8	28.26 ± 3.94	218.14 ± 6.62	0.32 ± 0.18	0.37 ± 0.26	0.37 ± 0.22	0.2 ± 0.07	0.19 ± 0.05	14.29 ± 1.38	0.11 ± 0.05
Ninox jacquinoti	6	97.86 ± 7.78	34.62 ± 1.9	202.14 ± 9.51	0.63 ± 0.28	0.46 ± 0.23	0.34 ± 0.14	0.23 ± 0.15	0.33 ± 0.15	11.83 ± 0.98	0.11 ± 0.03
Ninox meeki	5	117.57 ± 5.71	33.68 ± 2.57	234.71 ± 8.71	0.26 ± 0.08	0.36 ± 0.11	0.37 ± 0.17	0.24 ± 0.08	0.33 ± 0.1	11.17 ± 2.23	0.12 ± 0.04
Ninox novaeseelandiae	6	112.67 ± 8.09	30.12 ± 2.93	221 ± 6.2	0.6 ± 0.19	0.58 ± 0.14	0.36 ± 0.2	0.24 ± 0.1	0.26 ± 0.06	12.5 ± 1.05	0.15 ± 0.04
Ninox ochracea	4	91.75 ± 8.06	23.66 ± 1.57	191.25 ± 4.65	0.21 ± 0.16	0.19 ± 0.1	0.24 ± 0.11	0.17 ± 0.07	0.15 ± 0.06	9.5 ± 1.73	0.07 ± 0.03
Ninox odiosa	6	91.17 ± 5.27	26.98 ± 3.08	180.5 ± 5.28	0.41 ± 0.15	0.45 ± 0.18	0.4 ± 0.05	0.29 ± 0.1	0.35 ± 0.08	11.33 ± 1.21	0.17 ± 0.06
Ninox philippensis	11	82.91 ± 6.89	26.55 ± 3.68	179.18 ± 7.83	0.43 ± 0.41	0.28 ± 0.12	0.27 ± 0.14	0.2 ± 0.08	0.3 ± 0.08	10.91 ± 1.51	0.09 ± 0.03
Ninox punctulata	6	73.17 ± 4.96	29.85 ± 1.19	169.17 ± 2.32	0.75 ± 0.29	0.68 ± 0.23	0.48 ± 0.21	0.32 ± 0.16	0.27 ± 0.04	13.83 ± 0.75	0.12 ± 0.03

Ninox rufa	6	195 ± 11.8	40.61 ± 4.33	342.67 ± 20.48	0.81 ± 0.55	0.69 ± 0.42	0.46 ± 0.24	0.24 ± 0.11	0.27 ± 0.12	13.5 ± 1.38	0.12 ± 0.04
Ninox scutulata	6	110.83 ± 3.76	24.16 ± 2.62	228.5 ± 10.93	0.23 ± 0.11	0.25 ± 0.07	0.23 ± 0.08	0.16 ± 0.11	0.39 ± 0.1	9.83 ± 0.98	0.17 ± 0.05
Ninox squamipila	6	118.67 ± 5.92	30.76 ± 2.7	227.67 ± 5.28	0.38 ± 0.18	0.5 ± 0.31	0.32 ± 0.11	0.26 ± 0.08	0.37 ± 0.11	10.17 ± 0.75	0.13 ± 0.05
Ninox strenua	5	250 ± 6.12	47.86 ± 2.01	406.4 ± 11.28	1.17 ± 0.31	1.03 ± 0.43	0.3 ± 0.09	0.34 ± 0.26	0.23 ± 0.09	14.2 ± 1.1	0.13 ± 0.03
Ninox superciliaris	6	107.83 ± 4.88	27.16 ± 3.61	199.17 ± 5.23	0.41 ± 0.26	0.5 ± 0.28	0.44 ± 0.28	0.26 ± 0.06	0.32 ± 0.12	10.17 ± 1.72	0.15 ± 0.07
Ninox theomacha	6	92.17 ± 9.02	25.99 ± 1.72	190 ± 6.93	0.62 ± 0.47	0.56 ± 0.39	0.45 ± 0.36	0.22 ± 0.06	0.37 ± 0.12	11.83 ± 0.98	0.13 ± 0.04
Ninox variegata	6	109.33 ± 4.59	28.82 ± 0.83	208.67 ± 9.2	0.42 ± 0.38	0.35 ± 0.2	0.3 ± 0.13	0.15 ± 0.03	0.35 ± 0.12	10.5 ± 2.35	0.09 ± 0.03
Otus albogularis	6	108.67 ± 2.94	26.22 ± 0.72	208.83 ± 9.91	1.49 ± 0.86	1.22 ± 0.57	0.84 ± 0.54	0.59 ± 0.63	0.3 ± 0.11	11.17 ± 1.83	0.12 ± 0.05
Otus alfredi	2	72.5 ± 3.54	23.69 ± 0.62	158 ± 4.24	0.69 ± 0.51	0.6 ± 0.52	0.48 ± 0.32	0.17 ± 0.04	0.23 ± 0.03	15 ± 1.41	0.11 ± 0.06
Otus bakkamoena	5	80 ± 8.67	24.54 ± 3.77	165.5 ± 16.08	1.26 ± 0.46	1.38 ± 0.26	0.64 ± 0.34	0.23 ± 0.1	0.17 ± 0.05	15 ± 2	0.12 ± 0.03
Otus balli	2	73 ± 5.66	20.44 ± 3.5	145 ± 1.41	1.07 ± 0.6	1.2 ± 0.5	0.75 ± 0.19	0.27 ± 0.09	0.24 ± 0.05	14 ± 1.41	0.07 ± 0.01

Otus brucei	6	72.33 ± 5.47	25.6 ± 2.94	158.17 ± 6.18	0.55 ± 0.14	0.48 ± 0.14	0.34 ± 0.14	0.17 ± 0.1	0.16 ± 0.07	17.5 ± 1.87	0.09 ± 0.02
Otus clarkii	6	91.33 ± 7.12	28.62 ± 1.42	191.17 ± 2.93	1.05 ± 0.43	0.88 ± 0.27	0.75 ± 0.44	0.29 ± 0.12	0.15 ± 0.05	13.67 ± 2.16	0.1 ± 0.03
Otus flammeolus	6	61.61 ± 2.06	17.78 ± 0.97	133.17 ± 5.85	0.58 ± 0.27	0.45 ± 0.22	0.21 ± 0.07	0.15 ± 0.04	0.26 ± 0.04	13.17 ± 2.23	0.09 ± 0.01
Otus guatemalae	6	81 ± 5.1	23.78 ± 2.36	167.5 ± 11.66	1.23 ± 0.35	1.07 ± 0.34	0.59 ± 0.27	0.31 ± 0.1	0.25 ± 0.05	14.67 ± 1.37	0.11 ± 0.04
Otus hartlaubi	1	64	23.73	137	1.68	0.11	0.2	0.19	0.27	14	0.11
Otus icterorhynchus	5	79 ± 11.98	21.72 ± 3.36	138.8 ± 7.19	1.33 ± 0.75	1 ± 0.37	0.72 ± 0.48	0.41 ± 0.35	0.2 ± 0.12	15.2 ± 1.3	0.07 ± 0.03
Otus ingens	6	94.5 ± 16.17	25.01 ± 2.23	196.5 ± 9.27	1.22 ± 0.35	1.24 ± 0.43	0.87 ± 0.42	0.29 ± 0.03	0.29 ± 0.12	12.33 ± 1.75	0.14 ± 0.04
Otus insularis	1	81	27.64	163	0.58	0.73	0.42	0.17	0.22	16	0.06
Otus kennicotti	6	88.67 ± 4.72	26.16 ± 2.98	179.83 ± 7.91	2.71 ± 0.4	2.41 ± 0.65	1.02 ± 0.73	0.29 ± 0.14	0.36 ± 0.15	13.33 ± 1.03	0.11 ± 0.03
Otus magicus	6	72.17 ± 8.75	25.7 ± 6.41	164.5 ± 11.83	0.54 ± 0.2	0.5 ± 0.3	0.29 ± 0.12	0.17 ± 0.08	0.17 ± 0.04	15.17 ± 3.6	0.07 ± 0.02

Otus marshalli	4	86 ± 4.08	23.84 ± 0.55	169.25 ± 10.05	1.01 ± 0.25	1.08 ± 0.27	0.74 ± 0.34	0.28 ± 0.11	0.33 ± 0.04	12.5 ± 2.65	0.1 ± 0.02
Otus megalotis	6	82.83 ± 13.38	35.52 ± 13.14	177 ± 18.88	1.15 ± 0.25	1.16 ± 0.42	0.67 ± 0.6	0.19 ± 0.07	0.17 ± 0.06	17 ± 1.26	0.1 ± 0.02
Otus nudipes	6	98 ± 5.83	31.32 ± 4.08	177.33 ± 37.82	0.64 ± 0.3	0.76 ± 0.39	0.56 ± 0.3	0.24 ± 0.06	0.18 ± 0.04	14.81 ± 4	0.1 ± 0.04
Otus pembaensis	5	77.4 ± 4.34	24.08 ± 2.52	151.8 ± 1.64	0.55 ± 0.27	0.49 ± 0.21	0.24 ± 0.06	0.22 ± 0.14	0.2 ± 0.05	16.8 ± 3.35	0.07 ± 0.02
Otus peprsoni	1	90	26.79	175	0.99	0.74	0.34	0.24	0.16	14	0.11
Otus podorginus	5	83.4 ± 8.02	27.01 ± 1.78	161 ± 1.87	0.66 ± 0.18	0.79 ± 0.26	0.64 ± 0.25	0.38 ± 0.17	0.22 ± 0.04	10.2 ± 1.79	0.11 ± 0.02
Otus rufescens	6	63.67 ± 4.97	21.17 ± 4.07	128.17 ± 7.14	0.71 ± 0.39	0.57 ± 0.21	0.4 ± 0.17	0.2 ± 0.09	0.2 ± 0.07	15.5 ± 1.87	0.09 ± 0.01
Otus rutilus	5	83.2 ± 3.96	23.65 ± 3.89	163.2 ± 3.83	0.71 ± 0.46	0.67 ± 0.2	0.7 ± 0.35	0.31 ± 0.12	0.16 ± 0.07	14.4 ± 2.19	0.09 ± 0.02
Otus sagittatus	7	111.71 ± 6.75	25.99 ± 2.34	190.86 ± 4.14	1.4 ± 0.45	1.03 ± 0.5	0.64 ± 0.34	0.36 ± 0.14	0.24 ± 0.1	13 ± 0.82	0.13 ± 0.02
Otus scops	6	62.31 ± 7.41	19.26 ± 3.15	139.45 ± 7.32	0.28 ± 0.16	0.34 ± 0.15	0.31 ± 0.1	0.19 ± 0.09	0.22 ± 0.06	12.67 ± 2.16	0.13 ± 0.06

Otus senegalensis	10	73.91 ± 25.25	24.27 ± 7.45	159.5 ± 39.24	0.92 ± 0.62	1 ± 0.74	0.89 ± 0.54	0.35 ± 0.19	0.21 ± 0.07	14.2 ± 1.75	0.11 ± 0.05
Otus silvicola	3	100.33 ± 3.79	31.25 ± 1.36	207.33 ± 7.57	1.82 ± 0.42	1.58 ± 0.34	0.81 ± 0.05	0.26 ± 0.08	0.17 ± 0.03	15.67 ± 1.53	0.09 ± 0.03
Otus spilocephalus	6	72.67 ± 1.97	26.5 ± 1.34	151.33 ± 5.57	0.84 ± 0.32	1.1 ± 0.42	1.05 ± 0.53	0.34 ± 0.14	0.32 ± 0.22	15.5 ± 1.38	0.1 ± 0.07
Otus trichopsis	11	73.27 ± 4.58	21.79 ± 3.71	146.18 ± 6.81	1.24 ± 0.42	1.17 ± 0.53	0.84 ± 0.43	0.29 ± 0.12	0.3 ± 0.14	15.09 ± 2.26	0.11 ± 0.04
Otus umbra	1	63	21.23	144	0.25	0.31	0.34	0.21	0.45	12	0.1
Phodilus badius	7	85.43 ± 7.39	33.62 ± 4.07	208.86 ± 20.89	0.69 ± 0.32	0.8 ± 0.22	0.54 ± 0.13	0.39 ± 0.15	0.13 ± 0.03	25.29 ± 2.93	0.12 ± 0.05
Ptilopsis leucotis	10	92.8 ± 6.25	24.88 ± 2.89	192.1 ± 10.33	2.55 ± 0.54	2.4 ± 0.56	1.51 ± 0.47	0.54 ± 0.26	0.29 ± 0.07	15.9 ± 1.45	0.11 ± 0.03
Pulsatrix koeniswaldania	5	181.4 ± 11.61	36.45 ± 5.93	316 ± 7.68	1.71 ± 0.56	1.69 ± 0.61	1.15 ± 0.73	0.42 ± 0.11	0.29 ± 0.12	13.4 ± 0.55	0.11 ± 0.03
Pulsatrix melanonata	6	161.67 ± 4.76	36.92 ± 5.52	289.33 ± 9.75	1.6 ± 0.34	1.51 ± 0.58	0.85 ± 0.42	0.26 ± 0.1	0.32 ± 0.1	13.67 ± 1.37	0.13 ± 0.05
Pulsatrix perspicillata	6	181.17 ± 11.87	40.57 ± 6.11	306.5 ± 32.46	2.65 ± 0.39	2.54 ± 0.82	1.3 ± 0.91	0.31 ± 0.13	0.39 ± 0.09	12.33 ± 0.82	0.1 ± 0.05

Sceolglaux albifaces	4	141.75 ± 10.05	59.17 ± 9.79	262.75 ± 13.74	0.42 ± 0.28	0.51 ± 0.29	0.35 ± 0.4	0.28 ± 0.14	0.25 ± 0.09	12.75 ± 2.22	0.11 ± 0.04
Scops lucine	1	75	24.02	134	0.25	0.24	0.29	0.25	0.2	16	0.12
Scotopelia bouiveiri	5	174.6 ± 8.47	47.89 ± 3.78	311 ± 9.92	1.38 ± 1.03	0.74 ± 0.62	0.34 ± 0.14	0.25 ± 0.12	0.18 ± 0.04	12.6 ± 2.3	0.14 ± 0.04
Scotopelia peli	5	224 ± 17.89	65.02 ± 8.48	420.83 ± 12.94	0.97 ± 0.5	0.75 ± 0.52	0.52 ± 0.26	0.24 ± 0.15	0.19 ± 0.06	16 ± 1.87	0.12 ± 0.04
Scotopelia ussheri	1	200	63.21	345	2.96	2.37	0.63	0.52	0.27	13	0.08
Strix aluco	6	169.33 ± 13.19	35.07 ± 6.11	282.83 ± 15.82	4.05 ± 0.94	4.21 ± 0.6	1.49 ± 0.57	0.36 ± 0.11	0.43 ± 0.39	12.83 ± 0.98	0.09 ± 0.02
Strix butleri	3	147 ± 9	48.77 ± 2	249.33 ± 4.73	3.28 ± 0.81	3.04 ± 0.88	0.98 ± 0.38	0.27 ± 0.19	0.38 ± 0.11	15 ± 2	0.11 ± 0.03
Strix chacoensis	3	156 ± 13.23	43.99 ± 5.25	266.33 ± 9.07	3.18 ± 2.15	2.39 ± 1.23	1.04 ± 0.23	0.35 ± 0.07	0.31 ± 0.03	14 ± 2	0.07 ± 0.01
Strix fulvescens	1	190	35.69	315	1.65	1.52	0.99	0.28	0.28	15	0.14
Strix hylophilia	6	148 ± 4.29	38.01 ± 3.24	245.33 ± 5.92	2.06 ± 0.37	1.54 ± 0.75	0.67 ± 0.35	0.38 ± 0.11	0.29 ± 0.07	11.83 ± 0.41	0.14 ± 0.02
Strix leptogrammica	8	155 ± 7.19	40.68 ± 5.04	308.25 ± 14.68	1.21 ± 0.61	1.38 ± 0.66	0.52 ± 0.29	0.29 ± 0.09	0.32 ± 0.13	12.14 ± 1.35	0.17 ± 0.07

Strix nebulosa	6	286.5 ± 10.89	36.05 ± 3.36	443 ± 23.11	5.89 ± 1.15	5.34 ± 1.8	2.43 ± 0.62	0.38 ± 0.16	0.29 ± 0.12	10.5 ± 1.38	0.1 ± 0.05
Strix nigrolineata	5	156.33 ± 9.2	39.28 ± 5.93	271.17 ± 10.38	2.1 ± 0.6	2.12 ± 0.58	0.84 ± 0.38	0.23 ± 0.18	0.31 ± 0.1	12.5 ± 1.38	0.13 ± 0.04
Strix occidentalis	6	195 ± 10.2	44.82 ± 4.78	324.83 ± 11.32	4.86 ± 0.74	4.97 ± 0.65	1.96 ± 0.42	0.5 ± 0.25	0.44 ± 0.2	11.5 ± 1.76	0.1 ± 0.06
Strix ocellata	7	175.71 ± 16.41	44.94 ± 6.92	345.57 ± 14.05	2.06 ± 0.87	1.45 ± 0.7	0.43 ± 0.2	0.25 ± 0.18	0.32 ± 0.09	12.57 ± 1.27	0.13 ± 0.03
Strix rufipes	5	151.83 ± 7.25	34.29 ± 4.41	261.33 ± 12.74	2.03 ± 0.32	2.13 ± 0.33	1.09 ± 0.12	0.53 ± 0.04	0.38 ± 0.1	11.83 ± 0.75	0.19 ± 0.02
Strix seloputo	4	182.25 ± 14.73	46.42 ± 2.93	342.25 ± 22.91	2.23 ± 0.41	1.57 ± 0.6	0.44 ± 0.1	0.34 ± 0.17	0.3 ± 0.06	11.5 ± 1	0.18 ± 0.05
Strix uralensis	6	273.33 ± 11.71	43.92 ± 2.66	369.67 ± 12.44	3.65 ± 1.19	2.66 ± 1.02	0.91 ± 0.31	0.27 ± 0.13	0.32 ± 0.1	13.33 ± 1.03	0.15 ± 0.05
Strix varia	6	212.5 ± 8.17	39.08 ± 9.27	335.83 ± 14.91	3.58 ± 1.06	3.68 ± 0.86	1.26 ± 0.41	0.49 ± 0.25	0.47 ± 0.14	10.5 ± 1.22	0.14 ± 0.05
Strix virgata	6	141 ± 15.54	35.38 ± 2.74	247.5 ± 9.57	2.12 ± 0.91	1.94 ± 0.86	0.95 ± 1	0.36 ± 0.12	0.32 ± 0.09	14.33 ± 1.51	0.12 ± 0.02
Strix woodfordii	6	144.67 ± 11.33	36.07 ± 5.62	253.67 ± 26.88	2.24 ± 0.54	2.05 ± 0.67	0.84 ± 0.23	0.32 ± 0.1	0.37 ± 0.07	13 ± 2	0.18 ± 0.1

Surina ulula	8	177.56 ± 10.7	24.63 ± 6.86	230.78 ± 5.36	0.32 ± 0.11	0.3 ± 0.11	0.26 ± 0.06	0.2 ± 0.07	0.41 ± 0.1	11.38 ± 1.3	0.12 ± 0.03
Syrium whiteheadi	1	175	47.63	305	0.97	1.22	0.97	0.41	0.15	14	0.13
Tyto alba	6	115.7 ± 11.67	55.75 ± 5.48	301.67 ± 22.51	1.94 ± 0.51	1.63 ± 0.53	1.23 ± 0.58	0.83 ± 0.55	0.31 ± 0.08	17.83 ± 2.32	0.07 ± 0.02
Tyto alba punctatissma	6	110.33 ± 12.24	45.44 ± 2.84	217.83 ± 5.81	1.14 ± 0.23	1.04 ± 0.31	0.62 ± 0.19	0.24 ± 0.09	0.24 ± 0.1	19.5 ± 1.22	0.08 ± 0.02
Tyto aurantia	5	98.6 ± 12.58	57.26 ± 3.28	247.2 ± 24.17	1.43 ± 0.2	1.35 ± 0.2	0.78 ± 0.13	0.2 ± 0.05	0.17 ± 0.05	24.2 ± 0.84	0.1 ± 0.02
Tyto capensis	6	114.67 ± 4.93	73.48 ± 5.71	323.17 ± 16.93	0.86 ± 0.5	0.83 ± 0.41	0.65 ± 0.09	0.33 ± 0.08	0.2 ± 0.11	22.17 ± 1.33	0.1 ± 0.06
Tyto inexpectata	3	104.33 ± 8.5	53.34 ± 8.59	258.33 ± 11.93	1.07 ± 0.56	1.06 ± 0.41	0.89 ± 0.62	0.34 ± 0.09	0.2 ± 0.05	23.33 ± 1.53	0.09 ± 0.04
Tyto longimembris	1	110	76.34	330	0.56	0.85	0.64	0.17	0.13	17	0.12
Tyto novaehollandiae	6	119 ± 7.18	55.32 ± 15.43	305.5 ± 17.2	2.07 ± 0.44	1.7 ± 0.38	1.32 ± 0.13	0.56 ± 0.16	0.2 ± 0.06	19 ± 2.76	0.08 ± 0.03
Tyto rosenbergii	6	123.67 ± 17.42	62.83 ± 3.18	332.83 ± 8.52	1.47 ± 0.41	1.47 ± 0.21	1.28 ± 0.28	0.48 ± 0.2	0.4 ± 0.41	21 ± 1.26	0.08 ± 0.01

Tyto soumagnegi	1	94	29.11	235	1.92	1.88	1.74	0.31	0.16	23	0.13
Tyto tenebricosa	6	110.83 ± 11.87	57.42 ± 11.04	267.83 ± 17.7	1.43 ± 0.24	1.21 ± 0.18	0.78 ± 0.2	0.2 ± 0.07	0.14 ± 0.02	23.67 ± 2.34	0.11 ± 0.04

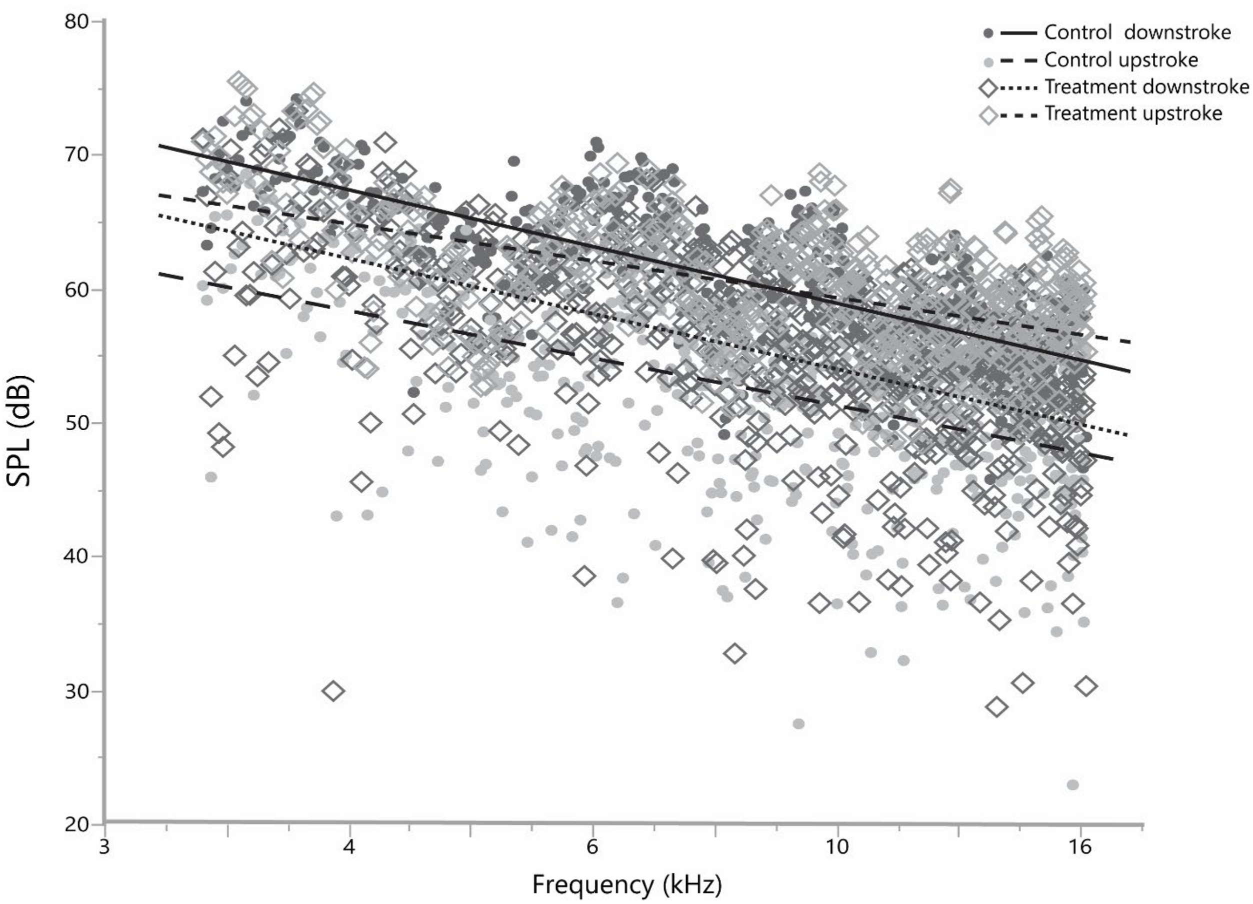

Figure 2.S1. Plot of sound production (3-16 kHz) during one control and treatment fight on log/log scale. X-axis is presented in kHz for reference. Regression lines of sound production across $\log_{10}$frequency of 3 kHz and above. Control downstroke R^2=0.58, slope= -21.2 dB/kHz; control upstroke R^2=0.26, slope= -17.7 dB/kHz; Treatment downstroke R^2=0.31, slope= -20.68 dB/kHz; Treatment upstroke R^2=0.30, slope= -13.8 dB/kHz.

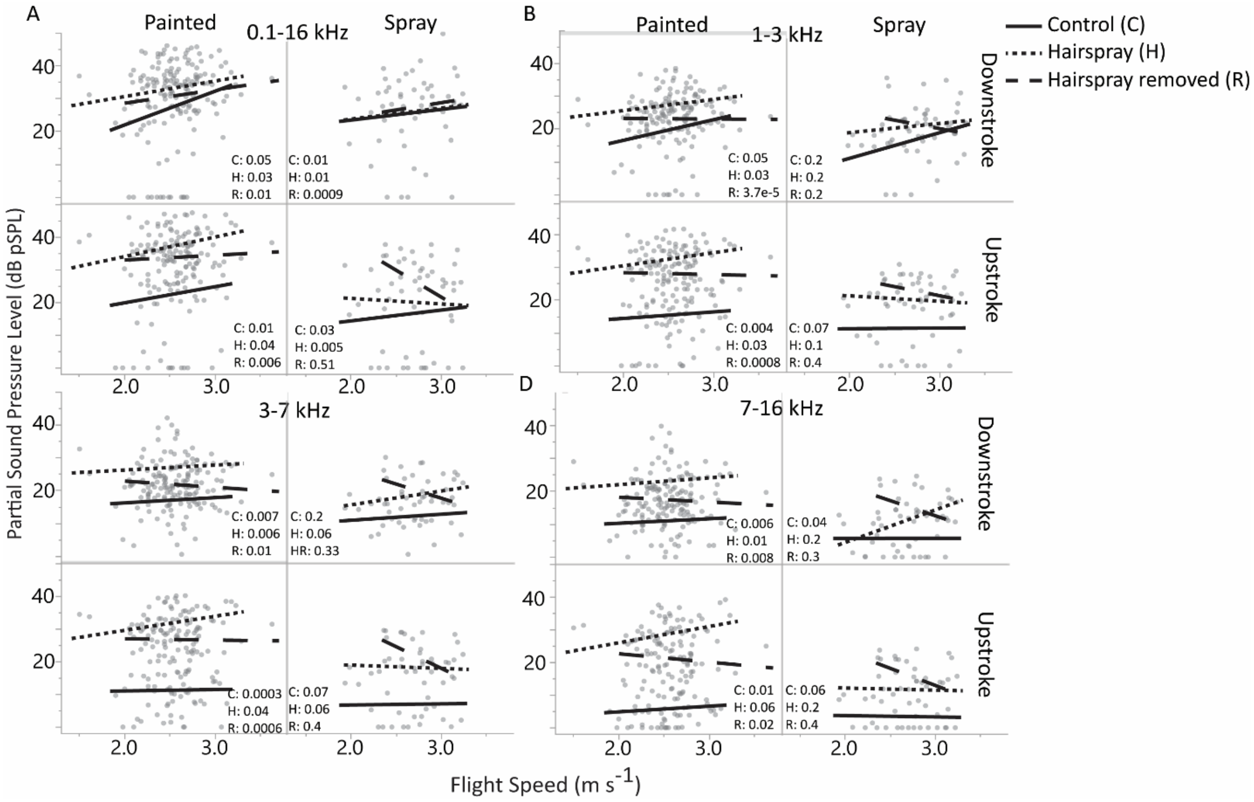

Figure 2.S2. Effect of flight speed on sound production of upstroke and downstroke. A) entire bandwidth (0.1-16 kHz), B) 1-3 kHz, C) 3-7 kHz, and D) 7-16 kHz. There was a positive relationship between flight speed and sound production in the control and hairspray groups in both treatment applications (painted and spray). In the hairspray-removed group, the relationship between flight speed and sound production is negative (N=217 flights).

Table 3.S1 Nearfield and Far-field sound production of the insects in this study.

	Nearfield sound (dB)		Farfield sound (dB)	
Distance (m)	*Chlorochroa say*i (0.37 mg)	*Hyles lineata* (1.03 mg)	*Chlorochroa sayi*	*Hyles lineata*
0.01	63	72	27 ± 0.2	33 ± 2.0
0.02	51	60	21 ± 0.2	27 ± 2.0
0.03	44	53	17 ± 0.2	23 ± 2.0
0.04	39	48	15 ± 0.2	21 ± 2.0
0.05	35	44	13 ± 0.2	19 ± 2.0
0.075	28	37	9.4 ± 0.2	15 ± 2.0
0.1	23	32	6.9 ± 0.2	13 ± 2.0
0.15	16	25	3.4 ± 0.2	9 ± 2.0
0.2	11	20	0.88 ± 0.2	6.7 ± 2.0
0.21	10	19	0.45 ± 0.2	6.2 ± 2.0
0.25	7.4	16	-1.1 ± 0.2	4.7 ± 2.0
0.3	4.2	13	-2.7 ± 0.2	3.1 ± 2.0
0.4	-0.8	8.2	-5.1 ± 0.2	0.63 ± 2.0
0.5	-4.7	4.3	-7.1 ± 0.2	-1.3 ± 2.0
0.75	-11	-2.8	-11 ± 0.2	-4.8 ± 2.0
1	-17	-7.8	-13 ± 0.2	-7.3 ± 2.0
1.25	-21	-12	-15 ± 0.2	-9.3 ± 2.0
1.5	-24	-15	-17 ± 0.2	-11 ± 2.0
1.75	-26	-17	-18 ± 0.2	-12 ± 2.0
2	-29	-20	-19 ± 0.2	-13 ± 2.0
2.35	-32	-23	-21 ± 0.2	-15 ± 2.0
3	-36	-27	-23 ± 0.2	-17 ± 2.0
3.5	-39	-30	-24 ± 0.2	-18 ± 2.0
4	-41	-32	-25 ± 0.2	-19 ± 2.0
4.5	-43	-34	-26 ± 0.2	-20 ± 2.0
5	-45	-36	-27 ± 0.2	-21 ± 2.0

Table 3.S2. Insect detection distances and hunting success for Lesser Nighthawks hunting from a perch and on the wing.

Foraging Strategy	Detection distance (m)	Success?	Insect evasion?	Insect evasion distance (m)
Perched	1.9	yes		
Perched	1.0	yes		
Perched	1.3	yes		
Perched	0.6	yes		
Perched	0.9	yes		
On the wing	2.6	yes		
On the wing	1.3	yes		
On the wing	0.9	yes		
On the wing	1.0	yes		
On the wing	2.3	yes		
On the wing	1.5	yes		
On the wing	3.6	yes		
On the wing	9.7	yes		
On the wing	3.2	yes		
On the wing	3.2	yes		
On the wing	1.6	yes		
On the wing	0.7	yes		
On the wing	2.0	unknown		
On the wing	3.9	unknown		
On the wing	3.4	no	no	
On the wing	0.8	no	no	
On the wing	7.1	no	no	
On the wing	3.0	no	no	
On the wing	1.2	no	no	
On the wing	2.7	no	no	
On the wing	0.6	no	no	
On the wing	1.0	no	yes	0.3
On the wing	2.4	no	no	
On the wing	3.6	no	no	
On the wing	1.3	no	no	
On the wing	1.4	no	yes	0.003
On the wing	1.1	no	no	
On the wing	0.7	no	yes	
On the wing	4.7	no	no	0.2